Award Number: W81XWH-10-2-0116

TITLE: “Treating Combat Hearing Loss with Atoh1 Gene Therapy”

PRINCIPAL INVESTIGATOR: Andrew K. Groves Ph.D.

CONTRACTING ORGANIZATION: Baylor College of Medicine
Houston, TX 77030

REPORT DATE: June 2015

TYPE OF REPORT: Final

PREPARED FOR: U.S. Army Medical Research and Materiel Command
Fort Detrick, Maryland 21702-5012

REPORT DOCUMENTATION PAGE

Form Approved
OMB No. 0704-0188

1. REPORT DATE	2. REPORT TYPE	3. DATES COVERED *(From - To)*
June 2015	Final	1Oct2010 - 31Mar2015

4. TITLE AND SUBTITLE
"Treating Combat Hearing Loss with Atoh1 Gene Therapy"

5a. CONTRACT NUMBER
W81XWH-10-2-0116

5b. GRANT NUMBER

5c. PROGRAM ELEMENT NUMBER

6. AUTHOR(S)

Andrew K. Groves Ph.D.

email: akgroves@bcm.edu

5d. PROJECT NUMBER

5e. TASK NUMBER

5f. WORK UNIT NUMBER

7. PERFORMING ORGANIZATION NAME(S) AND ADDRESS(ES)

AND ADDRESS(ES)
Baylor College of Medicine
Houston, TX 77030

8. PERFORMING ORGANIZATION REPORT NUMBER

9. SPONSORING / MONITORING AGENCY NAME(S) AND ADDRESS(ES)
U.S. Army Medical Research and Materiel Command
Fort Detrick, Maryland 21702-5012

10. SPONSOR/MONITOR'S ACRONYM(S)

11. SPONSOR/MONITOR'S REPORT NUMBER(S)

12. DISTRIBUTION / AVAILABILITY STATEMENT

Approved for public release; distribution unlimited

13. SUPPLEMENTARY NOTES

14. ABSTRACT

The goal of the project is to test experimental therapies for hearing loss in transgenic mouse models. We have identified a list of targets of the Atoh1 transcription factor which is a key to regenerating hair cells. We have shown that another candidate pathway, the Notch signaling pathway, is no longer active in the mature animal, and thus is not a viable therapeutic target for hearing loss. We have also generated the means to activate Atoh1 and a supporting factor, Gfi1, in deafened mice to promote hair cell regeneration.

15. SUBJECT TERMS
Noise-induced hearing loss, Mouse models, Gene Therapy, Regeneration

16. SECURITY CLASSIFICATION OF:			17. LIMITATION OF ABSTRACT	18. NUMBER OF PAGES	19a. NAME OF RESPONSIBLE PERSON
a. REPORT	b. ABSTRACT	c. THIS PAGE			19b. TELEPHONE NUMBER *(include area code)*
U	U	U	UU	52	

TABLE OF CONTENTS

1. INTRODUCTION:

Hearing and balance dysfunction are frequently seen in military personnel exposed to blast injuries. The most common cause of these disorders is the death of inner ear sensory hair cells. Once hair cells are killed, they are not replaced and combat-induced hearing and balance disorders are therefore permanent. At present, there is no treatment that allows the replacement of these sensory cells. The long term goal of this research is to develop gene or drug-based therapies that allow the regeneration of sensory hair cells and the restoration of hearing and balance in combat personnel. The transcription factor **Atoh1** is one of the first genes to be switched on when hair cells form. Atoh1 has been shown to induce new hair cells when activated in embryonic or neonatal inner ears. We have attempted to re-activate Atoh1 by genetic or pharmacological methods in an animal model to test its ability to promote regeneration of sensory hair cells.

2. KEYWORDS

Hearing Loss
Hair Cells
Cochlea
Atoh1
Gfi1
Mice
Regeneration
Supporting Cells
Adenovirus

3. OVERALL PROJECT SUMMARY:

Throughout this Final report, we have summarized the main findings discussed in previous Annual Reports and have provided a list of references to publications and abstracts that were generated by this work.

Aim 1: To determine the genetic targets of Atoh1

The transcription factor Atoh1 is both necessary and sufficient for the differentiation of hair cells, and is strongly up-regulated during hair cell regeneration in non-mammalian vertebrates. In order to understand more about the mechanism by which Atoh1 regulates the production of hair cells, we proposed the following goals for this Aim:

- to obtain comprehensive transcriptomic data sets from hair cells purified from wild type and Atoh1 mutant mice (which are unable to make hair cells)
- to use an epitope-tagged version of Atoh1 to identify direct targets of Atoh1 in cochlear hair cells by chromatin immunoprecipitation and sequencing (ChIP-Seq).

We initially began these studies by using microarray technology to identify transcripts present in purified hair cells, and we obtained microarray data from wild type hair cells purified by fluorescence-activated cell sorting. However, within the first six months of the project, the advent of RNA sequencing (RNA-seq), in particular the technology to obtain RNA-sequencing data from relatively small numbers of cells, allowed us to obtain much more representative and complete transcriptomic data from purified hair cells. As a result, we switched to RNA-seq for the remainder of the project and obtained high quality, reproducible, well-mapped RNA-seq data sets from purified neonatal cochlear hair cells (Cai et al., 2015).

Our original goal of generating RNA-seq data from Atoh1 mutant mouse cochleas was confounded by our discovery that in these mutants, the progenitors of hair cells in the cochlea die shortly after the time at which they would normally differentiate. Thus, Atoh1 is critically required for the *survival* of newly-generated hair cells. This result meant that it was not technically possible to purify the progenitors of hair cells from Atoh1 mutant mice, as they die almost as soon as they receive the signals to differentiate. However, we were able to use a conditional knockout mutant of Atoh1 to demonstrate that the requirement of Atoh1 for hair cell survival is only present for the first few days after hair cells differentiate. We were also able to publish the results of this study (Cai et al., 2013).

We carried out several attempts to perform ChIP-sequencing using transgenic mice that carried an epitope-tagged version of Atoh1. We did this both on whole cochleas and also on 300,000 purified hair cells carrying the tagged version of Atoh1. However, in both cases the signal-noise ratio we observed when analyzing the sequencing data made it impossible to accurately predict binding sites of Atoh1 in the hair cell genome. As a result, we adopted an alternative, bioinformatic-driven comparative strategy to identify potential targets of Atoh1 in hair cells. We cross-referenced our hair cell RNA-seq data with Atoh1 ChIP-seq data sets from two other populations that express Atoh1- cerebellar granule cells and intestinal epithelial cells. Our criteria for a candidate Atoh1 target gene was one of the following:

> - It was significantly expressed and enriched in hair cells (fold change>10, RPKM>3000) and contained at least one predicted Atoh1 binding site within 5kb of the gene's transcriptional start site, *OR*
> - It was shown to an Atoh1 binding region within 10kb of the transcriptional start site that was revealed through ChIP-seq in either cerebellum or intestinal epithelium.

Using these parameters, we identified 233 candidate Atoh1 target genes in cochlear hair cells, and demonstrated that 10 of them were indeed direct Atoh1 targets by ChIP-PCR. We also showed that some of these genes were down-regulated when Atoh1 was conditionally deleted from cochlear hair cells. This data was published earlier this year (Cai et al., 2015).

Aim 2: To activate Atoh1 in damaged cochlear organ cultures to promote hair cell regeneration

Aim 3: To activate Atoh1 in deafened mice to promote hair cell regeneration

These two aims used two different strategies to activate Atoh1, and we consider each of them in turn together with a discussion of how they were applied to organ culture and intact mouse model systems.

A: Inhibition of the Notch signaling pathway

It is well-established that hair cells use the Notch signaling pathway to inhibit surrounding supporting cells from adopting a hair cell fate. Accordingly, in animals that can regenerate their hair cells (such as birds), newly-regenerated hair cells that up-regulate Atoh1 re-express Notch ligands on their cell surface. Similarly, inhibition of the Notch signaling pathway in neonatal mammals leads to supporting cells switching on the Atoh1 transcription factor and differentiating into hair cells. Thus, in these two aims, we proposed to inhibit Notch signaling in organ cultures and in living, deafened mice using a variety of means.

We quickly found that although inhibition of the Notch signaling pathway works very well in neonatal animals, the ability of Notch inhibition to generate new hair cells declines precipitously after birth, such that very little effect is seen in three day old mouse cochleas and no effect is seen by the time the mice are six days old. We should stress that this decline simply reflects the aging or maturation of mouse supporting cells, as no supporting cells are either lost or gained during this time period. We obtained a similar result in a different way by using transgenic over-expression of Notch inhibitory molecule (a dominant negative version of the Mastermind co-activator protein), but again saw the same result. We characterized this effect at the level of organ cultures and the single cell level, and these results were recently published (Maass et al., 2015).

We then attempted to determine the transcriptional changes that occurred in supporting cells in the first week after birth in mice. We purified supporting cells from new born or 6 day old transgenic mice used by our lab to label supporting cells with GFP. We performed RNA-seq on relatively small numbers of cells from these mice and were able to identify hundreds of transcripts that were either significantly up- or down-regulated between these two ages. This work was presented in abstract form (Maass et al., 2014); we are currently preparing the work for publication.

To understand the reason for why a blockade of Notch signaling is effective in neonatal but not older animals, we considered a number of possibilities. It was formally possible that a large number of transcriptional changes were occurring in DAPT-treated cultures in six day old animals, but that these changes were simply insufficient to induce a hair cell differentiation program. To test this, we performed RNA-seq experiments on supporting cells purified from neonatal and six day old supporting cells that were treated with Notch inhibitors for 24 hours. In P1 supporting cells that were exposed to DAPT for 24 hours, over 2000 genes were significantly up- or down-regulated. However, in P6 supporting cells that were exposed to DAPT for 24 hours, only 2 genes were significantly up-regulated and 18 were down-regulated. Our results therefore demonstrate that supporting cells become essentially refractory to Notch signaling between P1 and P6, *and that Notch inhibition by itself is unlikely to be a viable therapy to restore hair cells.*

B: Genetic activation of Atoh1

Prior to our proposal, a number of studies had suggested that ectopic expression of Atoh1 in the inner ear was able to generate ectopic hair cells. The majority of these studies had been performed in neonatal animals, but a number of studies also used viruses to infect supporting cells with Atoh1 in older animals. The second strategy we proposed to activate Atoh1 in the cochlea was to use transgenic mice in which Atoh1 was expressed using the Cre-LoxP system – we proposed to mate an inner ear- or supporting cell-specific Cre driver line with mice in which Atoh1 could be expressed in a Cre-dependent fashion. Our first attempt to make these mice, using a transgenic chick beta-actin promoter and a LoxP-flanked stop cassette, gave very low expression of Atoh1. We therefore switched to targeting the

ubiquitously-expressed ROSA locus using previously published targeting cassettes incorporating a GFP reporter and a LoxP-flanked stop cassette. Once again, this line gave a very low induction of Atoh1, for reasons which are still unclear to us.

At the same time that we were testing these mice, two independent studies were published that also used two different Cre-inducible systems to activate expression of Atoh1 in the inner ear. Similar to our Notch studies reported above, these two papers showed that although transgenic activation of Atoh1 can generate large numbers of new hair cells in neonatal animals, the same transgenic approach does not produce new hair cells in animals older than about 7 days. We therefore proposed to test the hypothesis that additional transcription factors may be required to co-operate with Atoh1 in older animals. We chose to pursue the zinc finger transcription factor Gfi1, as its homologue in *Drosophila*, *senseless*, has been shown to co-operate with and enhance the function of the *Drosophila* Atoh1 homologue, *atonal*. We therefore generated a second set of transgenic mice in which Atoh1 and Gfi1 were co-expressed from the same transgenic construct in a Cre-inducible fashion. As discussed above, our first attempt to co-express these two genes, using transgenic mice made from a previously published targeting cassettes incorporating a GFP reporter and a LoxP-flanked stop cassette, proved unsuccessful. We therefore re-engineered our mice using an alternative Cre-inducible expression construct developed and published by the Allen Brain Institute. We also generated adenoviral constructs that allowed us to infect the cochlea with either Atoh1 and a reporter gene, or Atoh1 and Gfi1 together with a reporter gene

In the course of generating these new mice, we became concerned that the strategy we used for co-expression of Atoh1 and Gfi1 might be compromised by the picornavirus 2A sequence used to join the two gene coding regions together. After ribosomal cleavage of the 2A peptide to release Atoh1 and Gfi1 separately, a single proline residue was left attached to the N-terminus of Gfi1. Since the SNAG repressor domain of Gfi1 occurs immediately at the N-terminus of the protein, it is possible that the additional proline may interfere with this domain. We directly compared the repressive function of a Gf1-2A-TdTomato construct (in which Gfi1 has no N-terminal proline), with a TdTomato-2A-Gfi1 construct, and found that the latter construct had a significantly (75%) lower repressive activity. At this point, we do not know if the repressive function of Gfi1 is necessary for hair cell formation, as there is some evidence that Gfi1 can directly interact with Atoh1 without DNA binding, but in the light of these results, it will be prudent to re-engineer our constructs with Gfi1 as the first sequence in the construct. However, the grant terminated before we could complete this work.

As we were completing the project, we were able to demonstrate that unlike the adult cochlea, adenoviral transduction of Atoh1 into the adult utricle was able to generate large numbers of extra hair cells. Based on our candidate list of Atoh1 targets generated in Aim 1, we are now in an excellent position to interrogate these targets in the adult utricle and to find how these targets are differentially regulated in the cochlea and utricle, such that regeneration is possible in the adult utricle but not the cochlea.

4. KEY RESEARCH ACCOMPLISHMENTS:

• Developed techniques to purify supporting cells from cultured organ of Corti

• Generated a validated list of genes expressed in hair cells using RNA-seq

• Generated a list of Atoh1 target genes in cochlear hair cells

• Generated high-quality RNA-Seq library from neonatal and six day old supporting cells.

• Generated high-quality RNA-Seq libraries to compare the effects of DAPT on neonatal and six day old supporting cells

• Validated RNA-Seq library construction on small numbers of cells

• Confirmed that the new line of Sox2-CreER mice is able to efficiently cause gene activation or deletion in cochlear supporting cells.

• Generated a second set of targeting constructs to conditionally activate Atoh1 and Gfi1 in any cell or tissue type in the mouse.

• Generated adenoviral constructs to over-express Atoh1 and Gfi1 in any cell or tissue type in the mouse.

5. CONCLUSION:

The long-term goal of this project is to use activation of the Atoh1 gene by pharmacological or genetic means to promote hair cell production in the damaged cochlea as a means of hearing restoration.

The three goals of the proposal were to identify the genetic targets of Atoh1 and to demonstrate as a proof of principle that activation of Atoh1 can generate hair cells in organ culture and transgenic mouse models.

Aim 1 – to identify targets of Atoh1 itself – has now been completed and two manuscripts have been published. Mouse cochlear supporting cells execute their final division at late embryonic stages. One explanation for the failure of hair cell regeneration in mature animals is that direct transcriptional targets *of Atoh1* become epigenetically modified in supporting cells with increasing age and are rendered unavailable for transcription, even in the presence of ectopically expressed Atoh1. It is now accepted that genome-wide changes in epigenetic marks on promoters and enhancers accompany cell differentiation and maturation. In addition to DNA methylation of CpG sequences associated with transcriptional silencing, post-translational modification of histones can also render genes active or silent. In addition, many genes can be held in a transcriptionally "poised" state during development: they contain both repressive and activating histone marks and are transcriptionally silent, but can be rapidly activated by removal of the repressive epigenetic modifications. It is possible that Atoh1 targets are transcriptionally poised in neonatal supporting cells, but these targets become completely silent and associated with heterochromatin as supporting cells mature. Now that we have a panel of validated Atoh1 targets, these questions are now experimentally tractable.

Aims 2 and 3 – to activate Atoh1 in organ culture and in the intact animal by transgenic over-expression or by inhibition of Notch signaling – were been impeded for two reasons. First, we established in the course of years 1 and 2 that the Notch pathway is no longer active in the mature cochlea. We have now characterized this at the cellular and molecular level using organ cultures, gene expression analysis and RNA-seq of normal and Notch-inhibited supporting cells of different ages. We have shown beyond reasonable doubt that inhibiting the Notch signaling pathway in supporting cells from six day old mice causes almost no significant transcriptional changes at all. This suggests that any future therapies involving Notch inhibition in the inner ear are unlikely to work by themselves. Future work must now concentrate on how hair cell-specific genes are prevented from being re-activated in mature supporting cells, since they are clearly not being repressed by Notch signaling.

The second impediment to our in vivo experiments has been to generate suitable transgenic mice to over-express Atoh1 and Gfi1. We have re-targeted mouse ES cells with new targeting constructs, but our final conclusion is that another modification of the construct will be necessary to ensure that the Gfi1 protein expressed in these mice is maximally functional. Interestingly, a recent study showed that over-expression of Atoh1, Gfi1 and Pou4f3 in ES cells was sufficient to convert them into cells with some properties of hair cells. This study used a similar 2A fusion strategy to the one we have used, but in that study, Gfi1 was placed at the 5' end of the expression construct, a practice that we will adopt in the future.

6. BIBLIOGRAPHY OF PUBLICATIONS, ABSTRACTS AND PRESENTATIONS:

Maass, J.C., Gu, R., Waldhaus, J., Basch, M.L., Lopez, E.M., Wang, R., Oghalai, J.S., Heller, S. and Groves, A.K. (2015). Changes in regulation of the Notch signaling pathway contribute to regenerative failure in the mouse cochlea. *Frontiers in Cellular Neuroscience* **9,** 10. PMID 25873862

Cai, T, Jen, H.-I., Kang, H., Brown II, R.M. Klisch, T.J., Zoghbi, H.Y. and **Groves, A.K.** (2015). Characterization of the transcriptome of nascent hair cells and the identification of direct targets of the Atoh1 transcription factor. *J. Neuroscience* **35,** 5640-5654. PMID 25855195

Cai, T, Seymour, M.L., Zhang, H., Pereira, F. A. and **Groves, A.K.** (2013). Conditional deletion of Atoh1 reveals distinct critical periods for survival and function of hair cells in the organ of Corti. *J. Neuroscience* **33**, 10110-10122. PMID 23761906; PMC: 3682389

Maass, J.C., Asprer, J.S., Basch, M.L., Wan, Y.-W. and Groves, A.K.(2014). Gene Expression Profiling of Neonatal Supporting Cells by Next-Gen Sequencing. Presented at the Association for Research in Otolaryngology Mid-Winter meeting, February 2014.

LIST OF PERSONNEL WHO RECEIVED PAY FROM THE RESEARCH EFFORT, 2010-2015

Andrew K. Groves, Ph.D., Principal Investigator

Juan C. Maass, M.D., Ph.D., Postdoctoral Fellow
Eduardo Martin Lopez, Ph.D., Postdoctoral Fellow
Joanna Asprer, Ph.D., Postdoctoral Fellow

David Chung, Graduate Student

Rende Gu, M.D., Staff Scientist

Hongyuan Zhang, Research Technician

8. REPORTABLE OUTCOMES:

Informatics: We have compiled two databases of genes whose expression is enriched in hair cells by both microarray and RNA-seq. These data have been uploaded to a publicly accessible database (NCBI GEO, accession number GSE65633). We have cross-referenced these databases to extract genes in these lists that contain Atoh1-binding sites within 5kb upstream or downstream by bioinformatic interrogation with a consensus AtEAM site. We have established that the two different methods give distinct but overlapping results. We have identified over 200 Atoh1 targets and have manually validated 10 of these by ChIP-PCR. We have published two manuscripts on these findings.

ES cell production: We have generated successfully targeted ES cell lines to generate Cre-inducible forms of Atoh1 and both Atoh1 and Gfi1 simultaneously. We have also generated adenoviral expression constructs to express these genes in the organ of Corti if required.

Notch regulation in the organ of Corti: We have published one manuscript describing the cessation of Notch signaling in the organ of Corti. We have also generated RNA-seq data for genes expressed in P1 and P6 supporting cells and for supporting cell treated with DAPT; these data sets will be uploaded to NCBI GEO when a final paper describing them is published.

Development/Plasticity/Repair

Conditional Deletion of *Atoh1* Reveals Distinct Critical Periods for Survival and Function of Hair Cells in the Organ of Corti

Tiantian Cai,[1,5] Michelle L. Seymour,[3,6] Hongyuan Zhang,[1] Fred A. Pereira,[3,4,6] and Andrew K. Groves[1,2,5]

[1]Department of Neuroscience, [2]Department of Molecular and Human Genetics, [3]Department of Molecular and Cellular Biology, [4]Department of Otolaryngology–Head and Neck Surgery, [5]Program in Developmental Biology, and [6]Huffington Center on Aging, Baylor College of Medicine, Houston, Texas 77030

Atonal homolog1 (*Atoh1*) encodes a basic helix–loop–helix protein that is the first transcription factor to be expressed in differentiating hair cells. Previous work suggests that expression of *Atoh1* in prosensory precursors is necessary for the differentiation and survival of hair cells, but it is not clear whether *Atoh1* is required exclusively for these processes, or whether it regulates other functions later during hair cell maturation. We used EGFP-tagged *Atoh1* knock-in mice to demonstrate for the first time that Atoh1 protein is expressed in hair cell precursors several days before the appearance of differentiated markers, but not in the broad pattern expected of a proneural gene. We conditionally deleted *Atoh1* at different points in hair cell development and observe a rapid onset of hair cell defects, suggesting that the Atoh1 protein is unstable in differentiating hair cells and is necessary through an extended phase of their differentiation. Conditional deletion of *Atoh1* reveals multiple functions in hair cell survival, maturation of stereociliary bundles, and auditory function. We show the presence of distinct critical periods for *Atoh1* in each of these functions, suggesting that *Atoh1* may be directly regulating many aspects of hair cell function. Finally, we show that the supporting cell death that accompanies loss of *Atoh1* in hair cells is likely caused by the abortive *trans*-differentiation of supporting cells into hair cells. Together our data suggest that *Atoh1* regulates multiple aspects of hair cell development and function.

Introduction

The organ of Corti, the auditory sensory organ in mammals, comprises a precise and invariant pattern of mechanosensory hair cells and nonsensory supporting cells in the cochlea. Cochlear hair cells and supporting cells arise from a common postmitotic precursor population, the prosensory domain (Kelley, 2006). This differentiation follows a gradient, starting near the basal region of the cochlea and progressing toward the apex over a period of several days (Li and Ruben, 1979; Lim and Anniko, 1985; Chen et al., 2002; Lumpkin et al., 2003; Montcouquiol and Kelley, 2003; Kelley, 2006). *Atoh1*, the mouse homolog of the *Drosophila* proneural gene *atonal*, is a basic helix–loop–helix (bHLH) transcription factor that is the earliest known gene expressed in differentiating hair cells (Bermingham et al., 1999; Chen et al., 2002; Woods et al., 2004). In the cochlea, *Atoh1* is both necessary and sufficient for hair cell development: the absence of *Atoh1* results in a complete loss of hair cells (Bermingham et al., 1999), while ectopic expression of *Atoh1* is sufficient to direct ectopic hair cell formation in the greater epithelial ridge, the nonsensory epithelium next to the organ of Corti (Zheng and Gao, 2000). In *Atoh1*-null mice, massive cell death is observed within the presumptive sensory epithelia at the base of the cochlea at embryonic day (E) 15.5. Later, the apoptosis progresses to the whole cochlear duct (Chen et al., 2002). Transient expression of *Atoh1* in mice in which Atoh1 is conditionally deleted by an *Atoh1-Cre* transgene is not sufficient to prevent the majority of hair cells from dying and cannot support the proper function of the remaining hair cells (Pan et al., 2012), indicating the level and duration of *Atoh1* expression is critical for maintaining the viability and differentiation of hair cells. However, it remains unclear whether there is a critical period for *Atoh1* to keep hair cells alive and whether *Atoh1* functions differently at later stages of hair cell development. A recent genome-wide survey of *Atoh1* target genes in the cerebellum suggested that *Atoh1* regulates a broad range of biological processes, including cell proliferation, differentiation, migration, and metabolism (Klisch et al., 2011). The variety of pathways *Atoh1* might regulate during cerebellar

Received Dec. 5, 2012; revised May 7, 2013; accepted May 11, 2013.

Author contributions: T.C., M.L.S., and A.K.G. designed research; T.C., M.L.S., and H.Z. performed research; T.C., M.L.S., F.A.P., and A.K.G. analyzed data; T.C., M.L.S., F.A.P., and A.K.G. wrote the paper.

This work was supported by National Institutes of Health (NIH) Grants DC006185 (A.K.G.), Department of Defense Grant W81XWH1020116 (A.K.G.), a training fellowship from the Houston Laboratory and Population Sciences Training Program in Gene–Environment Interaction (T.C.), National Research Service Award Grant F31DC012503 (M.L.S.), and NIH Grant DC000354 (F.A.P.). We thank Alyssa Faught and Huiling Li for excellent technical assistance, members of the Groves laboratory for helpful discussions, and Kurt Chonko and Steven Maricich for discussing data and exchanging ideas before publication. We thank Matt Kelley and Tom Coate for a gift of Atoh1 antibody, Jim Bartles for a gift of anti-espin antibody, and Kenneth Johnson for a gift of anti-TMHS antibody. The Myo7a 138-1 monoclonal antibody developed by Dana Orten and Tama Hasson was obtained from the Developmental Studies Hybridoma Bank developed under the auspices of the National Institute of Child Health and Human Development and maintained by the University of Iowa, Department of Biology. We are extremely grateful to Huda Zoghbi for providing mouse lines, for her suggestions for experimental design, and her comments on the manuscript.

Correspondence should be addressed to Andrew Groves, Baylor College of Medicine, BCM295, 1 Baylor Plaza, Houston, TX 77030. E-mail: akgroves@bcm.edu.

DOI:10.1523/JNEUROSCI.5606-12.2013

 0270-6474/13/3310110-13$15.00/0

development suggests that *Atoh1* might be involved in multiple developmental processes in hair cells as well.

To dissect the function of *Atoh1* during hair cell development, we established a conditional knockout (CKO) system to delete *Atoh1* at specific developmental stages. By exposing pregnant or neonatal mice to tamoxifen to activate Cre-mediated recombination driven by an *Atoh1* autoregulatory enhancer (*Atoh1-CreER^{T2}*), we deleted *Atoh1* from hair cells at different embryonic and neonatal stages. We found a critical time window, ~2 d after initiation of *Atoh1* expression, in which *Atoh1* is absolutely required for hair cell survival. *Atoh1* deletion within this time window also led to the loss of the surrounding supporting cells, and we used a Cre reporter allele to show that some of these supporting cells attempt to upregulate *Atoh1* in response to hair cell loss. Significantly, later deletion of *Atoh1* also revealed a time-dependent requirement for its activity in hair bundle maturation and auditory function. Together, our data suggest *Atoh1* has multiple functions in the survival, differentiation, and maturation of hair cells during cochlear development.

Materials and Methods

Experimental animals. Atoh1 $^{-/-}$ [Mouse Genome Informatics (MGI): *Atoh1^{tm1Hzo}*], *Atoh1$^{A1GFP/A1GFP}$* (MGI: *Atoh1$^{tm4.1Hzo}$*), and *Atoh1$^{flox/flox}$* (MGI: *Atoh1^{tm3Hzo}*) mice were generated as previously described (Ben-Arie et al., 1997; Shroyer et al., 2007; Rose et al., 2009). *Atoh1- CreER^{T2}* [MGI: *Tg(Atoh1-cre/Esr1*)14Fsh*] (Machold and Fishell, 2005) and *R26R-YFP* [MGI: *Gt(ROSA)26Sor$^{tm1(EYFP)Cos}$*] (Srinivas et al., 2001) transgenic lines were obtained from Jackson Laboratories. Genotyping was performed by PCR using the following primers: for different *Atoh1* alleles, Atoh1-forward (ACG CAC TTC ATC ACT GGC), Atoh1-reverse (GGC ACT GGC TTC TCT TGG), and Neo-forward (GCA TCG CCT TCT ATC GCC) yield a 600 bp wild-type allele band and a 400 bp null allele band. HA-forward (GCG ATG ATG GCA CAG AAG G) and HA-reverse (GAA GGG CAT TTG GTT GTC TCA G) yield a 1 kb *Atoh1* EGFP-tagged allele band and a 350 bp floxed allele band. For *Atoh1-CreER^{T2}*, Cre1F (GCC TGC ATT ACC GGT CGA TGC AAC GA) and Cre1R (GTG GCA GAT GGC GCG GCA ACA CCA TT) yield a 700 bp band. For R26R-YFP, oIMR0316 (GGA GCG GGA GAA ATG GAT ATG), oIMR0883 (AAA GTC GCT CTG AGT TGT TAT) and oIMR4982 (AAG ACC GCG AAG AGT TTG TC) yield a 320 bp yellow fluorescent protein-positive (YFP+) band. To generate the inducible *Atoh1* CKO mice, *Atoh1-CreER^{T2}*; *Atoh1* $^{+/-}$ males were crossed with *Atoh1$^{flox/flox}$*; *R26R-YFP* homozygous females. One dose of 2 mg tamoxifen and 2 mg progesterone was administered to pregnant females at E15.5, E16.5, or E17.5 by oral gavage. Tamoxifen and progesterone were dissolved together in peanut oil, both at a concentration of 20 mg/ml. For delivering tamoxifen into newborn animals, tamoxifen was dissolved in peanut oil at a concentration of 10 mg/ml and subcutaneously injected into animals at a dose of 75–100 μg/g body weight. The genotypes of embryos or newborn pups from these crosses were determined as above. The Baylor College of Medicine Institutional Animal Care and Use Committee approved all animal experiments.

Cochlea isolation. Cochleas from E13.5 to E16.5 embryos were dissected in PBS and then incubated in calcium-magnesium-free PBS containing dispase (1 mg/ml; Invitrogen) and collagenase (1 mg/ml; Worthington) for 8 min at room temperature. The enzyme solution was then replaced by DMEM containing 10% FBS and the mesenchymal tissue was removed by fine syringes to free the cochlear duct. For neonatal pups, cochleas were dissected in PBS, with the spiral ganglia and Reissner's membrane removed to expose the organ of Corti. To obtain adult cochlear whole-mount preparations, temporal bones were dissected and the cochleas were slowly perfused through the oval window with 4% paraformaldehyde (PFA) in PBS, postfixed for 2 h at room temperature, and decalcified in 150 mM EDTA for 5–7 d at 4°C before further dissection.

Immunohistochemistry. Primary antibodies used in this study were anti-active Caspase 3 (1:500, rabbit; R&D Systems), anti-GFP (1:1000, chicken; Abcam; this detects GFP, EGFP, and YFP), anti-Hey2 (1:500, rabbit; Doetzlhofer et al., 2009), anti-Jag1 (1:200, rabbit; Santa Cruz Biotechnology), anti-Myosin6 (1:500, rabbit; Proteus), anti-Myosin7a (1:100, mouse; Developmental Studies Hybridoma Bank), anti-p27^{kip1} (1:250, mouse; NeoMarker), anti-Prox1 (1:500, rabbit; Millipore Bioscience Research Reagents), anti-Sox2 (1:500, rabbit; Millipore), anti-Sox10 (1:250, goat; Santa Cruz Biotechnology), anti-β tubulin (TuJ1, 1:1000, mouse; Covance), anti-TMHS (tetraspan transmembrane protein of hair cell stereocilia) (1:1000, rabbit; a gift from Kenneth Johnson; Longo-Guess et al., 2005), anti-espin (1:1000, rabbit; gift from Jim Bartles; Sekerkov á et al., 2004), and anti-Atoh1 (1:10,000, chick; a gift from Matthew Kelley and Thomas Coate; Driver et al., 2013). Secondary antibodies were Alexa 488, Alexa 594, or Alexa 647 (1:2000; Invitrogen). Actin in stereociliary bundles was labeled with Alexa 594-conjugated phalloidin (1:1000, Invitrogen). Cell nuclei were labeled by DAPI. For sections of ear tissue, animal heads were fixed 1–2 h in 4% PFA at room temperature, cryoprotected in 30% sucrose in PBS at 4°C, embedded in OCT compound, and cryosectioned at 12–14 μm. The immunohistochemistry procedure followed standard protocols with some minor modifications. For anti-Atoh1 staining, tissue was fixed in 4% paraformaldehyde for 30 min before sectioning, and sections were blocked in PBS containing 0.5% Triton X-100, 10% goat serum, and 10% Henblocker (Aves Labs). For anti-p27^{kip1}, Jag1, and Sox2 staining, sections were boiled for 10 min in 10 mM citric acid, pH 6.0.

Uptake of FM1-43. FM1-43 (Invitrogen) was prepared in water at a stock concentration of 5 mM. Cochleas were dissected from postnatal day (P) 5 mouse pups and briefly rinsed in HBSS (Invitrogen). Cochleas were exposed to a 5 μM solution of FM1-43 in HBSS for 15 s before being washed several times, mounted, and viewed with fluorescence microscopy.

Auditory brainstem response recording. Before testing, mice were anesthetized by intraperitoneal injection of a ketamine–xylazine mix at a dose of 100 mg/kg ketamine and 10 mg/kg xylazine. Testing was performed in a soundproof booth. Normal body temperature was maintained throughout the procedure by placing the mice on a heating pad. Pure tone bursts (0.1 ms rise/fall, 2 ms duration, 21 presentations/s) from 4 to 48 kHz were generated using System 3 digital signal processing hardware and software (Tucker Davis Technologies). The intensity of the tone stimuli was calibrated using a type 4938 one-quarter inch pressure-field calibration microphone (Brüel & Kjær). EC1 ultrasonic, low-distortion electrostatic speakers were coupled to the ear canal to deliver stimuli within 3 mm of the tympanic membrane. Response signals were recorded with subcutaneous needle electrodes inserted at the vertex of the scalp (channel 1), the postauricular bulla region (reference), and the back leg (ground), and averaged over 500 presentations of the tone bursts. Electrode-recorded activity was filtered (high pass, 300 Hz; low pass, 3kHz; notch, 60Hz) before averaging to minimize background noise. Auditory thresholds were determined by decreasing the sound intensity of each stimulus to 10 dB from 90 dB in 5 dB steps until the lowest sound intensity with reproducible and recognizable waveforms was detected. Thresholds were determined to within 5 dB for each frequency by two raters to ensure reliability. Mean hearing thresholds ± SD (dB SPL) were plotted as a function of stimulus frequency (kilohertz) and analyzed for group differences at individual frequencies using two-tailed *t* tests accompanied by a one-way ANOVA to reveal overall trends. R (version 2.13) was used for all statistical analyses.

Results

Atoh1 protein marks hair cell precursors during mouse cochlear development

The organ of Corti differentiates from a band of prosensory cells that runs along the length of the cochlear duct (Kelley, 2007; Kelly and Chen, 2009). This prosensory domain begins to exit the cell cycle in mice at E12.5, starting at the apex of the cochlea. Over the next 2–3 d, cell cycle exit proceeds along the cochlea from the apex to the base (Ruben, 1967; Lee et al., 2006). The differentiation of this postmitotic precursor domain into hair cells and supporting cells begins between E13 and E14, starting close to the

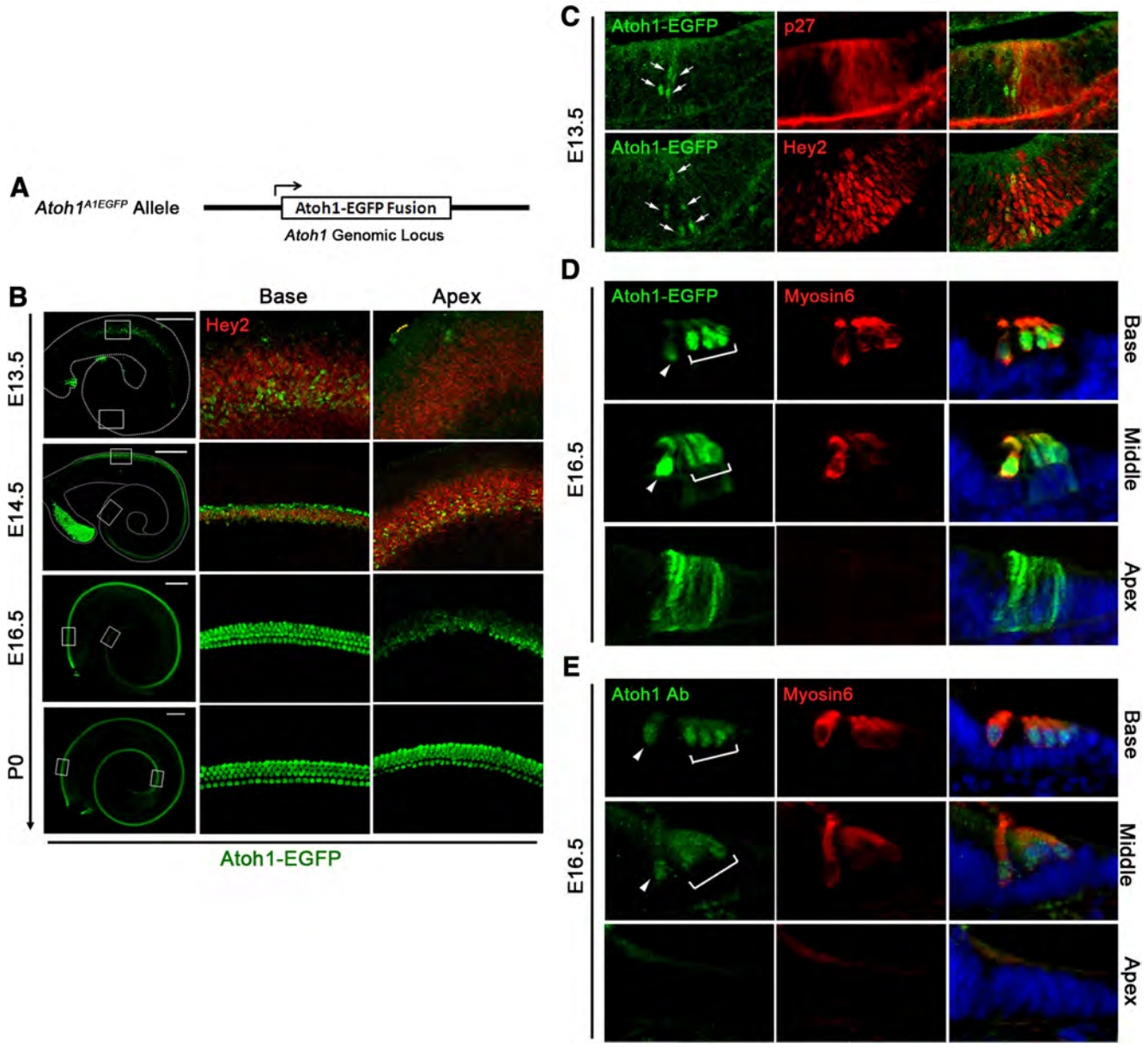

Figure 1. Atoh1 protein expression in the mouse cochlea. ***A***, Schematic diagram of the *Atoh1*$^{A1GFP/A1GFP}$ knock-in mouse line, referred to in the figure as Atoh1-EGFP. An *Atoh1-EGFP* fusion gene was targeted to the *Atoh1* genomic locus. ***B***, Whole-mount *Atoh1*$^{A1GFP/A1GFP}$ cochleas from E13.5 to P0. The right two rows show higher magnification of the base and apex regions marked by box at the left. Hey2 (red) was used to mark the prosensory domain at E13.5 and E14.5. Scale bars, 200 μm. ***C***, Sections of *Atoh1*$^{A1GFP/A1GFP}$ cochlea at E13.5. Scattered EGFP-labeled cells (arrows) were localized within the prosensory domain labeled by p27^{kip1} and Hey2. ***D***, Sections through different regions of E16.5 *Atoh1*$^{A1GFP/A1GFP}$ cochlea. Hair cells were labeled by Myosin6 (red). Hair cell differentiation begins near the base of the cochlea and spreads down to the apex over a period of days. Sections through the base, middle turn, and apex of the cochlea at E16.5 therefore reveal different stages in the differentiation of hair cell precursors. In the base, most Atoh1-EGFP protein is localized in the nucleus of Myosin6-expressing hair cells. However, in the apex, much cytoplasmic Atoh1-EGFP protein can be observed in precursors that have not yet expressed Myosin6. ***E***, An Atoh1 antibody also reveals nuclear staining in hair cells in the base of the cochlea, more cytoplasmic staining in the middle turn of the cochlea, but no detectable staining in the apex. Arrowhead, inner hair cells; bracket, outer hair cells.

base of the cochlea and spreading along the length of the cochlea to the apex over the next 4 d (Li and Ruben, 1979; Lim and Anniko, 1985; Chen et al., 2002; Montcouquiol and Kelley, 2003). At intermediate times, different regions of the cochlea are therefore at different stages of differentiation. For example, at E16, the basal region of cochlea contains a full complement of one row of inner hair cells and three rows of outer hair cells as revealed by the hair cell marker Myosin6, while at the apex of the cochlea, no Myosin6-expressing hair cells can be detected (Fig. 1*D*). In the middle regions of the cochlea, the first inner hair cells can be observed differentiating, but their neighboring outer hair cells and associated supporting cells have yet to differentiate. Thus, different regions of the cochlea contain hair cells or their precursors at different stages of differentiation.

Atoh1 is one of the first genes expressed in differentiating hair cells and is both necessary and in some circumstances sufficient for their differentiation (Bermingham et al., 1999; Zheng and Gao, 2000). However, the onset of *Atoh1* expression in the cochlea has been hard to visualize accurately, with different techniques giving different results. For example, using a β-gal reporter knocked in to the *Atoh1* locus, Woods et al. showed that *Atoh1* promoter activity can be observed in a wide patch of cells along most of the cochlear duct at E13 (Woods et al., 2004), suggesting *Atoh1* is a marker of hair cell and supporting cell pre-

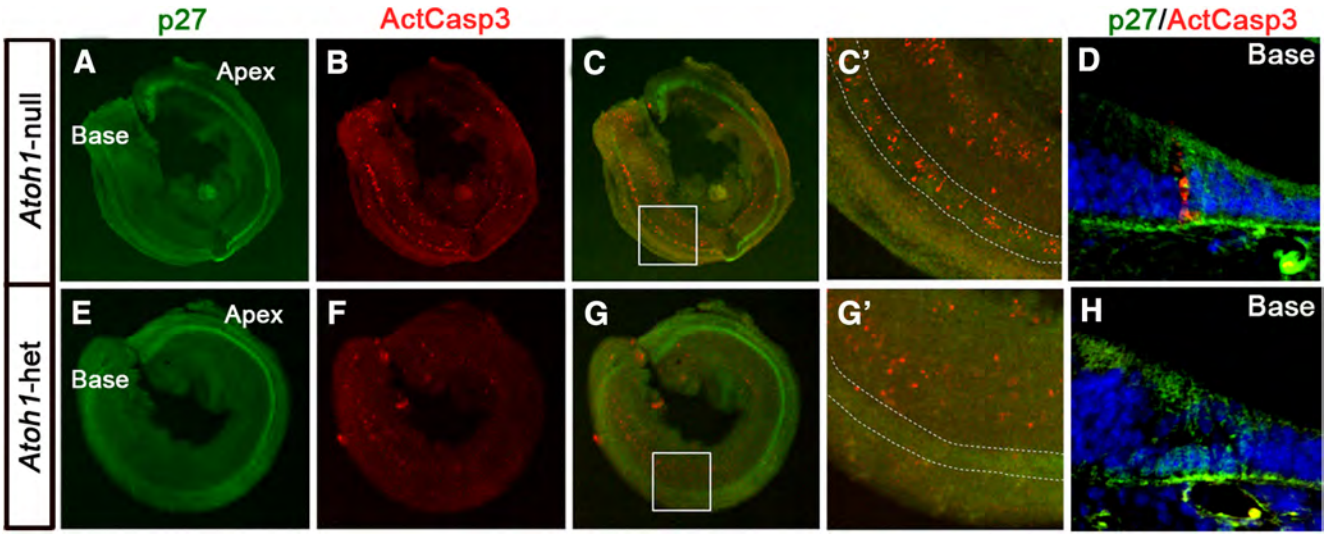

Figure 2. Precursor cells in the sensory epithelia start to undergo apoptosis at E15.5 in the *Atoh1*-null (−/−) mice. ***A–C***, ***E–G***, Whole-mount cochleas from E15.5 *Atoh1*-null (***A–C***) and *Atoh1* heterozygous (***E–G***) littermates. $p27^{kip1}$ (green) marks the prosensory epithelial region. ActCasp3 (red) labels apoptotic cells in the prosensory epithelium of the *Atoh1*-null cochlea. ***C'***, ***G'***, Higher-power magnifications of the midbasal region of the cochlea marked by box in ***C*** and ***G***, respectively. The dotted lines highlight the prosensory epithelium. ***D***, ***H***, Sections of the basal cochlea at E15.5. ActCasp3 (red) staining was only observed in the *Atoh1* mutants (***D***) but not their heterozygous littermates (***H***).

cursors in the prosensory epithelium. Such a pattern of expression would be consistent with *Atoh1* functioning as a proneural gene. To clarify the expression pattern of Atoh1 protein in the mouse cochlea, we made use of $Atoh1^{A1GFP/A1GFP}$ knock-in mice, in which the endogenous *Atoh1* gene is tagged with EGFP (Fig. 1*A*; Rose et al., 2009). Homozygous $Atoh1^{A1GFP/A1GFP}$ mice are viable, breed normally, and exhibit no observable phenotype in any organ (Rose et al., 2009). We used these mice to visualize Atoh1 protein by staining with antibodies against EGFP together with markers of the prosensory domain and hair cells.

The earliest stage at which we could detect Atoh1-EGFP expression in the $Atoh1^{A1GFP/A1GFP}$ cochlea was E13.5 (Fig. 1*B*,*C*). In whole-mount preparations of the E13.5 cochlea, we observed expression of EGFP in a diffuse, salt-and-pepper patch of cells in the midbasal region, localized within the prosensory domain marked by the transcription factor Hey2 (Fig. 1*B*) (Hayashi et al., 2008; Doetzlhofer et al., 2009). We did not observe broad domains of Atoh1 protein expression in sections of the $Atoh1^{A1GFP/A1GFP}$ cochlea. Instead, cells expressing Atoh1-EGFP frequently lined up in columns in the sensory epithelium or existed as single cells (Fig. 1*C*). Costaining with $p27^{kip1}$ and Hey2 indicated that these columns or isolated EGFP-labeled cells localized within the prosensory domain on its neural side (Fig. 1*C*). This arrangement of the earliest Atoh1-expressing cells in the $Atoh1^{A1GFP/A1GFP}$ cochlea was consistent with previous immunohistochemical studies using anti-Atoh1 antibodies (Chen et al., 2002; Driver et al., 2013). However, the higher sensitivity of the anti-EGFP antibody in our study suggests that the onset of Atoh1 protein expression in the mouse cochlea begins as early as E13.5.

At E16.5 in the basal cochlea, Atoh1-EGFP protein was restricted to hair cells that express the early hair cell differentiation marker Myosin6, forming one row of inner hair cells and three rows of outer hair cells (Fig. 1*D*). However, in the middle turn region, where Myosin6 is just beginning to be expressed in outer hair cells, Atoh1-EGFP was expressed in columns of cells spanning the sensory epithelium. This pattern of EGFP-expressing cells was also seen in the apex of E16.5 cochlea, where there were no signs of Myosin6 expression (Fig. 1*D*). This suggests that Atoh1 is expressed in a subset of postmitotic precursors within the cochlear sensory primordium, before the differentiation of hair cells. As differentiation proceeds, Atoh1 becomes restricted to Myosin6-labeled hair cells (Fig. 1*D*). Intriguingly, we observed that Atoh1-EGFP expression in hair cells in the basal third of the cochlea was largely restricted to the nucleus. However, in the middle turn and apical regions that contain Myosin6-negative hair cell precursors at earlier stages of differentiation, EGFP was diffusely localized throughout the cell cytoplasm (Fig. 1*D*). These changes in subcellular distribution of Atoh1 protein between precursors and differentiating hair cells suggests there is a redistribution of cytosolic Atoh1 or an active transport of Atoh1 protein from the cytoplasm into the nucleus during hair cell differentiation.

It is possible that the cytoplasmic localization of the Atoh1-EGFP fusion protein in hair cell precursors is a consequence of the EGFP tag. To test this, we stained E16.5 cochlear sections with a recently described chicken antibody to the Atoh1 protein (Driver et al., 2013). Although the staining we observed with this antibody was significantly fainter than that seen with the Atoh1-EGFP fusion protein and absent at the apex of the cochlea, we were able to observe a diffuse cytoplasmic staining in middle turn regions of the cochlea, with nuclear staining becoming more distinct in the most basal regions of the cochlea (Fig. 1*E*).

Cell death in the prosensory domain of *Atoh1* mutant mice

Genetic inactivation of *Atoh1* in mice results in the death of a subpopulation of cells in the prosensory domain and a consequent failure of hair cell formation (Chen et al., 2002; Pan et al., 2011, 2012). To examine the time of onset of the apoptosis in detail, we performed immunohistochemistry on whole-mount *Atoh1*-null ($Atoh1^{-/-}$; Bermingham et al., 1999) cochleas at different stages, using antibody against the active form of Caspase3 (ActCasp3). No apoptotic cells were observed in the prosensory domain of the *Atoh1*-null cochlea at E14.5 (data not shown), but we observed many ActCasp3-labeling cells at the base of E15.5 cochleas (Fig. 2*A*–*C*'). Staining of the cochlear sections showed the dying cells were located within the sensory epithelial region labeled by $p27^{kip1}$ (Fig. 2*D*). These data suggest there is an ~48 h delay between the time at which Atoh1 protein expression would

normally initiate in the cochlea and the death of hair cell precursors in the absence of *Atoh1*.

A transgenic mouse system to conditionally delete *Atoh1*

Our immunohistochemistry data from *Atoh1*$^{A1GFP/A1GFP}$ cochleas suggest *Atoh1* expression is sustained in cochlear hair cells for at least a week after hair cell differentiation. We next asked whether *Atoh1* is continuously required for the survival of hair cells after differentiation has begun. We established a CKO system to remove *Atoh1* from hair cells at different stages using the inducible Cre-lox system. We crossed *Atoh1*$^{+/-}$; *Atoh1-CreER*^{T2} males with *Atoh1*$^{flox/flox}$; *R26R-YFP* female mice. By oral gavage of the pregnant females or injecting mouse pups subcutaneously with tamoxifen, we were able to generate *Atoh1* CKO (*Atoh1*$^{flox/-}$; *Atoh1-CreER*^{T2}; *R26R-YFP*) and control (*Atoh1*$^{flox/+}$; *Atoh1-CreER*^{T2}; *R26R-YFP*) animals (Fig. 3*A*). One advantage of this system is that the *R26R-YFP* reporter provides a clear visualization of the Cre recombination efficiency in the cochlea and reveals cells in which *Atoh1* has been deleted. The system displayed almost no recombination in the absence of tamoxifen. Figure 3*B* shows regions from a neonatal *Atoh1*$^{flox/+}$; *Atoh1-CreER*^{T2}; *R26R-YFP* mouse that had not been exposed to tamoxifen. No YFP can be seen in either apical or basal regions of the cochlea; we typically saw one YFP-labeled cell in every five cochleas from untreated control mice. Moreover, we saw no evidence of YFP-labeled supporting cells in control animals treated with tamoxifen at any age between E15.5 and P2 (data not shown).

Tamoxifen-mediated recombination occurred rapidly in our CKO system. Figure 3*C* shows examples of embryos in which tamoxifen was administered at E17.5 and the animals killed 8, 24, or 48 h later. We could readily detect YFP expression in the embryonic cochleas 8 h after tamoxifen treatment. After 24 h, >80% of hair cells in the base of the cochlea were labeled with YFP. At the apex, which contains less mature hair cells, fewer (50%) hair cells were labeled by Cre recombination, but by 48 h, similar numbers (80–85%) of YFP-labeled cells could be seen in both apical and basal regions.

Atoh1 expression is gradually downregulated in cochlear hair cells in the first few days after birth, commencing at the base of the cochlea and finally being extinguished at the apex several days later. For example, at P0, Atoh1 is being downregu-

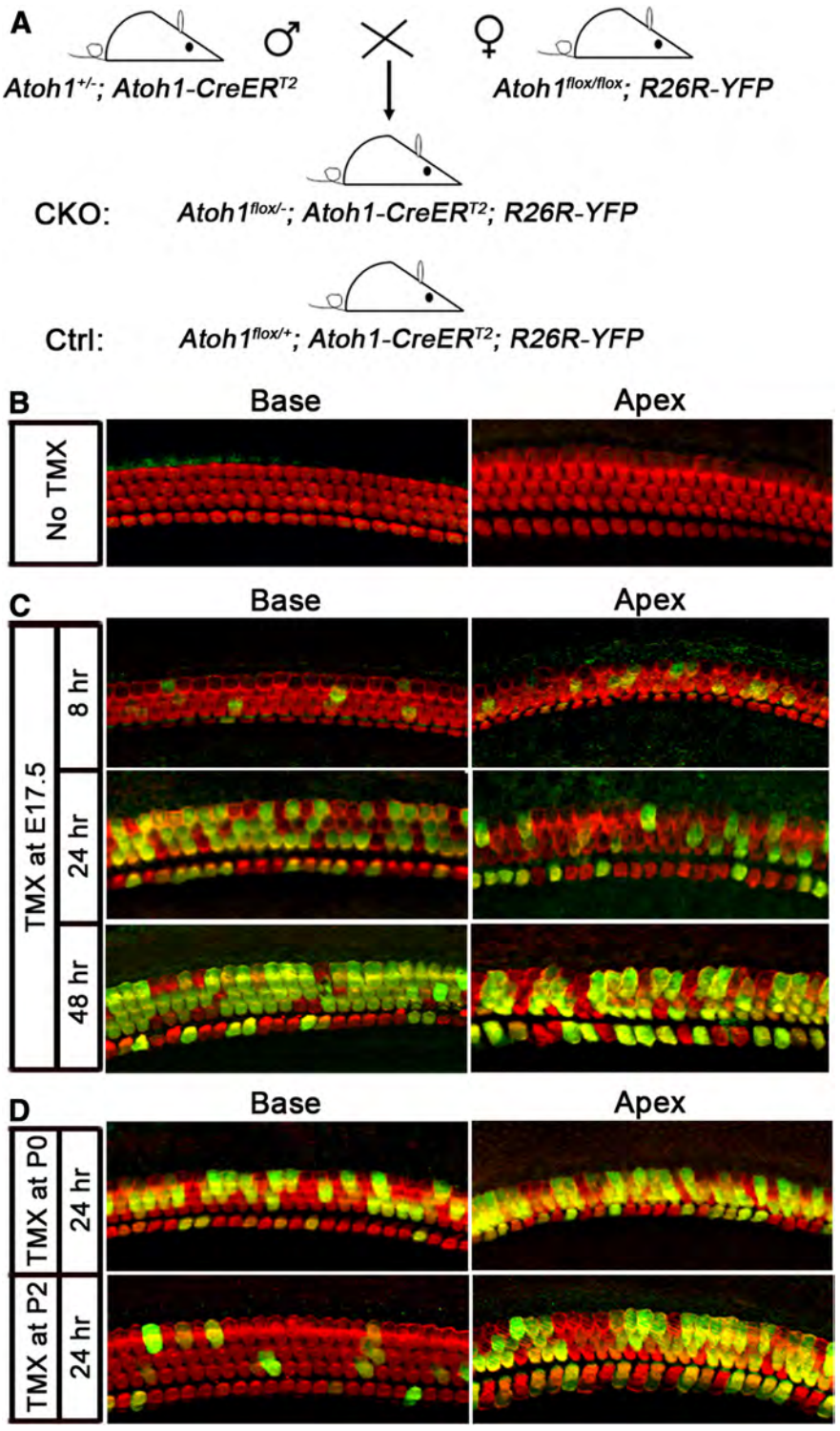

Figure 3. ***A***, Breeding scheme to generate *Atoh1*-CKO mice. Female *Atoh1*$^{flox/flox}$; *R26R-YFP* mice were mated with *Atoh1*$^{+/-}$; *Atoh1-CreER*^{T2} males to generate mice that carried the *CreER*^{T2} allele, one copy of the *R26R-YFP* Cre reporter, and either an *Atoh1*$^{flox/+}$ (50%) or *Atoh1*$^{flox/-}$ (50%) allele. Use of the *R26R-YFP* Cre reporter provides a readout of the leakiness, speed, and efficiency of the system. ***B***, The base and apex of a cochlea from a P3 *Atoh1*$^{flox/-}$; *Atoh1-CreER*^{T2}; *R26R-YFP* mouse whose mother did not receive tamoxifen during pregnancy. No YFP-labeled cells can be detected in either region of the cochlea, and we typically observed an average of 1 YFP+ cell in every five cochleas examined. ***C***, The base and apex of cochleas from *Atoh1*$^{flox/+}$; *Atoh1-CreER*^{T2}; *R26R-YFP* mice whose mothers received a single dose of tamoxifen (TMX) at E17.5. The embryos were collected 8, 24, and 48 h after tamoxifen dosing. A small number of YFP cells can be observed in both base and apex after 8 h. After 24 h, significantly more labeled cells can be observed in the base, in which hair cells differentiate first, compared with the apex. After 48 h, similar numbers of YFP-labeled cells (80–85%) are present in both regions of the cochlea. ***D***, The *Atoh1-CreER*^{T2} transgene remains active until at least 2 d after birth. Neonatal pups were injected with tamoxifen at either P0 or P2 and allowed to develop for 24 h. After birth, Atoh1 starts to be downregulated from the cochlea, starting at the base and proceeding down to the apex. Consequently, significantly fewer YFP-labeled cells can be seen in the base at both ages, but ~50% YFP+ cells are seen in the apex.

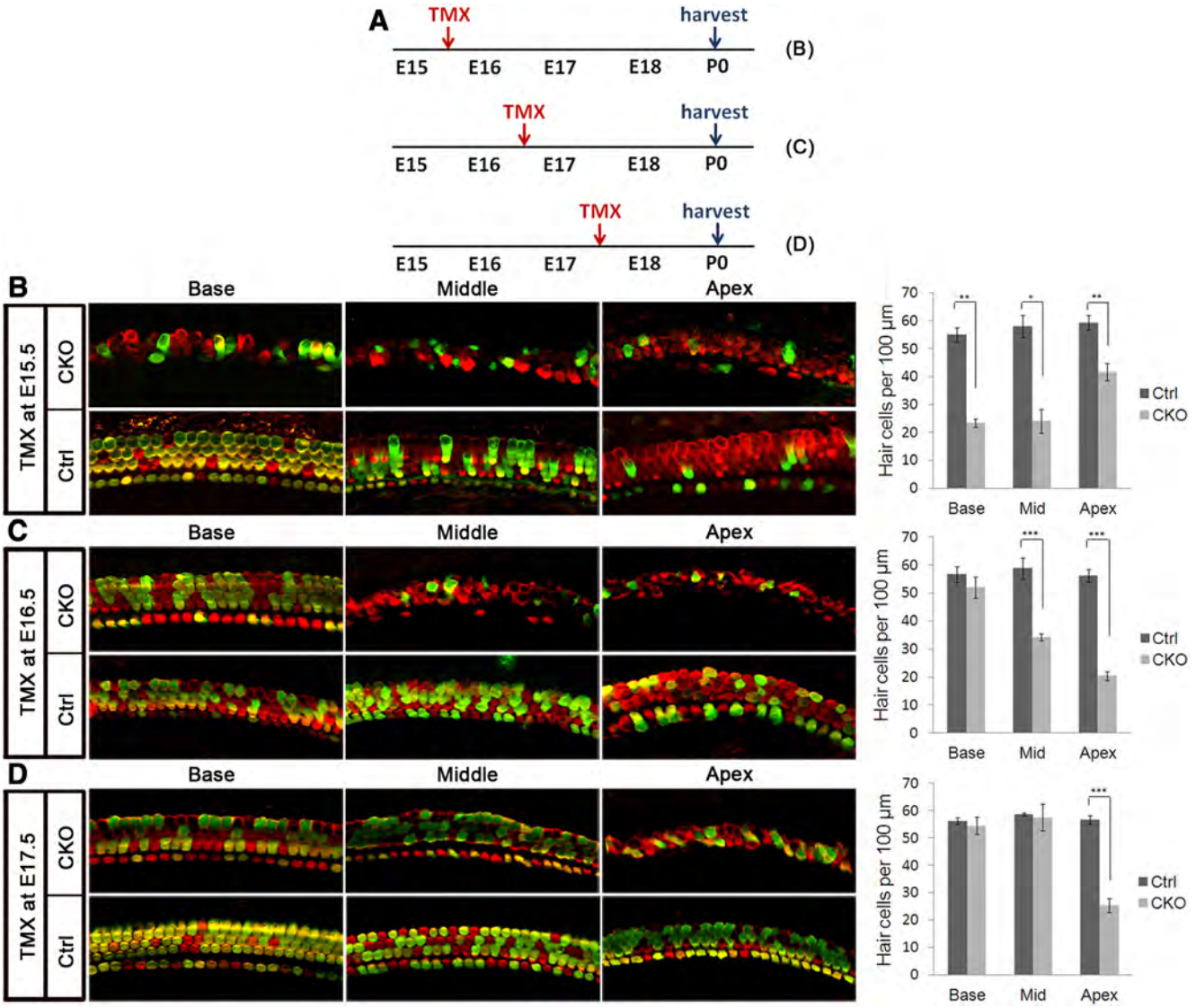

Figure 4. *Atoh1* is required for the survival of hair cells in a time-dependent manner. ***A***, Diagram showing the experimental design for the analysis of *Atoh1*-CKO cochleas in ***B–D***. Female *Atoh1*$^{flox/flox}$; *R26R-YFP* mice were mated with *Atoh1*$^{+/-}$; *Atoh1-CreER*^{T2} males and received a single dose of tamoxifen (TMX) at E15.5, E16.5, or E17.5. Mouse pups were analyzed on the day of birth (P0). ***B–D***, Different regions of whole-mount cochleas from P0 *Atoh1*-CKO and control littermates in which one dose of tamoxifen was administered at E15.5 (***B***), E16.5 (***C***), and E17.5 (***D***). YFP (green) was used as a reporter to show Cre-mediated recombination. Red, Myosin6-labeled hair cells. The number of hair cells in both CKO and control cochleas is quantified and shown in the graphs at the right ($n \geq 3$, error bars show SD).

lated in the base of the cochlea and is strongly expressed in the apex. Accordingly, when tamoxifen was injected into P0 pups, we saw few YFP-labeled cells in the base of the cochlea but many more (~50%) in the apex (Fig. 3*D*). We continued to see ~50% labeled cells in the apical third of the cochlea when tamoxifen was administered at P2 (Fig. 3*D*), suggesting that the *Atoh1-CreER*^{T2} allele is still active at this time.

Identification of a critical period for *Atoh1* function in hair cell survival

To test whether there is a critical time window for *Atoh1* to maintain the survival of hair cells, we delivered one dose of tamoxifen to pregnant females at three stages, E15.5, E16.5, or E17.5 (Fig. 4*A*). Animals were allowed to develop to the day of birth (P0), when offspring were genotyped and the cochleas collected from both CKO and control animals (Fig. 4*A*). We labeled and counted hair cells in whole-mount cochlea preparations using anti-Myosin6 antibodies and detected cells in which Atoh1 had been deleted by visualizing the YFP reporter (Fig. 3*A*). As described above, hair cell differentiation in the cochlea follows a basal-to-apical gradient, in which differentiation at the apex starts ~3 d later than at the base (Li and Ruben, 1979; Lim and Anniko, 1985; Chen et al., 2002; Montcouquiol and Kelley, 2003). We therefore divided each cochlea into three parts along the length of the cochlear duct (base, middle turn, and apex) and quantified the hair cells in each region separately. When tamoxifen was administered at E15.5, hair cell numbers were significantly reduced along the entire length of CKO cochleas (Fig. 4*B*) compared with controls. When tamoxifen was administered at E16.5, we observed significant loss of hair cells in the middle turn to apical parts of the CKO cochleas, but not at the base (Fig. 4*C*), where hair cells are more mature. When tamoxifen was administered at E17.5, significantly reduced numbers of hair cells were only observed in the apex of the CKO cochleas (Fig. 4*D*). We examined the timing of cell death in the sensory epithelia by labeling the cochleas with antibodies to ActCasp3. In the CKO

cochleas, we first observed apoptotic cells 20 h after tamoxifen treatment, with large numbers of dying cells observed by 24 h (see Fig. 8*A*). Since we first detect recombination in our mice 8 h after tamoxifen administration (Fig. 3*C*), this suggests that Atoh1 protein is unstable and that loss of Atoh1 from differentiating hair cells causes rapid cell death. Moreover, since hair cells mature in a basal–apical gradient along the cochlea starting at E13.5, our data suggest that Atoh1 is required for the survival of hair cell precursors in the base of the cochlea for 72 h after the first appearance of Atoh1 protein, but that deletion of *Atoh1* after this critical period (for example, at E16.5 or later in the base of the cochlea) does not compromise hair cell survival.

Identification of a second critical period for *Atoh1* in hair cell function

We next addressed whether surviving hair cells in the *Atoh1* CKO cochlea retain any aspects of normal structure or function. We tested the effect of *Atoh1* deletion on hair bundle structure by staining the actin-rich stereocilia with fluorescently labeled phalloidin. Administration of tamoxifen at E17.5 causes hair cell loss in the apex, but not in the midregion or basal region (Fig. 4*D*). In these animals, we observed disorganized hair bundles in both in the middle turn (where hair cell numbers were normal) and in the apical regions of the cochlea (which show significant hair cell loss; Fig. 5*A*). We did not observe abnormal hair bundle structure in the basal, more mature hair cells of CKO cochleas (Fig. 5*A*). We saw similar results with antibodies to the hair bundle proteins Espin (Sekerkov á et al., 2004; Fig. 5*B*) and TMHS (Longo-Guess et al., 2005; data not shown). We also examined cochleas in which we delivered tamoxifen to neonatal pups at P0, and only observed very subtle defects at the apex of the CKO organs (Fig. 5*A*). These data suggest that *Atoh1* plays an additional role in hair bundle development as well as in regulating hair cell survival. Since deletion of *Atoh1* at E17.5 can cause hair cell defects without hair cell death, this suggests that there is a second delayed critical period for *Atoh1* in the regulation of hair bundle morphology independent of cell survival.

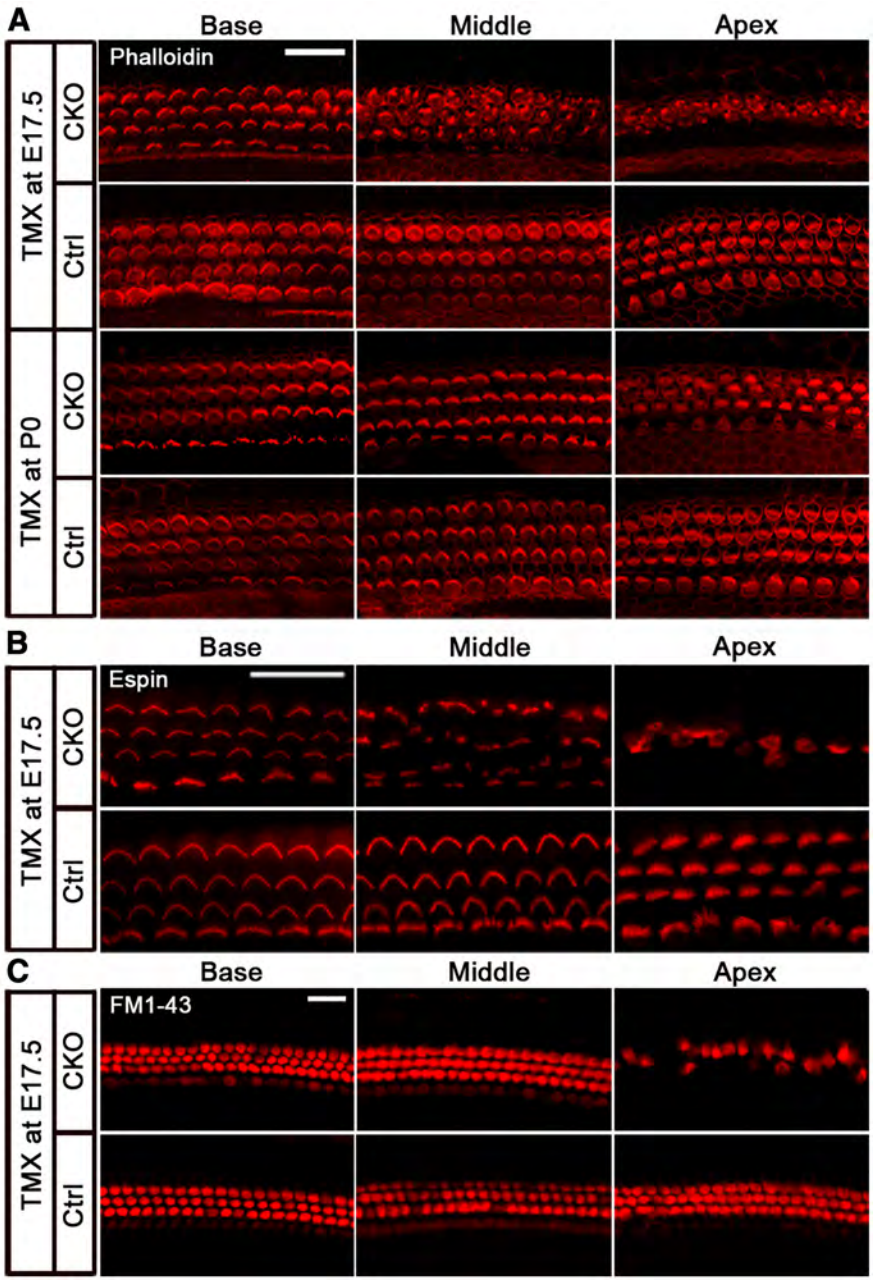

Figure 5. *Atoh1* is required for stereociliary bundle development in hair cells. ***A***, Phalloidin staining of different regions of whole-mount cochlea preparations from P2 *Atoh1*-CKO and control littermates. One dose of tamoxifen administration at E17.5 resulted in disorganized hair bundles in the middle and apical turns of CKO cochleas, but no defects in the more mature hair cells in the basal region. However, only very subtle defects in hair bundles were observed in the apical cochlea of CKO animals that received one dose of tamoxifen at P0. This suggests that Atoh1 is initially required for hair cell survival, but later for other functions, including hair bundle morphology ***B***, Whole-mount cochleas from *Atoh1*-CKO and control animals receiving one dose of tamoxifen at E17.5 and stained with anti-espin antibodies at P2. ***C***, Whole-mount cochleas from *Atoh1*-CKO and control animals receiving one dose of tamoxifen at E17.5 and then dissected at P5 and exposed to 5 μM of the styryl dye FM1-43 for 15 s to detect dye uptake through mechanotransduction channels. Surviving hair cells from apical regions of the cochlea displaying abnormal bundle morphology (***A***, ***B***) still take up FM1-43. Scale bars, 20 μm. TMX, tamoxifen.

To determine whether *Atoh1* can influence assembly of the mechanotransduction machinery in hair cell stereociliary bundles, we labeled living cochleas with FM1-43, a fluorescent styryl dye that can rapidly enter hair cells through open mechanotransduction channels (Meyers et al., 2003; Lelli et al., 2009). We administered tamoxifen at E17.5 and let the mice develop for 5 d after birth. Dissected cochleas were then bath-exposed to FM1-43 for 15 s and then washed and examined for FM1-43 fluorescence. We detected dye uptake in hair cells all along the CKO cochleas regardless of bundle morphology, even at the apex, where significant hair cell loss had occurred (Fig. 5*C*). Similar results were observed by injecting mouse pups with the fixable dye AM1-43 (data not shown). This suggests that deletion of *Atoh1* does not affect the correct expression of mechanotransduction channels in hair cells over the time period examined, and that the assembly of mechanotransduction apparatus does not require morphologically normal hair bundles.

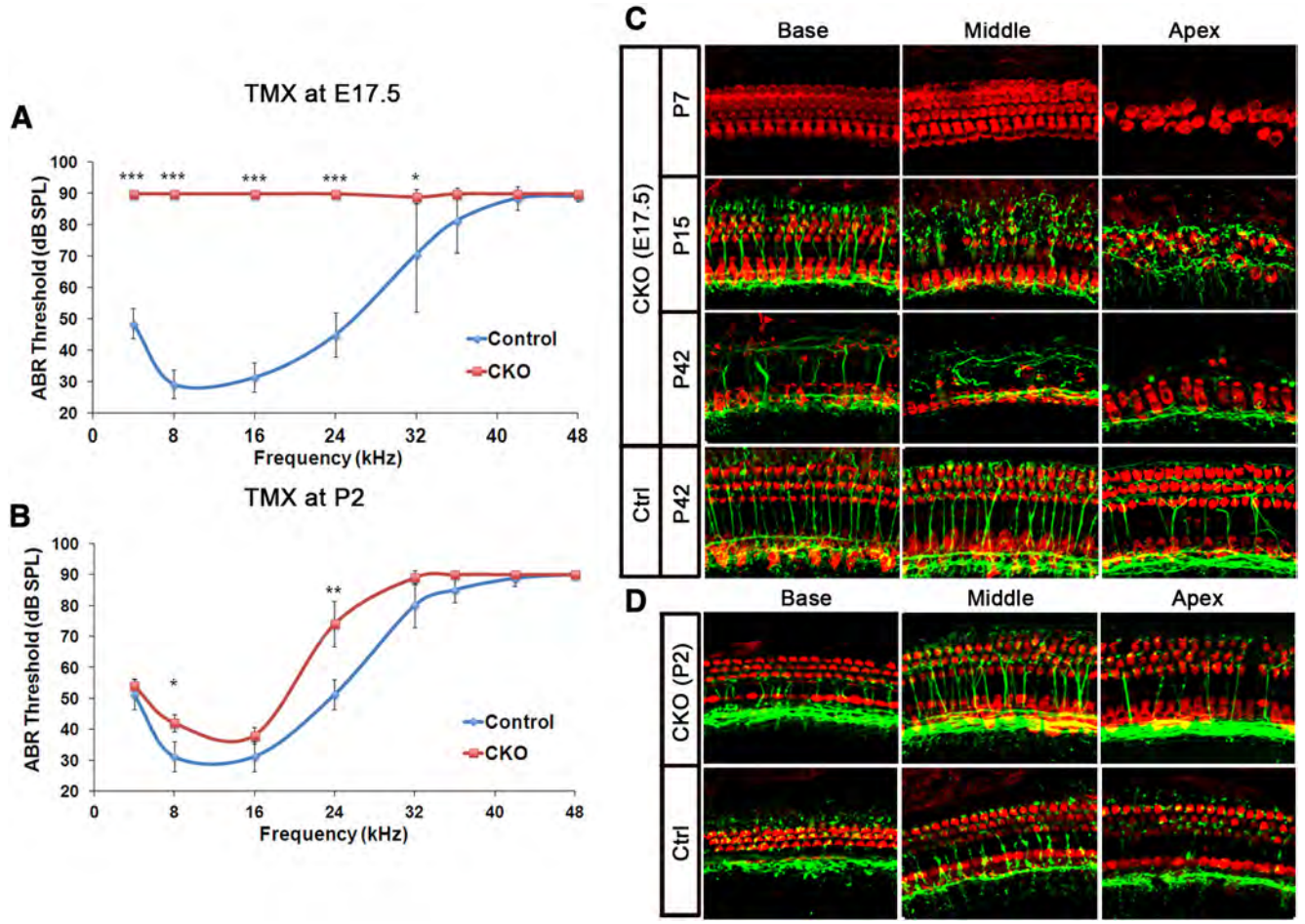

Figure 6. Timing of *Atoh1* deletion affects extent of hair cell survival and preservation of hearing function. ***A***, ***B***, *Atoh1* CKO mice have profound hearing loss when tamoxifen is administered at E17.5 (ANOVA $p = 7.96e{-}11$) (***A***), but only mild hearing loss when tamoxifen administration is delayed until P2 (ANOVA $p = 0.1849$) (***B***). Error bars represent SD. The Student's *t* test with Benjamini–Hochberg adjustment of *p* values for multiple comparisons was used to estimate statistical significance between genotypes at individual frequencies. $^{*}p < 0.05$, $^{**}p < 0.02$, $^{***}p < 0.001$. ***C***, When tamoxifen is administered at E17.5, hair cells, visualized with Myosin6 immunostaining (red), are only missing from the apex of the cochlea at P7. However, by P15, hair cell loss is seen in the middle turn of the cochlea and, by P42, at the base. Control animals show no hair cell loss. Regions lacking hair cells also have defects in afferent and efferent innervation, revealed by staining with the TuJ1 antibody (green). ***D***, When tamoxifen is administered at P2, no significant defects are seen in either hair cell numbers or innervation.

To determine the degree of hearing loss caused by deletion of *Atoh1*, we performed auditory brainstem response (ABR) measurements on 6-week-old Atoh1-CKO animals in which tamoxifen was administered at E17.5. We were surprised to see that these mice had a severe hearing loss at all frequencies tested (Fig. 6*A*), despite the fact that mice given tamoxifen at E17.5 only display apical hair cell loss at birth (Fig. 4*D*). This suggested that the loss of *Atoh1* might lead to further hair cell loss or dysfunction as the animals age. We therefore treated mice with tamoxifen at E17.5 and isolated cochleas from these CKO at different postnatal stages and performed immunohistochemistry for Myosin6 to label hair cells and the TuJ1 anti-tubulin antibody to label neuronal fibers. At P7, no hair cells loss was observed in basal or middle turn regions of the CKO cochleas (Fig. 6*C*), although significant hair cell loss was seen in the apical regions, as we had observed at P0 (Fig. 4*D*). However, by P15, we started to observe loss of outer hair cells in the middle turn region of the cochlea (Fig. 6*C*). In 6-week-old adult mice, most outer hair cells were missing along the entire length of the cochlea (Fig. 6*C*) and efferent innervation of the outer hair cell region was severely disrupted. These data suggest that although outer hair cells in the basal and middle turns of the cochlea initially survive following loss of *Atoh1*, it is required for their integrity and survival in the week before the onset of hearing.

To determine whether this delayed effect of *Atoh1* loss on hair cell survival also occurred within a critical time window, we administered tamoxifen to CKO pups at 2 d after birth and again measured hearing and cochlear morphology at 6 weeks of age. At P2, *Atoh1* is still expressed in the apex of the cochlea, and *Atoh1*-CKO mice still show recombination in ~50% of hair cells (Fig. 3*D*). In contrast to mice in which *Atoh1* was deleted at E17.5, P2 CKO mice had ABR thresholds only marginally higher than those of controls (Fig. 6*B*). Moreover, the morphology and innervation of the cochlea of 6-week-old CKO was similar to controls along the length of the cochlea, and only very few missing outer hair cells were observed at the apex (Fig. 6*D*). These data suggest that although deletion of *Atoh1* hair cells at E17.5 can cause delayed, severe hair cell death, hair cells in P2 mice no longer require *Atoh1* for their short-term or long-term survival.

Atoh1 is indirectly required for differentiation and survival of cochlear supporting cells

Previous studies have suggested *Atoh1* expression in hair cells might play an indirect role in the development and maturation of

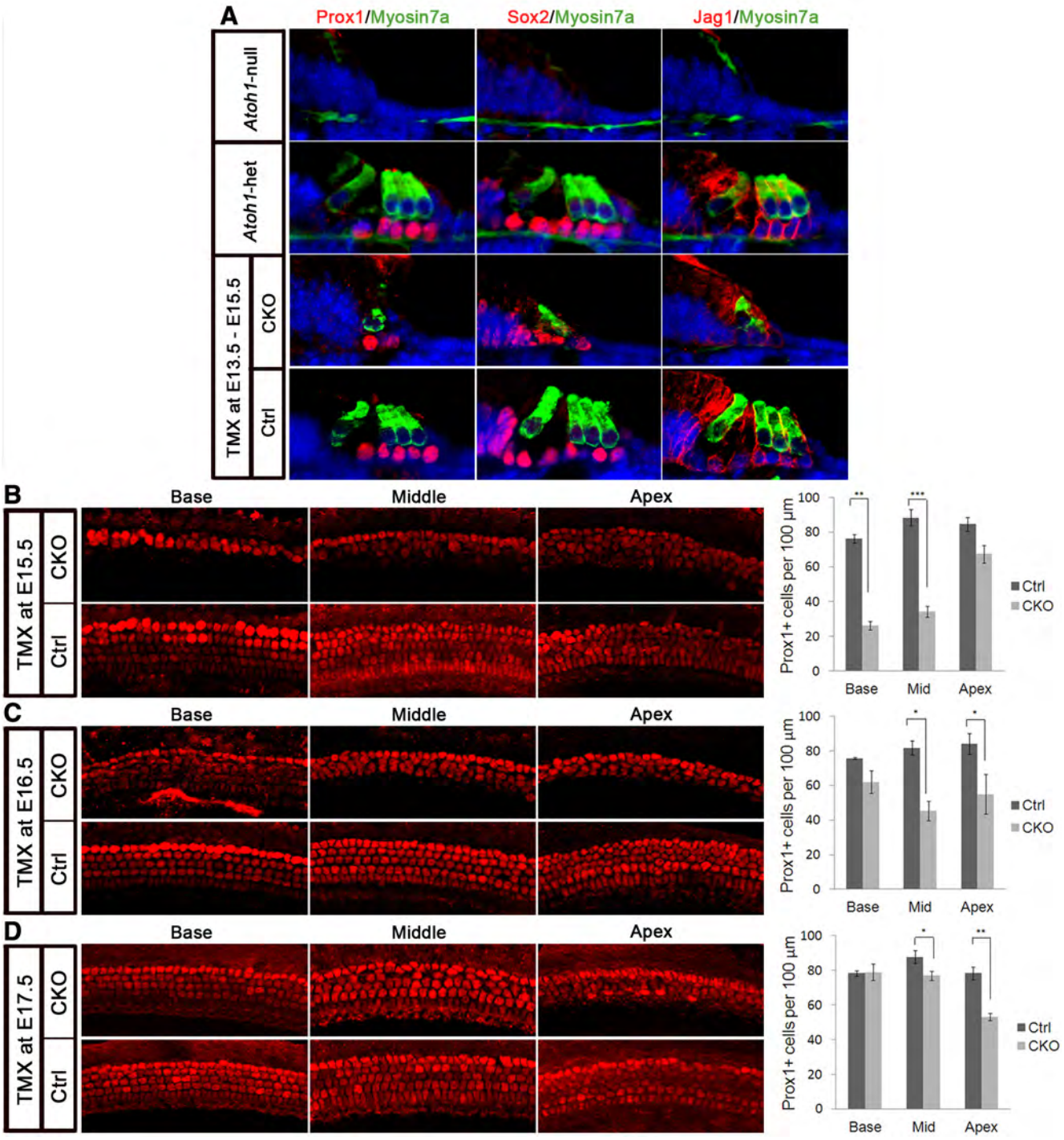

Figure 7. *Atoh1* is required for the survival of the surrounding supporting cells in a time-dependent manner. ***A***, Sections of middle turn regions of the cochlea from *Atoh1*-null and heterozygous embryos at E19. The expression of supporting markers Prox1, Sox2, and Jag1 was abolished in the knock-out mutants. Similar, albeit slightly milder phenotypes were also seen in *Atoh1*-CKO mice that received three daily doses of tamoxifen between E13.5 and E15.5 and were killed at E19. ***B–D***, Whole-mount cochleas from P0 *Atoh1*-CKO and control littermates receiving one dose of tamoxifen at E15.5 (***B***), E16.5 (***C***), and E17.5 (***D***). This is the same experimental regimen shown in Figure 4*A*. Supporting cells were visualized by staining with a Prox1 antibody (red). The number of Prox1-labeled cells in both CKO and control cochleas on each injection day is quantified and shown in the graph.

the neighboring supporting cells (Woods et al., 2004). Consistent with this idea, immunostaining of cochleas from *Atoh1*-null E19 mice or cochleas from *Atoh1-CKO* E19 mice that received tamoxifen between E13.5 and E15.5 showed significantly decreased expression or loss of several supporting cell markers, including Prox1, Sox2, and Jag1 (Fig. 7*A*). To examine whether deleting *Atoh1* from hair cells affects the development or survival of the surrounding supporting cells, we collected neonatal CKO cochleas after tamoxifen treatment at E15.5, E16.5, or E17.5 (an identical schedule to that shown in Fig. 4*A*) and performed immunohistochemistry for Prox1 as a marker of Deiters' and pillar cells (Fig. 7*B–D*). For quantification, each cochlea was divided into three regions: base, middle turn, and apex. When tamoxifen was administered at E15.5, there was a significant loss of support-

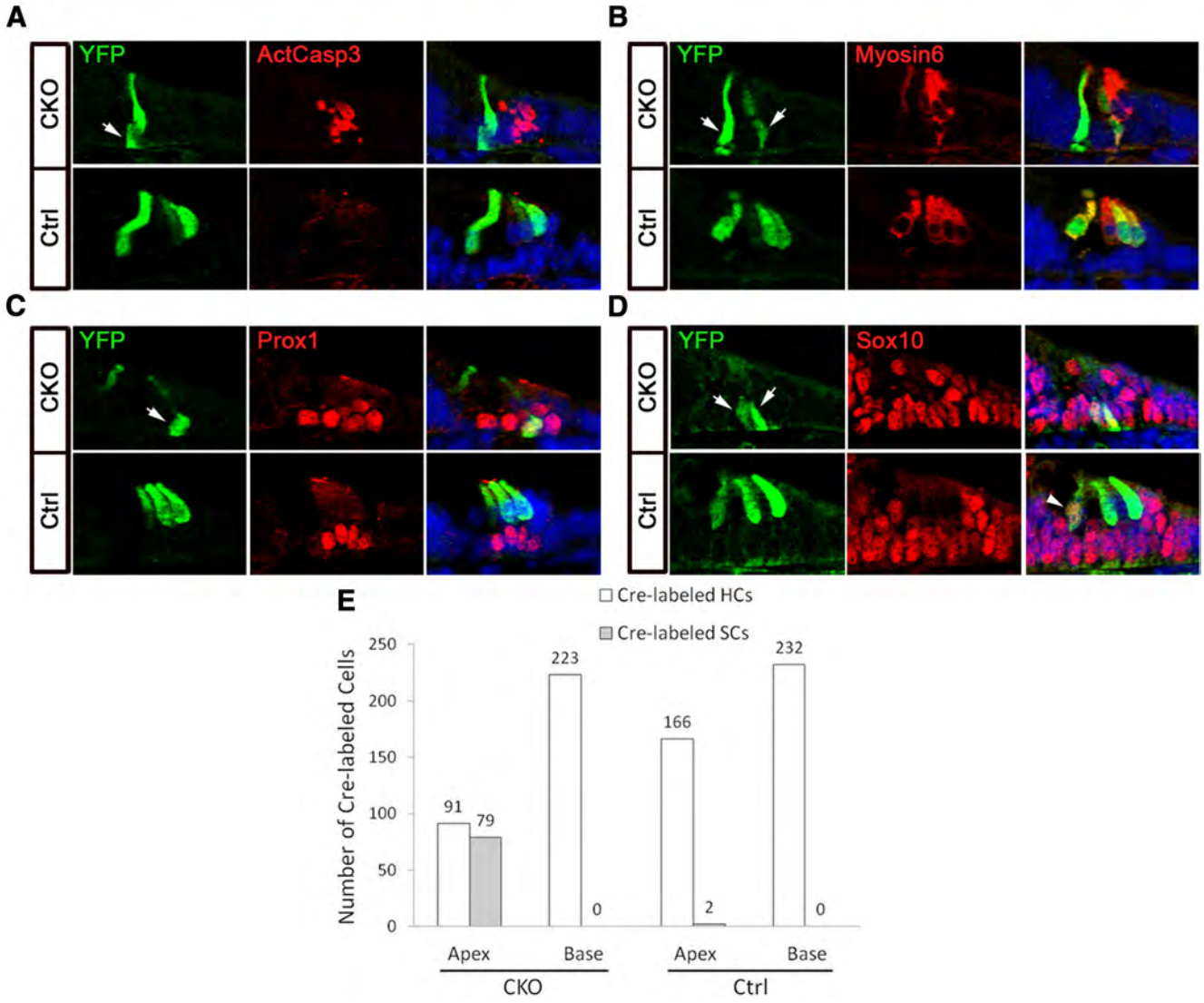

Figure 8. *Atoh1* is indirectly required for differentiation and survival of cochlear supporting cells. ***A–D***, Sections of apical regions of the cochlea from *Atoh1*-CKO and control animals harvested 24 h after tamoxifen treatment at E17.5. YFP shows cells that underwent recombination after tamoxifen administration. ActCasp3 (red) labels apoptotic cells in the apex of CKO organ (***A***). Myosin6 labels differentiated hair cells (***B***). Prox1 (***C***) and Sox10 (***D***) were used to examine supporting cell development. YFP+ cells (arrow) in the supporting cell layer were only observed in the apical region of CKO cochlea. This suggested that cells in the supporting cell layer of the CKO, but not wild-type cochlea, were activating the *Atoh1*-CreER^{T2} transgene. In the apex of control cochlea, we often saw inner hair cells labeled by Sox10 (***D***, arrowhead). ***E***, Quantification of YFP+ cells in the hair cell and supporting cell layers of *Atoh1*-CKO and control mice harvested 24 h after tamoxifen treatment at E17.5. The total number of YFP+ cells was quantified in regions approximating to the basal and apical thirds of the cochlea from three different specimens of each genotype. Cells were assigned based on their position in the hair cell or supporting cell layers. Significant numbers of YFP-labeled cells (79) were observed in the supporting cell layer from the apical regions of three *Atoh1*-CKO cochleas. In contrast, only two YFP-labeled supporting cells from three cochleas could be observed in the apical turn of control cochleas. HC, hair cell; SC, supporting cell.

ing cells from basal to middle turn regions of the CKO cochleas (Fig. 7*B*). However, when tamoxifen was administered at E17.5, supporting cell numbers were comparable between CKO and control organs at the base. Significant decrease of supporting cells was only observed in the middle turn to apical regions (Fig. 7*D*). The loss of supporting cells in the *Atoh1*-CKO cochlea closely followed the loss of hair cells (Fig. 4*B–D*). These data suggest that the critical period of *Atoh1* requirement for the survival of hair cells is approximately the same as that which indirectly regulates the survival of surrounding supporting cells.

To gain more insight into the mechanism of supporting cell death, we used anti-ActCasp3 antibodies to identify cells undergoing apoptosis in the cochlear sections of CKO mice that we harvested at 24 h after tamoxifen treatment at E17.5. Within the sensory epithelial region, we only observed ActCasp3 staining in the apex of the CKO cochleas, consistent with the restriction of hair cell and supporting cell loss to this region (Figs. 4*D*, 7*D*). Although many of the apoptotic cells were present in the upper hair cell layer, significant numbers of ActCasp3-labeled cells were located in the supporting cell layer close to the basilar membrane, suggesting that *Atoh1* deletion in hair cells results in the death of surrounding supporting cells as well (Fig. 8*A*). Interestingly, when we examined *Atoh1-CreER*-mediated recombination in these mice, we observed some cells expressing the supporting cell markers Prox1 and Sox10 that were also labeled by YFP in the apical region of the CKO cochleas (Fig. 8*C*,*D*). However, we did not observe coexpression of YFP and Prox1 in any region of the control cochleas (Fig. 8*C*), nor at the base of the CKO organs. This suggested that the loss of hair cells leads to activation of *Atoh1*, and hence the *Atoh1-CreER*^{T2} transgene in supporting cells. We quantified the YFP-labeled cells within the hair cell layer and supporting cell layer (Fig. 8*E*). In the apex of the CKO co-

chleas, about half of the YFP+ cells were localized in the supporting cell layer (79 cells of a total of 170 YFP+ cells counted from 3 different cochleas; Fig. 8*E*). In contrast, we observed only two YFP+ cells in total within the supporting cell layer in the apical regions of three control cochleas (Fig. 8*E*). Since the *Atoh1* autoregulatory enhancer used to drive $CreER^{T2}$ expression requires *Atoh1* expression (Helms et al., 2000; Machold and Fishell, 2005; Raft et al., 2007), the presence of YFP in the supporting cell layer suggests that loss of hair cells induces the upregulation of *Atoh1* in the surrounding supporting cells, followed by Cre-mediated deletion of *Atoh1* in these cells and their rapid death.

Discussion

Atoh1 is first expressed in a subset of precursors before hair cell differentiation

In *Drosophila*, *atonal* acts as a proneural gene: it is expressed in proneural clusters and the sensory precursors that give rise to the chordotonal organs, and is both necessary and sufficient for the differentiation of sensory organ precursors (Jarman et al., 1993). However, different techniques to reveal Atoh1 mRNA or protein expression in the mouse cochlea have yielded inconsistent results (Chen et al., 2002; Woods et al., 2004). We attempted to resolve this issue by using an *Atoh1-EGFP* fusion construct knocked into the *Atoh1* locus. The *Atoh1-EGFP* allele is fully functional (Rose et al., 2009) and displays no observable phenotypes, being able to breed normally and survive to adulthood, unlike *Atoh1*-null mice. Our data show that Atoh1 protein is expressed before the expression of hair cell and supporting cell markers, but its expression is restricted to a subset of precursors in a salt-and-pepper pattern close to the border of the prosensory domain with the greater epithelial ridge (Fig. 1*B*,*C*). This region will give rise to inner hair cells, the first hair cell type to differentiate in the organ of Corti (Lim and Anniko, 1985; Chen et al., 2002; Lumpkin et al., 2003; Jacques et al., 2007). The restricted expression of Atoh1 suggests that, unlike *atonal* in *Drosophila*, *Atoh1* is not expressed in a manner consistent with a proneural gene in the mammalian cochlea.

We observed a striking change in the subcellular localization of Atoh1-EGFP protein as hair cell precursors differentiated. Before hair cell differentiation, Atoh1-EGFP is ubiquitously expressed in the nucleus and cytoplasm of hair cell precursors (Fig. 1*D*). However, as cells started expressing the hair cell differentiation marker Myosin6, Atoh1-EGFP becomes restricted to the nucleus. We observed similar results with a recently described polyclonal antibody to Atoh1 (Driver et al., 2013), although the antibody appeared to be less sensitive than the Atoh1-EGFP fusion protein (compare Fig. 1*D* and 1*E*) . The change in Atoh1 subcellular localization might be caused by the nuclear transport of Atoh1 when precursors differentiate into hair cells. Although nuclear-cytoplasmic shuttling has been reported for many transcription factors, there are few examples of this process regulating bHLH genes (Ghosh and Baltimore, 1990; Van Der Heide et al., 2004; Reich and Liu, 2006; MacDonald et al., 2009). At present, we do not know whether this translocation is regulated by post-translational modification of Atoh1 itself, or by accessory proteins that actively import Atoh1 into the nucleus. Regardless of the mechanism, it is intriguing to consider that the onset of nuclear restriction of Atoh1 coincides with the first appearance of differentiated hair cell markers, such as Myosin6 (Fig. 1*D*,*E*), and with the timing of hair cell precursor death in *Atoh1*-null embryos (see below). We are currently exploring the significance of the altered subcellular localization of Atoh1 in more detail.

Recent studies using Cre recombinase-mediated lineage tracing of *Atoh1*-expressing precursors suggests that at least some cells expressing *Atoh1* will ultimately differentiate as supporting cells (Yang et al., 2010; Driver et al., 2013). We therefore cannot be certain that all of the Atoh1-EGFP-labeled cells we observe are destined to become hair cells. The random and variable distribution of cochlear supporting cells labeled by *Atoh1* lineage tracing in these studies suggests that some *Atoh1*-expressing cells may be diverted to a supporting cell fate, possibly through Notch-mediated lateral inhibition (Jarman and Groves, 2013).

Atoh1 regulates the survival of hair cells and hair cell precursors

We and others have observed the first signs of apoptosis in the *Atoh1*-null cochlea at E15.5, 2 d after Atoh1 protein can be visualized in the wild-type organ (Chen et al., 2002; Pan et al., 2012). However, when we conditionally removed *Atoh1* at stages between E15.5 and E17.5, conspicuous cell death was observed much more rapidly, starting at 20 h after tamoxifen treatment. The rapid cell death in our *Atoh1* CKO mice is especially striking because we first observe recombination of the R26R-YFP locus in these mice 8 h after tamoxifen gavage. The fact that only 12 h elapses between the first cessation of *Atoh1* transcription and the onset of cell death suggests that Atoh1 protein is quite unstable and that its absence rapidly leads to hair cell death. However, this critical period in which hair cells are vulnerable to loss of *Atoh1* lasts for only 72 h in the base of the cochlea, as deletion of *Atoh1* after E16.5, 72 h after the first expression of Atoh1 protein, does not cause cell death. It is likely that hair cells begin to express additional factors that promote hair cell survival toward the end of this critical period. Although we currently do not know the identity of these factors, two possible candidates are the transcription factors *Gfi1* and *Pou4f3*, as mutant mice for either gene show significant hair cell death in the cochlea at later developmental stages (Xiang et al., 1998; Wallis et al., 2003). Atonal also participates in cell fate decisions mediating survival and death in the *Drosophila* antenna, where only sensory lineages specified by Atonal can respond to EGF signaling and survive (Sekerkov á et al., 2004). This suggests *Atoh1* might also regulate cell survival in the cochlea by modulating hair cell responses to trophic factors.

The role of *Atoh1* in hair bundle development and function

Previous studies on *Atoh1* function in the cochlea focused mainly on the regulation of hair cell differentiation (Mulvaney and Dabdoub, 2012). However, the sustained expression of *Atoh1* in differentiating hair cells until after birth suggests *Atoh1* might also participate in other biological programs involved in the maturation and function of hair cells. We observed disorganized hair bundles in *Atoh1*-CKO cochleas when *Atoh1* was deleted at E17.5, but not when *Atoh1* was removed at P0, suggesting *Atoh1* is required for the formation and orientation of stereocilia in a time-dependent manner. The fact that disorganized hair bundles can be observed in regions of *Atoh1*-CKO cochleas that have a normal complement of hair cells and supporting cells (Fig. 5*A*,*B*) suggests that this effect is a direct result of *Atoh1* loss, rather than morphological rearrangements as an indirect consequence of cell death. Our FM1-43 labeling data suggests that mechanotransduction channels are still present in surviving *Atoh1*-CKO hair cells bearing disorganized stereociliary bundles (Fig. 5*C*). However, our ABR measurements of *Atoh1*-CKO mice suggest that animals in which *Atoh1* is deleted at E17.5 have severe hearing loss at 6 weeks. Our whole-mount data suggests the hearing loss results from the degeneration of hair cells, particularly outer hair cells, and that this degeneration is already apparent by the onset of hearing at 2 weeks. We suggest that one factor contributing to

the delayed loss of hair cells in the CKO animals seen at adult stages might be disrupted formation of stereocilia. It has been previously shown that loss of genes involved in stereocilia development, such as *Whirlin*, *Cadherin23* and *Pcdh15*, can cause hair cell degeneration with age (Alagramam et al., 2001; Holme et al., 2002; Mustapha et al., 2007; Kane et al., 2012), suggesting healthy stereociliary bundles are essential for the long-term survival of hair cells. Once again, we observe another critical period in which *Atoh1* is required for hair bundle formation and long-term hair cell survival, as we observed far less severe hearing loss and hair cell loss in CKO mice treated with tamoxifen at P2. Our histology data show that despite significant (>50%) recombination in the apex of the P2 cochlea, these mice lack only a few outer hair cells in this region, with no obvious signs of hair cell degeneration in basal and middle turn regions. The slight loss of hair cells in the apex may explain why these CKO mice show some degree of hearing loss at lower frequencies (<16 kHz).

Hair cell loss leads to *trans*-differentiation and death of surrounding supporting cells

Previous studies have shown that *Atoh1*-null mice lack both hair cells and supporting cells (Woods et al., 2004; Pan et al., 2012). It has been proposed that nascent hair cells may regulate the differentiation of supporting cells, but the ongoing role of hair cells in supporting cell survival is more controversial (Woods et al., 2004). We show here that conditional deletion of *Atoh1* in cochlear hair cells leads to supporting cell death, but only in regions in which hair cells are also missing. This suggests that hair cells are indirectly regulating the survival of supporting cells. A possible mechanism for this death is suggested by our observation of Cre-mediated recombination in some supporting cells after tamoxifen treatment. We see strong expression of EGFP in cells in the lower layer of the CKO cochlea, colocalizing with both Prox1 and Sox10. We have never observed this expression in control cochleas or in regions of the CKO cochlea that show no hair cell death, suggesting that *Atoh1* is upregulated in supporting cells in regions of the cochlea where hair cells are dying. It has been proposed that nascent hair cells normally send inhibitory signals (likely through the Notch pathway) to neighboring supporting cells, preventing their differentiation into hair cells (Lanford et al., 1999; Kiernan et al., 2005). Moreover, a number of previous studies in embryonic or neonatal mammals have shown that loss of hair cells following trauma can cause supporting cells to *trans*-differentiate into hair cells (Kelley et al., 1995; Burns et al., 2012). Atoh1 upregulation in the supporting cells of CKO cochleas might therefore be the consequence of loss of lateral inhibition following hair cell death. This would suggest that supporting cells might undergo an ill-fated attempt to *trans*-differentiate into hair cells, which then undergo *Atoh1* deletion due to the continuing presence of circulating tamoxifen (Reinert et al., 2012).

In conclusion, our data suggest that *Atoh1* fulfills several separate functions during the development and maturation of hair cells. In addition to being required for the initial differentiation of hair cells, conditional deletion of *Atoh1* has also revealed the existence of distinct critical periods for hair cell survival, stereociliary bundle maturation, and the long-term viability of hair cells. By analogy to the recent finding that *Atoh1* can directly regulate a wide variety of cellular functions in the developing cerebellum (Klisch et al., 2011), we suggest that *Atoh1* may have a similarly diverse set of functions during the maturation of hair cells. A systematic survey of *Atoh1* targets in hair cells, similar to that performed in the cerebellum, is likely to reveal further candidates and pathways that promote hair cell survival and function.

References

Alagramam KN, Murcia CL, Kwon HY, Pawlowski KS, Wright CG, Woychik RP (2001) The mouse Ames waltzer hearing-loss mutant is caused by mutation of Pcdh15, a novel protocadherin gene. Nat Genet 27:99–102. CrossRef Medline

Ben-Arie N, Bellen HJ, Armstrong DL, McCall AE, Gordadze PR, Guo Q, Matzuk MM, Zoghbi HY (1997) Math1 is essential for genesis of cerebellar granule neurons. Nature 390:169–172. CrossRef Medline

Bermingham NA, Hassan BA, Price SD, Vollrath MA, Ben-Arie N, Eatock RA, Bellen HJ, Lysakowski A, Zoghbi HY (1999) Math1: an essential gene for the generation of inner ear hair cells. Science 284:1837–1841. CrossRef Medline

Burns JC, Cox BC, Thiede BR, Zuo J, Corwin JT (2012) *In vivo* proliferative regeneration of balance hair cells in newborn mice. J Neurosci 32:6570–6577. CrossRef Medline

Chen P, Johnson JE, Zoghbi HY, Segil N (2002) The role of Math1 in inner ear development: uncoupling the establishment of the sensory primordium from hair cell fate determination. Development 129:2495–2505. Medline

Doetzlhofer A, Basch ML, Ohyama T, Gessler M, Groves AK, Segil N (2009) Hey2 regulation by FGF provides a Notch-independent mechanism for maintaining pillar cell fate in the organ of Corti. Dev Cell 16:58–69. CrossRef Medline

Driver EC, Sillers L, Coate TM, Rose MF, Kelley MW (2013) The Atoh1-lineage gives rise to hair cells and supporting cells within the mammalian cochlea. Dev Biol 376:86–98. CrossRef Medline

Ghosh S, Baltimore D (1990) Activation in vitro of NF-kappa B by phosphorylation of its inhibitor I kappa B. Nature 344:678–682. CrossRef Medline

Hayashi T, Kokubo H, Hartman BH, Ray CA, Reh TA, Bermingham-McDonogh O (2008) Hesr1 and Hesr2 may act as early effectors of Notch signaling in the developing cochlea. Dev Biol 316:87–99. CrossRef Medline

Helms AW, Abney AL, Ben-Arie N, Zoghbi HY, Johnson JE (2000) Autoregulation and multiple enhancers control Math1 expression in the developing nervous system. Development 127:1185–1196. Medline

Holme RH, Kiernan BW, Brown SD, Steel KP (2002) Elongation of hair cell stereocilia is defective in the mouse mutant whirler. J Comp Neurol 450:94–102. CrossRef Medline

Jacques BE, Montcouquiol ME, Layman EM, Lewandoski M, Kelley MW (2007) Fgf8 induces pillar cell fate and regulates cellular patterning in the mammalian cochlea. Development 134:3021–3029. Advance online publication. Retrieved March 30, 2013. doi:10.1016/j.semcdb.2013.03.010. CrossRef Medline

Jarman AP, Groves AK (2013) The role of Atonal transcription factors in the development of mechanosensitive cells. Semin Cell Dev Biol.

Jarman AP, Grau Y, Jan LY, Jan YN (1993) atonal is a proneural gene that directs chordotonal organ formation in the *Drosophila* peripheral nervous system. Cell 73:1307–1321. CrossRef Medline

Kane KL, Longo-Guess CM, Gagnon LH, Ding D, Salvi RJ, Johnson KR (2012) Genetic background effects on age-related hearing loss associated with Cdh23 variants in mice. Hear Res 283:80–88. CrossRef Medline

Kelley MW (2006) Regulation of cell fate in the sensory epithelia of the inner ear. Nat Rev Neurosci 7:837–849. CrossRef Medline

Kelley MW (2007) Cellular commitment and differentiation in the organ of Corti. Int J Dev Biol 51:571–583. CrossRef Medline

Kelley MW, Talreja DR, Corwin JT (1995) Replacement of hair cells after laser microbeam irradiation in cultured organs of corti from embryonic and neonatal mice. J Neurosci 15:3013–3026. Medline

Kelly MC, Chen P (2009) Development of form and function in the mammalian cochlea. Curr Opin Neurobiol 19:395–401. CrossRef Medline

Kiernan AE, Cordes R, Kopan R, Gossler A, Gridley T (2005) The Notch ligands DLL1 and JAG2 act synergistically to regulate hair cell development in the mammalian inner ear. Development 132:4353–4362. CrossRef Medline

Klisch TJ, Xi Y, Flora A, Wang L, Li W, Zoghbi HY (2011) In vivo Atoh1 targetome reveals how a proneural transcription factor regulates cerebellar development. Proc Natl Acad Sci U S A 108:3288–3293. CrossRef Medline

Lanford PJ, Lan Y, Jiang R, Lindsell C, Weinmaster G, Gridley T, Kelley MW (1999) Notch signalling pathway mediates hair cell development in mammalian cochlea. Nat Genet 21:289–292. CrossRef Medline

Lee YS, Liu F, Segil N (2006) A morphogenetic wave of p27Kip1 transcription directs cell cycle exit during organ of Corti development. Development 133:2817–2826. CrossRef Medline

Lelli A, Asai Y, Forge A, Holt JR, Géléoc GS (2009) Tonotopic gradient in the developmental acquisition of sensory transduction in outer hair cells of the mouse cochlea. J Neurophysiol 101:2961–2973. CrossRef Medline

Li CW, Ruben RJ (1979) Further study of the surface morphology of the embryonic mouse cochlear sensory epithelia. Otolaryngol Head Neck Surg (1979) 87:479–485. Medline

Lim DJ, Anniko M (1985) Developmental morphology of the mouse inner ear. A scanning electron microscopic observation. Acta Otolaryngol Suppl 422:1–69. Medline

Longo-Guess CM, Gagnon LH, Cook SA, Wu J, Zheng QY, Johnson KR (2005) A missense mutation in the previously undescribed gene Tmhs underlies deafness in hurry-scurry (hscy) mice. Proc Natl Acad Sci U S A 102:7894–7899. CrossRef Medline

Lumpkin EA, Collisson T, Parab P, Omer-Abdalla A, Haeberle H, Chen P, Doetzlhofer A, White P, Groves A, Segil N, Johnson JE (2003) Math1-driven GFP expression in the developing nervous system of transgenic mice. Gene Expr Patterns 3:389–395. CrossRef Medline

MacDonald BT, Tamai K, He X (2009) Wnt/beta-catenin signaling: components, mechanisms, and diseases. Dev Cell 17:9–26. CrossRef Medline

Machold R, Fishell G (2005) Math1 is expressed in temporally discrete pools of cerebellar rhombic-lip neural progenitors. Neuron 48:17–24. CrossRef Medline

Meyers JR, MacDonald RB, Duggan A, Lenzi D, Standaert DG, Corwin JT, Corey DP (2003) Lighting up the senses: FM1-43 loading of sensory cells through nonselective ion channels. J Neurosci 23:4054–4065. Medline

Montcouquiol M, Kelley MW (2003) Planar and vertical signals control cellular differentiation and patterning in the mammalian cochlea. J Neurosci 23:9469–9478. Medline

Mulvaney J, Dabdoub A (2012) Atoh1, an essential transcription factor in neurogenesis and intestinal and inner ear development: function, regulation, and context dependency. J Assoc Res Otolaryngol 13:281–293. CrossRef Medline

Mustapha M, Beyer LA, Izumikawa M, Swiderski DL, Dolan DF, Raphael Y, Camper SA (2007) Whirler mutant hair cells have less severe pathology than shaker 2 or double mutants. J Assoc Res Otolaryngol 8:329–337. CrossRef Medline

Pan N, Jahan I, Kersigo J, Kopecky B, Santi P, Johnson S, Schmitz H, Fritzsch B (2011) Conditional deletion of Atoh1 using Pax2-Cre results in viable mice without differentiated cochlear hair cells that have lost most of the organ of Corti. Hear Res 275:66–80. CrossRef Medline

Pan N, Jahan I, Kersigo J, Duncan JS, Kopecky B, Fritzsch B (2012) A novel Atoh1 "self-terminating" mouse model reveals the necessity of proper Atoh1 level and duration for hair cell differentiation and viability. PLoS One 7:e30358. CrossRef Medline

Raft S, Koundakjian EJ, Quinones H, Jayasena CS, Goodrich LV, Johnson JE, Segil N, Groves AK (2007) Cross-regulation of Ngn1 and Math1 coordinates the production of neurons and sensory hair cells during inner ear development. Development 134:4405–4415. CrossRef Medline

Reich NC, Liu L (2006) Tracking STAT nuclear traffic. Nat Rev Immunol 6:602–612. CrossRef Medline

Reinert RB, Kantz J, Misfeldt AA, Poffenberger G, Gannon M, Brissova M, Powers AC (2012) Tamoxifen-induced Cre-loxP recombination is prolonged in pancreatic islets of adult mice. PLoS One 7:e33529. CrossRef Medline

Rose MF, Ren J, Ahmad KA, Chao HT, Klisch TJ, Flora A, Greer JJ, Zoghbi HY (2009) Math1 is essential for the development of hindbrain neurons critical for perinatal breathing. Neuron 64:341–354. CrossRef Medline

Ruben RJ (1967) Development of the inner ear of the mouse: a radioautographic study of terminal mitoses. Acta Otolaryngol 220:1–44. Medline

Sekerkov á G, Zheng L, Loomis PA, Changyaleket B, Whitlon DS, Mugnaini E, Bartles JR (2004) Espins are multifunctional actin cytoskeletal regulatory proteins in the microvilli of chemosensory and mechanosensory cells. J Neurosci 24:5445–5456. CrossRef Medline

Shroyer NF, Helmrath MA, Wang VY, Antalffy B, Henning SJ, Zoghbi HY (2007) Intestine-specific ablation of mouse atonal homolog 1 (Math1) reveals a role in cellular homeostasis. Gastroenterology 132:2478–2488. CrossRef Medline

Srinivas S, Watanabe T, Lin CS, William CM, Tanabe Y, Jessell TM, Costantini F (2001) Cre reporter strains produced by targeted insertion of EYFP and ECFP into the ROSA26 locus. BMC Dev Biol 1:4. CrossRef Medline

Van Der Heide LP, Hoekman MF, Smidt MP (2004) The ins and outs of FoxO shuttling: mechanisms of FoxO translocation and transcriptional regulation. Biochem J 380:297–309. CrossRef Medline

Wallis D, Hamblen M, Zhou Y, Venken KJ, Schumacher A, Grimes HL, Zoghbi HY, Orkin SH, Bellen HJ (2003) The zinc finger transcription factor Gfi1, implicated in lymphomagenesis, is required for inner ear hair cell differentiation and survival. Development 130:221–232. CrossRef Medline

Woods C, Montcouquiol M, Kelley MW (2004) Math1 regulates development of the sensory epithelium in the mammalian cochlea. Nat Neurosci 7:1310–1318. CrossRef Medline

Xiang M, Gao WQ, Hasson T, Shin JJ (1998) Requirement for Brn-3c in maturation and survival, but not in fate determination of inner ear hair cells. Development 125:3935–3946. Medline

Yang H, Xie X, Deng M, Chen X, Gan L (2010) Generation and characterization of Atoh1-Cre knock-in mouse line. Genesis 48:407–413. CrossRef Medline

Zheng JL, Gao WQ (2000) Overexpression of Math1 induces robust production of extra hair cells in postnatal rat inner ears. Nat Neurosci 3:580–586. CrossRef Medline

Development/Plasticity/Repair

Characterization of the Transcriptome of Nascent Hair Cells and Identification of Direct Targets of the Atoh1 Transcription Factor

Tiantian Cai,[1]* Hsin-I Jen,[1]* Hyojin Kang,[3,5] Tiemo J. Klisch,[3,5] Huda Y. Zoghbi,[1,2,3,4,5] and Andrew K. Groves[1,2,3]

[1]Program in Developmental Biology, [2]Departments of Neuroscience, [3]Molecular and Human Genetics, and [4]Howard Hughes Medical Institute, Baylor College of Medicine, Texas 77030, and [5]The Jan and Dan Duncan Neurological Research Institute, Texas Children's Hospital, Houston, Texas 77030

Hair cells are sensory receptors for the auditory and vestibular system in vertebrates. The transcription factor *Atoh1* is both necessary and sufficient for the differentiation of hair cells, and is strongly upregulated during hair-cell regeneration in nonmammalian vertebrates. To identify genes involved in hair cell development and function, we performed RNA-seq profiling of purified Atoh1-expressing hair cells from the neonatal mouse cochlea. We identified >600 enriched transcripts in cochlear hair cells, of which 90% have not been previously shown to be expressed in hair cells. We identified 233 of these hair cell genes as candidates to be directly regulated by Atoh1 based on the presence of Atoh1 binding sites in their regulatory regions and by analyzing Atoh1 ChIP-seq datasets from the cerebellum and small intestine. We confirmed 10 of these genes as being direct Atoh1 targets in the cochlea by ChIP-PCR. The identification of candidate Atoh1 target genes is a first step in identifying gene regulatory networks for hair-cell development and may inform future studies on the potential role of Atoh1 in mammalian hair cell regeneration.

Key words: **Atoh1; cochlea; hair cells; inner ear**

Introduction

Atoh1 is the first transcription factor to be expressed in hair cells, and is essential for hair-cell development. Previous studies of *Atoh1* mutant mice have revealed multiple functions of *Atoh1* in the genesis, survival, maturation, and function of hair cells (Bermingham et al., 1999; Chen et al., 2002; Woods et al., 2004; Pan et al., 2012; Yang et al., 2012b; Cai et al., 2013). Overexpression of *Atoh1* in immature rodent inner ears can induce ectopic hair cells in both sensory and nonsensory regions of the cochlea (Zheng and Gao, 2000; Woods et al., 2004), suggesting the sufficiency of *Atoh1* for hair-cell formation in parts of the inner ear. However, the ability of *Atoh1* to induce new hair cells in the cochlea declines precipitously with age (Liu et al., 2012; Yang et al., 2012a), although the reasons for this decline are currently not known.

Although *Atoh1* is both necessary and sufficient for hair-cell development, the precise molecular mechanism by which *Atoh1* mediates hair-cell genesis is unknown. A very small number of Atoh1 targets have been identified by expression profiling of tissues or cell lines (Krizhanovsky et al., 2006; Scheffer et al., 2007a,b). Genome-wide studies have also identified Atoh1 targets in the nervous system and intestine (Klisch et al., 2011; Kim et al., 2014). A previous study combined Atoh1 ChIP-seq (to identify Atoh1 binding sites) together with histone-seq (to identify global H3K4 methylation status), and RNA-seq (to compare expression profiles of wild-type and *Atoh1-null* cerebella; Klisch et al., 2011). The resultant Atoh1 "targetome" suggests that *Atoh1* regulates the expression of genes responsible for diverse biological processes, including cell proliferation, differentiation, migration, and metabolism. This study also pinpointed an extended E-box-containing sequence termed AtEAM as a consensus binding site for *Atoh1* (Klisch et al., 2011). A second strategy combining the cerebellar Atoh1 targetome with microarray data from the dorsal spinal cord identified several additional Atoh1 targets specific for dorsal spinal cord interneurons (Lai et al., 2011).

The small number of hair cells in the cochlea has militated against identification of Atoh1 target genes in hair cells by ChIP-seq. However, the success of Atoh1 target identification in the dorsal spinal cord suggests a strategy of hair cell RNA-seq combined with ChIP-seq data from other tissues may allow the identification of some Atoh1 targets in hair cells. We used RNA-sequencing to

Received Dec. 15, 2014; revised Feb. 11, 2015; accepted March 2, 2015.

Author contributions: T.C., H.-I.J., H.K., T.J.K., H.Y.Z., and A.K.G. designed research; T.C., H.-I.J., and T.J.K. performed research; T.C., H.-I.J., H.K., T.J.K., H.Y.Z., and A.K.G. analyzed data; T.C., H.-I.J., H.K., H.Y.Z., and A.K.G. wrote the paper.

This project was supported in part by The Genomic and RNA Profiling Core and the RNA In Situ Core at Baylor College of Medicine with the expert assistance of Drs Lisa D. White and Cecilia Ljunberg, funding from NIH Grant P30HD024064 from the Eunice Kennedy Shriver National Institute of Child Health and Human Development, The Cytometry and Cell Sorting Core at Baylor College of Medicine with the expert assistance of Joel M. Sederstrom, funding from NIH Grants P30 AI036211, P30 CA125123, and S10 RR024574, NIH Grants DC006185 and DC011657 to A.K.G., Department of Defense Grant DOD W81XWH-11-2-004 to A.K.G., and H.Y.Z. is an investigator of the Howard Hughes Medical Institute. We thank Hongyuan Zhang, Alyssa Crowder, and Huiling Li for excellent technical assistance and members of the Groves laboratory for their advice and comments; David He for advice and sharing data with us; and Ying-Wooi Wan for help in handling sequencing data.

The authors declare no competing financial interests.

*T.C. and H.-I.J. contributed equally to this work.

Correspondence should be addressed to Andrew Groves, Baylor College of Medicine, BCM295, 1 Baylor Plaza, Houston, TX 77030. E-mail: akgroves@bcm.edu.

H. Kang's present address: National Institute of Supercomputing and Networking, Korea Institute of Science and Technology Information, Daejeon 305-806, Korea.

DOI:10.1523/JNEUROSCI.5083-14.2015

 0270-6474/15/355870-14$15.00/0

identify transcripts in *Atoh1*-expressing cells from the neonatal mouse cochlea and found 614 genes enriched over tenfold in *Atoh1*-expressing cells. We performed an *in situ* hybridization screen to validate the expression of 60 of these enriched genes, of which 34 showed specific hair cell expression. We searched for the Atoh1-binding sites in 10 of the validated genes and verified direct Atoh1 binding in these gene loci by ChIP-PCR. These Atoh1 targets may be useful tools in the assembly of a hair cell gene regulatory network and may allow us to understand why the ability of Atoh1 to induce hair-cell transdifferentiation declines with age.

Materials and Methods

Experimental animals. *Atoh1* $^{-/-}$ (MGI: *Atoh1*^{tm1Hzo}), *Atoh1*$^{A1GFP/A1GFP}$ (MGI: *Atoh1*$^{tm4.1Hzo}$), and *Atoh1*$^{flox/flox}$ (MGI: *Atoh1*^{tm3Hzo}) mice were generated as previously described (Ben-Arie et al., 1997; Shroyer et al., 2007; Rose et al., 2009). *Atoh1-CreER*^{T2} (MGI: Tg(Atoh1-cre/Esr1*)14Fsh; (Machold and Fishell, 2005) and *R26R-YFP* (MGI: Gt(ROSA)26Sor$^{tm1(EYFP)Cos}$; (Srinivas et al., 2001) transgenic lines were obtained from Jackson Laboratories. Genotyping was performed by PCR using the following primers: for different *Atoh1* alleles, Atoh1-forward (ACG CAC TTC ATC ACT GGC), Atoh1-reverse (GGC ACT GGC TTC TCT TGG), and Neo-forward (GCA TCG CCT TCT ATC GCC) yield a 600 bp wild-type allele band and a 400 bp null allele band. HA-forward (GCG ATG ATG GCA CAG AAG G) and HA-reverse (GAA GGG CAT TTG GTT GTC TCA G) yield a 1 kb *Atoh1* EGFP-tagged allele band and a 350 bp floxed allele band. For *Atoh1-CreER*^{T2}, Cre1F (GCC TGC ATT ACC GGT CGA TGC AAC GA),and Cre1R (GTG GCA GAT GGC GCG GCA ACA CCA TT) yield a 700 bp band. For R26R-YFP, oIMR0316 (GGA GCG GGA GAA ATG GAT ATG), oIMR0883 (AAA GTC GCT CTG AGT TGT TAT), and oIMR4982 (AAG ACC GCG AAG AGT TTG TC) yield a 320 bp YFP+ band. To generate the inducible *Atoh1* conditional knock-out (CKO) mice, *Atoh1-CreER*^{T2}; *Atoh1*$^{\pm}$ males were crossed with *Atoh1*$^{flox/flox}$; *R26R-YFP* homozygous females. One dose of 2 mg tamoxifen and 2 mg progesterone was administered to pregnant females at embryonic day (E)17.5 by oral gavage. Progesterone was co-administered to prevent late fetal abortions (Nakamura et al., 2006). Tamoxifen and progesterone were dissolved together in peanut oil, both at a concentration of 20 mg/ml. The genotypes of embryos or newborn pups from these crosses were determined as above. The Baylor College of Medicine Institutional Animal Care and Use committee approved all animal experiments.

Hair-cell purification. Whole inner ears were dissected from homozygous P0 *Atoh1*$^{A1GFP/A1GFP}$ mice and incubated in Ca^{2+}, Mg^{2+}-free (CMF) PBS. The cochleae were isolated and the spiral ganglia and Reissner's membrane removed to expose the organ of Corti. Isolated cochleae were washed with CMF-PBS and then incubated in 0.1% Trypsin-EDTA (Sigma-Aldrich) diluted in CMF-PBS for 10 min at 37°C. The trypsin solution was removed and the tissue rinsed in DMEM with 5% fetal calf serum (FCS). The tissue was then gently triturated with a 1000 μl pipette tip in CMF-PBS containing 5% FCS for ~100 times to generate a single-cell suspension. Hair cells were purified on a BD FACSAria cell-sorting flow cytometer using a 100 μm nozzle and 488 nm excitation. Gates were set each time using small number of cells from the same sample to identify the viable cells and GFP fluorescence. GFP^+ and GFP^- cells were individually collected in CMF-PBS with 5% FCS. Sorted cells were spun down at 1000 × *g* for 10 min at 4°C. The supernatant was carefully removed and pellets were suspended in cell lysis buffer from an RNeasy Plus Micro kit (Qiagen) and stored at −80°C for future RNA extraction.

qPCR. Total RNA was extracted from fluorescence-activated cell sorting (FACS)-purified cells using an RNeasy Plus Micro kit (Qiagen). cDNA was generated using Superscript III Reverse Transcriptase (Invitrogen). Quantitative PCR (qPCR) was performed with Master SYBR Green Kit (Applied Biosystems) on a Step One Plus real-time PCR system (Applied Biosystems). Each reaction was performed in triplicate. Relative quantification of gene expression was analyzed by the $\Delta\Delta C_T$ method (Livak and Schmittgen, 2001) using the ribosomal gene L19 as an internal control. Gene-specific primer sets used for qPCR were as follows: Atoh1-F (ATG CAC GGG CTG AAC CA) and Atoh1-R (TCG TTG TTG AAG GAC GGG ATA); L19-F (GGT CTG GTT GGA TCC CAA TG), and L19-R (CCC GGG AAT GGA CAG TCA).

RNA-sequencing. RNA-seq libraries of FACS purified cells were generated as previously described (Lott et al., 2011). Total RNA was extracted from FACS-purified cells (~100,000 cells for each library) using an RNeasy Plus Micro kit (Qiagen). mRNA purification, RNA fragmentation, first strand and second strand cDNA synthesis, adaptor ligation, and PCR amplification were performed using the Illumina mRNA-Seq Sample Prep Kit. SPRI beads (Ampure XP, Beckman) were used in each purification step after RNA fragmentation for size selection. Duplicate libraries were made for GFP^+ cells and GFP^- cells. All libraries were analyzed for quality and concentration using an Agilent Bioanalyzer. A sample from each library was also cloned into the TOPO-Blunt vector. Ten clones were randomly picked and sequenced to verify that ribosomal RNA was depleted from the libraries. Sequencing was performed at the Genomic and RNA Profiling Core in Baylor College of Medicine using Illumina HiSeq2000 100bp Paired-End Platform. Fastq files of paired-end reads and BigWig files have been deposited in the NCBI GEO database, Accession No. GSE65633.

RNA-seq data analysis. RNA-seq reads were mapped to the mouse reference genome (mm9) using TopHat (Trapnell et al., 2009). Read counts per gene were obtained by counting the number of reads, which overlap the exons of genes defined by RefGene (NCBI). Read counts were normalized to a library size and differentially expressed genes were identified by performing a negative binomial test using the DESeq package (Anders and Huber, 2010). *P* values were adjusted using the Benjamini and Hochberg (1995) multiple testing procedure. Genes with adjusted *p* values $<1 \times 10^{-10}$ were marked as significant.

Prediction of Atoh1 binding sites. To predict Atoh1 binding sites, the MACS package (Zhang et al., 2008) was used to select the top 5000 Atoh1 binding sites from ChIP-Seq data obtained from the neonatal cerebellum (Klisch et al., 2011). MEME-ChIP (Machanick and Bailey, 2011) was used to analyze the flanking sequences of the top 5000 sites, from which 87 motifs were selected that were present >10 times in these 5000 sites. Conserved promoter or enhancer regions within 5 kb of the transcriptional start site of each gene were identified from the UCSC browser conservation track and these regions were searched for the 87 Atoh1 binding motifs.

RNA probe synthesis. Primer sets for each candidate gene were selected to target a 500–700 bp DNA fragment in a single exon of each gene for screen. A T7 RNA polymerase sequence (5′-GGATCCTAATACG ACTCACTATAGGGAG-3′) was added to the 5′ end of each reverse primer. Mouse genomic DNA was used as the template for PCR. The PCR product of the correct size was purified with a PCR Purification Kit (Qiagen). Purified DNA was used as the template for RNA probe synthesis with T7 polymerase (Promega) using standard protocols (Stern, 1998).

In situ *hybridization.* Heads of neonatal mouse pups were fixed in 4% paraformaldehyde in PBS overnight at 4°C, cryoprotected in 30% sucrose in PBS at 4°C, embedded in OCT compound (Sakura Finetek), and cryosectioned at 14 μm. The *in situ* hybridization procedure was modified from previous protocols (Harland, 1991; Birren et al., 1993; Groves et al., 1995). Sections were fixed in 4% paraformaldehyde in PBS, pH 7.2, for 10 min at room temperature, followed by three 5 min washes in DEPC-treated PBS. The sections were treated with 1 μg/ml proteinase K in DEPC-PBS for 5 min at room temperature, followed by three 5 min washes in DEPC-PBS and refixation in 4% paraformaldehyde in PBS, pH 7.2, for 10 min at room temperature. Sections were acetylated in 0.25% acetic anhydride in 0.1 M triethanolamine, pH 8.0, for 10 min at room temperature, followed by three 5 min washes in DEPC-PBS. Slides were incubated in hybridization buffer (50% Formamide, 5× SSC, 50 μg/ml Yeast tRNA, 100 μg/ml heparin, 1× Denhardt's Solution, 0.1% Tween 20, 0.1% CHAPS, 5 mM EDTA) for 1–2 h at 65°C. One-hundred microliters of digoxygenin-labeled probe (1 mg/ml) was added to each slide and the slides covered with glass coverslips. The slides were incubated in a chamber humidified with 5× SSC, 50% formamide at 65°C overnight. Coverslips were removed by rinsing in 0.2× SSC and the slides washed in 0.2× SSC at 65°C for 1 h. The slides were then washed in 0.2× SSC for 5

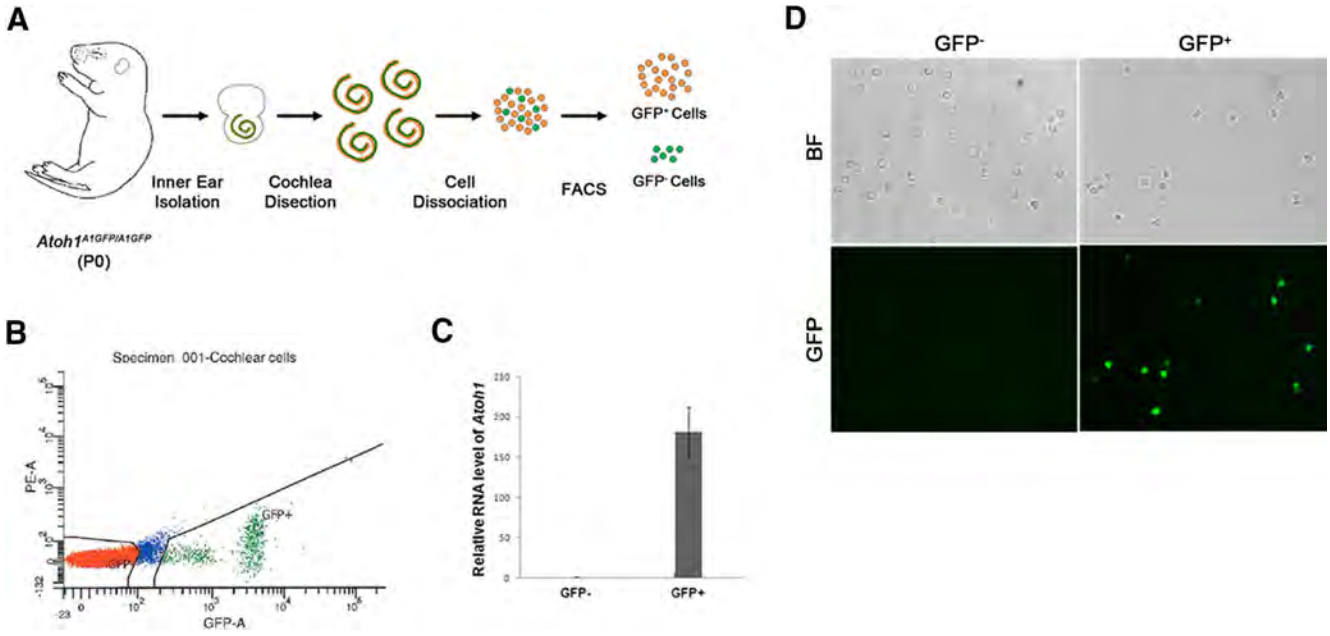

Figure 1. ***A***, Schematic diagram of the purification of GFP cells from the neonatal *Atoh1*$^{A1GFP/A1GFP}$ mouse cochlea. ***B***, Sample FACS profile showing the distribution of GFP-expressing cells (green). ***C***, Q-PCR analysis of GFP-positive and -negative cells sorted from the *Atoh1*$^{A1GFP/A1GFP}$ cochlea shows an almost 180-fold enrichment of *Atoh1* mRNA in the GFP+ population. ***D***, Fluorescence and bright field images of the GFP-positive and -negative cell populations.

min at room temperature, followed by another 5 min wash in 0.1% Tween 20 in PBS (PTw). The slides were blocked in 10% lamb serum in PTw at room temperature for 1 h and then stained with anti-digoxygenin-alkaline phosphatase antibody (1:2000) for 1–3 h at room temperature in a humidified chamber. The slides were then washed three times for 5 min each in PTw and equilibrated with freshly made alkaline phosphatase buffer (100 mM Tris, pH 9.5, 50 mM $MgCl_2$, 100 mM NaCl, 0.1% Tween 20) for 10 min. The slides were developed in alkaline phosphatase buffer containing 0.33 mg/ml NBT and 0.18 mg/ml BCIP in the dark at room temperature until the purple reaction product had developed to a satisfactory degree. The reaction was stopped by washing the slides in PBS three times for 15 min each, followed by fixation in 4% paraformaldehyde in PBS, pH 7.2, for 30 min. The slides were then rinsed and mounted in 80% glycerol in PBS.

Chromatin immunoprecipitation. Cochleae were dissected from P0 *Atoh1*$^{A1GFP/GFP}$ pups and stored in DMEM with 5% FBS. Cochleae were incubated with 500 μM thermolysin in DMEM for 30–45 min at 37°C and washed in DMEM with 5% FBS. The sensory epithelium from each cochlea was dissected out and pooled together in PBS. Eight sensory epithelia were collected for each sample and centrifuged at 470 × *g* for 10 min at 4°C. The pooled sensory epithelia were cross-linked with 500 μl PBS containing 13.5 μl of 36.5% formaldehyde solution for 20 min; the sample was vortexed every 5 min during the incubation. The fixation was then quenched with 57 μl of 1.25 M glycine for 5 min. The cross-linked tissue was centrifuged at 470 × *g* for 10 min at 4°C with soft deceleration. The supernatant was then removed, and the pellet was washed with 500 μl of ice-cold PBS three times. The PBS was removed without disturbing the pellet and the sample snap frozen in liquid nitrogen, and stored at −80°C.

Chromatin immunoprecipitation was performed using the "micro-ChIP" protocol of Dahl and Collas (2009) with some modification. Cross-linked sensory epithelia in the tube were lysed in 120 μl lysis buffer (50 mM Tris-HCl, pH 8.0, 10 mM EDTA, 1% SDS with fresh 1% protease inhibitor and 1 mM PMSF), and incubate for 5 min on ice. The sample was sonicated using a Bioruptor (Diagenode) programmed for 30 s on, 30 s off, for 15 cycles, with vortexing after every five cycles. Four-hundred microliters of RIPA ChIP buffer (10 mM Tris-HCl, pH 7.5, 140 mM NaCl, 1 mM EDTA, 0.5 mM EGTA, 1% Triton X-100, 0.1% SDS, 0.1% Na-deoxycholate, 1% protease inhibitor and 1 mM PMSF) was added to the tube. The sample was then mixed and centrifuged at 12,000 × *g* for 10 min at 4°C. Supernatant (450 μl) was collected into a new tube and the pellet re-extracted with another 400 μl of RIPA ChIP buffer. To precipitate Atoh1^{GFP}-bound DNA, 10 μl of blocking magnetic beads and 10 μl of anti-GFP magnetic beads (Chromotek, GFP-Trap-M) were washed twice with dilution buffer (1.0 M Tris, pH 7.5, 150 mM NaCl, 1 mM EDTA). The ChIP sample solution (400 μl) was added to 400 μl dilution buffer containing the blocking magnetic beads. The sample mixture was then incubated for 30 min at 4°C. After incubation, the tube was placed on a magnetic rack, the beads were captured, and the solution was extracted and mixed with anti-GFP magnetic beads. This mixture was vortexed and incubated for 2 h at 4°C with moderate shaking. The bead-containing solution was placed on the ice-cold magnetic rack to capture the beads and the beads then washed three times with 1 ml ice-cold RIPA buffer at 4°C with moderate shaking for 10 min each. After the final wash, 1 ml TE buffer was added to the beads and incubated for 10 min at 4°C with moderate shaking. After removal of TE, 100 μl of a 10% solution of Chelex-100 beads was added and the sample vortexed for 10 s and boiled for 10 min. One microliter of 25 mg/ml proteinase K was added to the sample, vortexed, and incubated for 40 min at 56°C, with vortexing every 10 min followed by boiling again for 10 min. The sample was cooled to room temperature, centrifuged for 10 s and the supernatant transferred to a chilled clean tube. The sample was then stored at −20°C for up to 1 week or used directly for ChIP-PCR with appropriate primers. As a negative control, GFP ChIP was performed as above from a wild-type mouse.

Results

RNA-seq analysis identifies transcripts enriched in Atoh1-expressing hair cells

We used FACS on cells isolated from *Atoh1*$^{A1GFP/A1GFP}$ knock-in mice (Rose et al., 2009) to purify differentiating hair cells that express Atoh1 (Fig. 1*A*). Cochleae were dissected from newborn (P0) *Atoh1*$^{A1GFP/A1GFP}$ mice, dissociated into single cells, and GFP$^+$ and GFP$^-$ cells were isolated by FACS sorting based on the intensity of GFP fluorescence (Fig. 1*B*). At P0 we saw no observable apical-basal differences in GFP intensity in the intact cochleae of *Atoh1*$^{A1GFP/A1GFP}$ mice (Cai et al., 2013). To confirm Atoh1-GFP expression, both sorted populations were fixed and GFP fluorescence was examined under a microscope. In the

GFP$^+$ population, ~ 90% expressed levels of GFP that were detectable by eye and by costaining with antibodies to Myosin6. No GFP$^+$ cells were detected in the GFP$^-$ population (Fig. 1*C*). To further examine *Atoh1* expression level in the sorted cell populations, we extracted total RNA from both GFP$^+$ and GFP$^-$ populations and performed quantitative reverse-transcriptase PCR to measure the relative mRNA level of *Atoh1*. *Atoh1* transcripts were highly enriched in the GFP$^+$ population by almost 180-fold (Fig. 1*D*).

To identify genes that are enriched in differentiating hair cells, we compared the transcripts in GFP$^+$ and GFP$^-$ cells from P0 *Atoh1*$^{A1GFP/A1GFP}$ mice using RNA-sequencing. We obtained between 98,000,000 and 189,000,000 reads for each sample, with 83–85% of the paired reads mapping correctly to the reference genome. Two biological replicates of each population showed high reproducibility ($r = 0.98$ for the GFP$^+$ populations and 0.96 for the GFP$^-$ populations). By comparing the transcripts between GFP$^+$ and GFP$^-$ populations, we identified 614 transcripts that have over tenfold enrichment in the GFP$^+$ cell population ($p < 1.0E-30$). We also identified 329 transcripts that were downregulated over tenfold in the GFP$^+$ population (data not shown). Of the 614 upregulated genes, 57 have been previously identified as hair cell-specific genes (Table 1), 82 have been identified in adult inner or outer hair cells (Liu et al., 2014), and 74 have also been identified as candidate hair cell genes based on the behavior of chick homologues of these genes during utricle regeneration (Ku et al., 2014). Finally, we also identified 22 enriched transcripts in the GFP$^+$ population that are known deafness genes (*Cabp2*, *Cib2*, *Cldn14*, *Dfnb59*, *Gipc3*, *Gxcr1*, *Gxcr2*, *Ildr1*, *Lhfpl5*, *Msrb3*, *Myo3a*, *Myo6*, *Myo7a*, *Pdzd7*, *Pou4f3*, *Ptprq*, *Smpx*, *Tmc1*, *Tmie*, *Ush1 g*, *Ush2a*).

Genes enriched in Atoh1-expressing hair cells are involved in biological processes associated with sensory organ and neuronal development

To analyze the function of the genes enriched in *Atoh1*-expressing cells, we made use of the gene ontology (GO) database DAVID (Huang et al., 2009a,b). We focused on 313 genes that were enriched by at least tenfold and showed transcript levels at >3000 RPKM. GO analysis suggests several of these genes are involved in biological process associated with sensory organ development (Table 2; 24 genes, $p = 2.11E-10$), as well as molecular functions that are known to be critical for hair cell development, such as cytoskeletal protein binding (20 genes, $p = 2.68E-04$), channel activity (17 genes, $p = 0.001439$), and motor activity (11 genes, $p = 0.001123$). It is known that sensory hair cells share some properties with neurons, such as synapse formation, synaptic vesicle release, and the regulation of membrane potential. Accordingly, we identified a number of genes associated with neuron differentiation in Atoh1-expressing cells (30 genes, $p = 4.92E-11$) and genes known to be synapse components (23 genes, $p = 2.05E-06$).

In situ validation of genes enriched in Atoh1-expressing cochlear cells

We performed an *in situ* hybridization screen in the P0 mouse cochlea to validate the expression of the genes enriched in Atoh1-expressing cochlear cells. We focused on the 313 genes that showed high ranks in both expression and fold-change in our RNA-seq result (expression level >3000 RPKM, fold-change >10). We chose an expression of RPKM>3000 as an arbitrary filter based on our empirical correlation of RPKM values with a positive signal by *in situ* hybridization. We designed RNA probes for 60 genes from this list, and performed *in situ* hybridization on sections of neonatal mouse cochlea to validate their expression. Surprisingly, only 34 of 60 genes showed specific expression in cochlear hair cells (Table 3; Fig. 2*A*,*B*). Although the remaining 26 genes were expressed in hair cells, we observed additional sites of expression such as supporting cells, Kölliker's organ, or the outer sulcus. Some of the validated hair-cell-specific genes were previously shown to be expressed in the inner ear hair cells or associated with hair-cell development and hearing-defect phenotypes, such as *Lhx3* (Hertzano et al., 2007; Rajab et al., 2008), *Lhfpl5* (Kalay et al., 2006), and *Srrm4* (Nakano et al., 2012). However, many of the genes in our screen have never been studied in the inner ear before (Table 3; Fig. 2*B*). These include the phospholipid binding protein *Annexin A4*, the transcription factor and tumor suppressor Castor (*Casz1*; Charpentier et al., 2013), *RBM24*, an RNA-binding protein implicated in Notch-Delta signaling (Maragh et al., 2014), the Notch receptor modifying enzyme *Mfng*, and the lysosome regulatory gene melanoregulin (*Mreg*). Some genes associated with cytoskeletal binding and motor activity are specifically expressed in cochlear hair cells, such as *Eps8l2*, *Kif21b*, and *Pacsin1* (Table 3; Fig. 2*A*,*B*). Several ion channels also show a hair-cell-restricted expression pattern, such as *Chrna9*, *Chrna10*, *Kcnh6*, and *Scn11a* (Table 3; Fig. 2*A*,*B*). Because *Atoh1* is expressed in all differentiating hair cells in both the auditory and vestibular end organs, we also checked the expression of our validated genes in the vestibular organs. All the genes we found to be specifically expressed in cochlear hair cells also show expression in vestibular hair cells at neonatal stages (Table 3; Fig. 2*C*).

Atoh1 expression initiates in the basal region of the cochlea at E13.5 and spreads along the cochlear duct to the apex (Chen et al., 2002; Cai et al., 2013). However, by the day of birth, *Atoh1* expression is beginning to be downregulated in the hair cells in the basal turn of the cochlea, and this downregulation continues for several days along the length of the cochlea to the apex (Groves et al., 2013). Many of the genes in our screen also show a gradient of expression in hair cells along the apical-basal axis of the cochlear duct (Table 3; Fig. 3). Some genes are expressed more strongly in apical hair cells than in the basal ones at P0 in a similar gradient to *Atoh1*, such as *Srrm4* and *Scn11a* (Fig. 3). These genes are likely to be regulated by Atoh1 (although they may not necessarily be direct targets) and like Atoh1 are downregulated as hair cells mature. In contrast, some genes, such as *Chrna10* and *Mreg*, showed an opposite gradient, with higher expression in basal hair cells compared with apical hair cells (Fig. 3). It is likely that these genes reflect the ongoing basal-apical wave of differentiation of hair cells and represent markers of maturing hair cells. Alternatively, it is possible that some of the genes showing differential apical-basal expression maintain this differential expression as the cochlea matures and might, for example, be involved in regulating tonotopic differences in hair cells along the cochlear duct.

Identification of Atoh1 direct target genes in neonatal cochlear hair cells

Although Atoh1 is both necessary and sufficient for hair cell development, little is known about the molecular function of Atoh1 in hair cells and very few genes have been identified as direct targets of Atoh1 in hair cells. To select potential Atoh1 targets, we cross-referenced our validated hair-cell-specific genes from the P0 cochlea with Atoh1 ChIP-seq datasets from mouse cerebellum and intestine (Klisch et al., 2011; Kim et al., 2014). We found that genes for 233 of 313 hair-cell-enriched transcripts contain Atoh1 binding regions within 10 kb of the transcriptional start site in

Table 1. Previously characterized hair cell genes identified in RNA-seq of P1 Atoh1-GFP+ cells

Gene	Expression in GFP+ cells (RPKM)	Expression in GFP− cells (RPKM)	Fold-change (GFP+ vs GFP−)	*p*	References
Atoh1	19042.084	40.151	474.258	6.23E-130	Bermingham et al., 1999; Chen et al., 2002; Cai et al., 2013
Atp7b	1270.502	64.270	19.768	5.07E-43	Ding et al., 2011
Barhl1	561.825	1.982	12.810	2.54E-73	Li et al., 2002
Bdnf	156.249	0.500	283.453	6.73E-44	Ylikoski et al., 1993; Wheeler et al., 1994
Cacnb2	3669.813	288.711	312.498	5.67E-37	Neef et al., 2009
Calb2	9535.022	754.472	12.711	1.41E-35	Dechesne et al., 1991, 1993
Calm1	200561.183	12606.473	12.638	1.84E-42	Walker et al., 1993
Cdh23	45229.825	347.607	15.909	8.06E-27	Müller, 2008
Celsr3	3879.836	63.198	61.391	6.77E-74	Shima et al., 2002
Chrm4	594.397	33.833	17.568	1.21E-34	Maison et al., 2010
Chrna10	25097.049	49.883	503.115	6.37E-127	Elgoyhen et al., 2001
Chrna9	12030.115	17.392	691.694	2.97E-86	Elgoyhen et al., 1994
Cldn14	446.603	5.849	76.361	1.95E-54	Ben-Yosef et al., 2003
Cldn9	23743.783	1413.451	16.798	4.54E-44	Nunes et al., 2006
Ctbp2	2032.242	8.167	70.452	1.72E-31	Schmitz et al., 2000
Dll1	4063.849	57.682	239.864	8.02E-78	Morrison et al., 1999
Dll3	14095.426	58.764	119.103	4.46E-111	Hartman et al., 2007
Foxj1	10620.589	89.172	133.781	3.26E-93	Yu et al., 2011
Fscn2	8200.816	61.300	205.116	3.45E-45	Shin et al., 2010
Gfi1	10651.143	51.927	52.077	5.78E-105	Wallis et al., 2003
Gpr98	17877.609	343.293	505.351	1.37E-37	McGee et al., 2006
Grxcr1	10736.947	21.247	584.267	1.63E-126	Odeh et al., 2010
Grxcr2	8326.395	14.251	19.827	2.45E-127	Imtiaz et al., 2014
Hes6	27504.001	1387.183	75.974	6.40E-47	Qian et al., 2006
Jag2	41818.936	550.437	573.769	2.72E-58	Lanford et al., 1999
Lhfpl5	32615.662	56.845	452.087	5.35E-135	Longo-Guess et al., 2005
Lhx3	14148.409	31.296	21.718	5.58E-128	Hertzano et al., 2007
Lmo1	12269.408	564.951	277.373	2.62E-49	Deng et al., 2006
Loxhd1	6198.799	22.348	22.931	4.21E-81	Grillet et al., 2009
Mcoln3	4954.974	216.084	618.731	1.38E-51	Di Palma et al., 2002
Myo3a	7421.246	11.994	374.468	1.51E-128	Walsh et al., 2002
Myo3b	10718.111	28.622	15.678	2.62E-123	Merritt et al., 2012
Myo6	176638.988	11266.614	49.712	1.76E-43	Avraham et al., 1997
Myo7a	74294.144	1494.476	380.593	1.83E-37	Hasson et al., 1995
Nhlh1	9522.399	25.020	259.873	4.27E-121	Krüger et al., 2006
Pcp4	26486.479	101.921	602.423	1.04E-115	Thomas et al., 2003
Pou4f3	25774.460	42.785	331.022	2.01E-76	Erkman et al., 1996; Xiang et al., 1998
Ptprq	32675.674	98.711	98.435	2.41E-71	Goodyear et al., 2003
Pvalb	23332.031	237.031	13.086	6.02E-88	Pack and Slepecky, 1995
Pvrl1	21596.648	1650.421	17.679	8.31E-38	Togashi et al., 2011
Rab15	32493.128	1837.926	18.510	2.82E-46	Lai et al., 2011
Rassf4	14720.011	795.253	10.701	5.97E-48	Lai et al., 2011
Selm	26344.158	2461.804	275.918	4.66E-32	Lai et al., 2011
Smpx	11162.484	40.456	195.793	2.51E-113	Yoon et al., 2011
Sstr2	480.310	2.453	161.149	5.35E-66	Bodmer et al., 2012
Strc	11791.437	14.699	802.190	3.93E-55	Verpy et al., 2001
Tmc1	1173.027	98.556	11.902	8.21E-33	Kawashima et al., 2011
Tmc2	1621.727	3.260	497.489	5.12E-103	Kawashima et al., 2011
Tmie	4513.184	369.072	12.228	1.03E-35	Mitchem et al., 2002
Tomt	9470.009	143.013	66.218	2.92E-78	Ahmed et al., 2008
Ush1g	815.769	5.931	137.532	3.25E-60	Kikkawa et al., 2003
Ush2a	32496.762	48.641	668.099	2.46E-40	Pearsall et al., 2002

List of known hair cell genes whose transcripts are enriched in neonatal Atoh1-GFP+ cells. The gene name is indicated, together with the expression and fold-change in expression level (RPKM) compared with GFP− cells and the calculated *p* value for difference between the GFP+ and GFP− populations.

either cerebellar or intestinal ChIP-seq experiments, or have AtEAM binding sites within 5 kb of their transcriptional start site (Klisch et al., 2011). We designed specific primers for the binding locus of nine candidate genes (*Anxa4*, *Chrna10*, *Mgat5b*, *Mreg*, *Pcp4*, *Rasd2*, *Rbm24*, *Scn11a*, and *Srrm4*), as well as *Atoh1*, as it is known to regulate its own expression by binding to an autoregulatory enhancer (Helms et al., 2000; Groves et al., 2013; Jarman and Groves, 2013). We isolated sensory epithelia of P0 $Atoh1^{A1GFP/A1GFP}$ cochleae and performed chromatin immunoprecipitation with camelid nanobodies against the Atoh1-GFP fusion protein. By PCR amplification of the immunoprecipitated DNA, we verified all 10 genes to contain upstream or downstream elements that are directly bound by Atoh1 in the neonatal cochlear sensory epithelium. We also analyzed two genes, *Fgf18* and *Cntn1* that have been shown to be direct targets of Atoh1 in the cerebellum (Klisch et al., 2011), but which are not expressed at significant levels in cochlear hair cells. Neither gene region gave a positive result in our ChIP-PCR experiments (Fig. 4). The nine newly identified Atoh1 direct targets include genes that have been previously reported to be essential for cochlear development,

Table 2. Gene ontology analysis of genes identified in RNA-seq of P1 Atoh1-GFP+ cells

GO category	GO term	No. of genes	Genes
Biological process	Neuron differentiation	30	*Myo7a, Uchl1, Jag2, Atoh1, Mcoln3, Lhx3, Pou4f3, Rtn4rl2, Gfi1, Nefl, Kndc1, Ush2a, Cdh23, Tomt, Myo6, Fscn2, Kif5c, Celsr3, Dll1, Gpr98, Sall3, Bbs1, Lhfpl5, 6530402F18Rik, 2610109H07Rik, Chrnb2, Ngfr, Slitrk6, Wnt7a, Grk1*
	Sensory organ development	24	*Tomt, Myo6, Fscn2, Cryab, Myo7a, Tmie, Jag2, Dll1, Pax2, Prph2, Prox1, Gpr98, Ptprq, Lhfpl5, Atoh1, Pvrl1, Chrna9, Mcoln3, Pou4f3, Gfi1, Chrna10, Ush2a, Cdh23, Grk1*
Molecular function	Calcium ion binding	32	*Spock2, Clstn3, Jag2, Cacnb2, Dlk2, Cdh1, Calb2, Necab2, Mmp24, Syp, Pvalb, Pcp4, Pls1, Cib2, S100a1, Cdh23, Dtna, Tesc, Hpcal1, Celsr3, Dll1, Actn3, Anxa4, Gas6, S100a13, Gpr98, Pkd2l1, Chga, Umodl1, Cadps2, Dll4, Calm1*
	Cytoskeletal protein binding	20	*Obscn, Myo6, Baiap2l2, Fscn2, Myo3a, Myo7a, Myo3b, Lmo7, Actn3, Rph3a, Gpr98, Pacsin1, Fhod3, Myo16, Pls1, AI428936, Lmod1, Eps8l2, Ush2a, Tmod1*
	Channel activity	17	*Scn1b, Cacnb2, Pkd2l1, Kcnmb2, Kcna10, Accn4, Chrna9, Mcoln3, P2rx3, Kcnh6, Kcnf1, Scn11a, Chrnb2, Kcnh2, Chrna1, Chrna10, Chrng*
	Motor activity	11	*Myo6, Kif27, Myo3a, Myo7a, Myo3b, Kif5c, Myo16, Kif19a, Dynlrb2, Kif21b, Dnaic2*
Cell component	Cell junction	24	*Gpr156, Ica1, Cldn9, Dlgap3, Rimbp2, Ctnnd2, Lmo7, Cdh1, Rims2, Rph3a, Calb2, Syp, Cbln1, Pvrl1, Cadps2, Pcp4, Snph, Chrnb2, Ssx2ip, Tjp3, Chrna1, Chrna10, Chrng, Dtna*
	Synapse	23	*Gpr156, Rab3b, Ica1, Cplx1, Myo6, Dlgap3, Clstn3, Myo7a, Rimbp2, Rims2, Rph3a, Syp, Cbln1, Chrna9, Cadps2, Snph, Chrnb2, Chrna1, Chrna10, Nefm, Chrng, Cdh23, Dtna*

Gene ontology analysis of the 313 genes whose transcripts showed high ranks in both expression and fold-change in our RNA-seq result (expression level >3000 RPKM, fold-change >10). A representative number of GO categories and terms are shown with >10 genes per category.

Table 3. Summary of hair cell genes validated by *in situ* hybridization

	Expression	Fold-change	P0 vestibule	Gradient (high to low)	Published HC gene	ChIP-seq	Atoh1 direct targets	Expression in Atoh1-CKO
Anxa4	58650.61	74.378	HC	Base to apex	No	Intestine	Yes	Decreased
Atoh1	19042.08	474.258	HC	Apex to base	Yes	Cerebellum, intestine	Yes	Decreased
Calb2	9535.022	12.638	HC	Not observed	Yes	Cerebellum	ND	ND
Casz1	9969.698	85.483	HC	Not observed	No	Cerebellum, intestine	ND	ND
Chrna10	25097.05	503.115	HC	Base to apex	Yes	Intestine	Yes	ND
Chrna9	12030.11	691.694	HC	Not observed	Yes	None	ND	ND
Eps8l2	15530.19	64.052	HC	Base to apex	Yes	Intestine	ND	ND
Grxcr2	8326.395	584.267	HC	Not observed	Yes	None	ND	No change
Kcnh6	12791.54	154.773	HC	Not observed	No	Intestine	ND	ND
Kif21b	8369.936	11.176	HC	Base to apex	No	Cerebellum, intestine	ND	ND
Lhfpl5	32615.66	573.769	HC	Not observed	Yes	Intestine	ND	ND
Lhx3	14148.41	452.087	HC	Not observed	Yes	Intestine	ND	Decreased
Mfng	10493.52	76.080	HC	Not observed	No	Cerebellum, intestine	ND	Decreased
Mgat5b	22037.06	214.706	HC	Not observed	No	Cerebellum, intestine	Yes	No change
Mreg	16063.03	139.686	HC	Base to apex	No	Cerebellum, intestine	Yes	No change
Mycl1	26009.33	41.131	HC	Not observed	Yes	Cerebellum, intestine	ND	ND
Myo3b	10718.11	374.468	HC	Base to apex	Yes	Cerebellum, intestine	ND	ND
Naca	10408.7	24.968	ND	Base to apex	No	Cerebellum, intestine	ND	ND
Pacsin1	4302.44	40.762	HC	Base to apex	No	Cerebellum, intestine	ND	ND
Pcp4	26486.48	259.873	HC	Base to apex	Yes	Cerebellum	Yes	No change
Ptgir	4722.92	133.553	No	Base to apex	No	None	ND	ND
Ptprq	32675.67	331.022	HC	Base to apex	Yes	None	ND	No change
Rab11fip1	3025.383	89.836	HC	Not observed	No	Intestine	ND	ND
Rasd2	127825.8	507.234	HC	Not observed	No	Cerebellum, intestine	Yes	Decreased
Rbm24	16001.61	229.243	HC	Not observed	No	Intestine	Yes	Decreased
Scn11a	11604.04	797.871	HC	Apex to base	Yes	Cerebellum	Yes	Decreased
Sema5b	32913.11	29.366	ND	Base to apex	No	Cerebellum, intestine	ND	ND
Slc6a11	13126.97	309.753	HC	Not observed	No	Cerebellum, intestine	ND	No change
Smpx	11162.48	275.918	HC	Not observed	Yes	Cerebellum	ND	ND
Srrm4	8899.872	164.984	HC	Apex to base	Yes	Cerebellum, intestine	Yes	Decreased
Stard10	30766.48	25.747	HC	Not observed	No	Intestine	ND	ND
Thsd7b	28906.74	298.100	HC	Not observed	No	Intestine	ND	No change
Ttc21a	16745.86	329.525	HC	Not observed	No	Cerebellum, intestine	ND	ND
Umodl1	10437.93	331.222	HC	Not observed	No	Cerebellum, intestine	ND	ND

Summary of genes whose specific expression in hair cells was validated by *in situ* hybridization. Gene name, expression level (RPKM), and fold-change over GFP− cells are indicated, together with expression pattern in the cochlea or vestibular system. If a transcript showed a gradient of expression in the cochlea, this is indicated. The table also lists whether each gene was identified as an Atoh1 target by ChIP-seq in either the cerebellum (Klisch et al., 2011) or small intestine (Kim et al., 2014), as well as whether the gene was shown to be a direct target of Atoh1 in the cochlea by ChIP-PCR (Fig. 5). Finally, the expression of direct Atoh1 target genes was measured *in vivo* 24 h after deletion of *Atoh1* (Fig. 5).

HC, Hair cell; IHC, inner hair cell; ND, not determined.

such as *Chrna10* and *Srrm4* (Simmons and Morley, 2011; Nakano et al., 2012), and genes that have not previously been described in ear development, such as *Anxa4*, *Mgat5b*, *Mreg*, *Pcp4*, *Rasd2*, *Rbm24*, and *Scn11a* (Fig. 4).

We have previously shown that Atoh1 protein is quite unstable in cochlear hair cells, as conditional deletion of *Atoh1* using the Cre-Lox system leads to hair cell death 12 h after the onset of Cre-mediated recombination (Cai et al., 2013). We tested to what

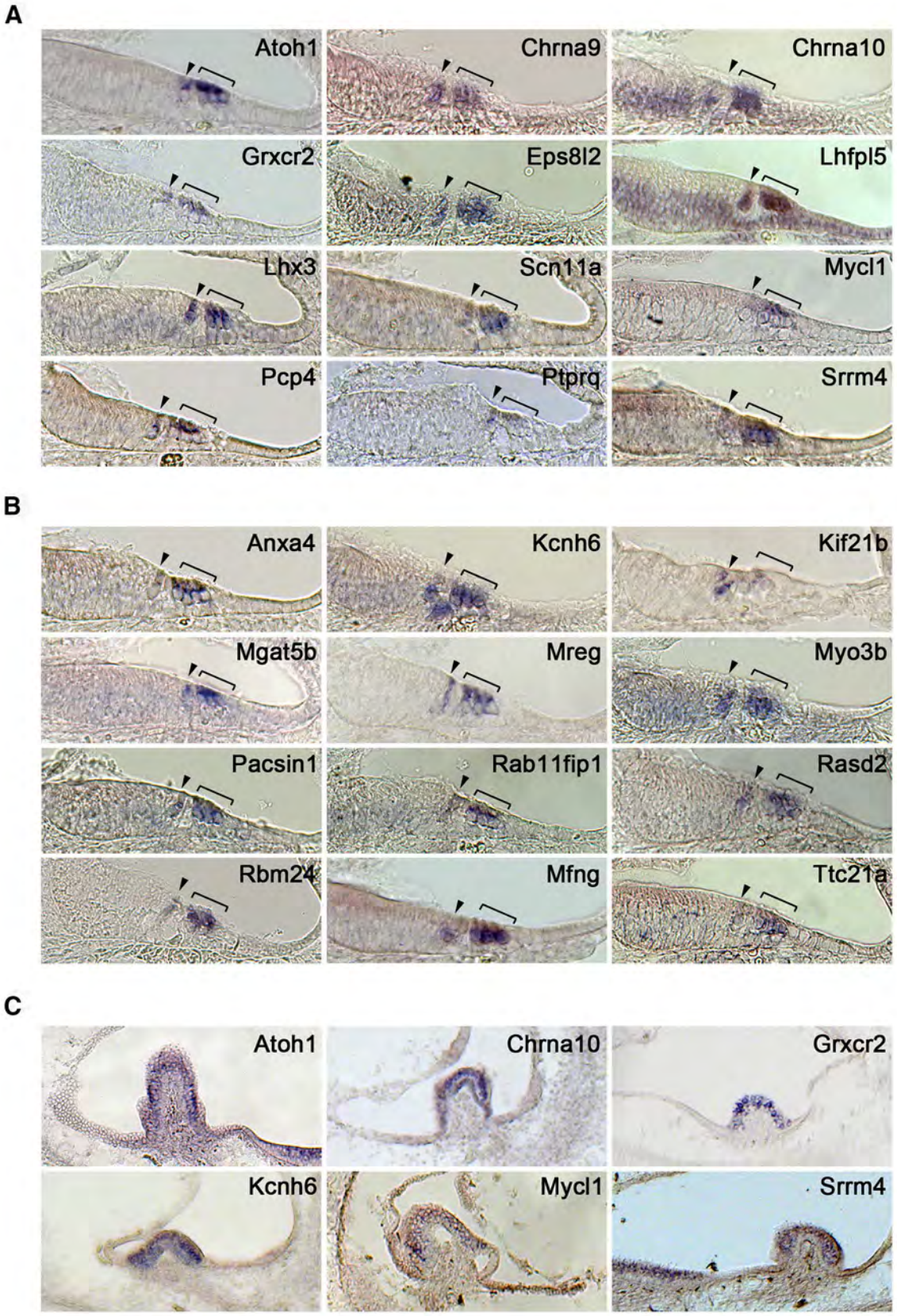

Figure 2. *In situ* hybridization validation of transcripts enriched in Atoh1-GFP+ cells. ***A***, Representative sample of 12 genes whose expression has previously been reported in hair cells. Images are taken from the basal turn of a neonatal mouse cochlea. ***B***, Representative sample of 12 genes whose expression has not previously been reported in hair cells. Images are taken from the basal turn of a neonatal mouse cochlea. Brackets mark the outer hair cell region; arrowhead marks the inner hair cell region. ***C***, Expression of sample of enriched transcripts in the cristae of the neonatal mouse vestibular system.

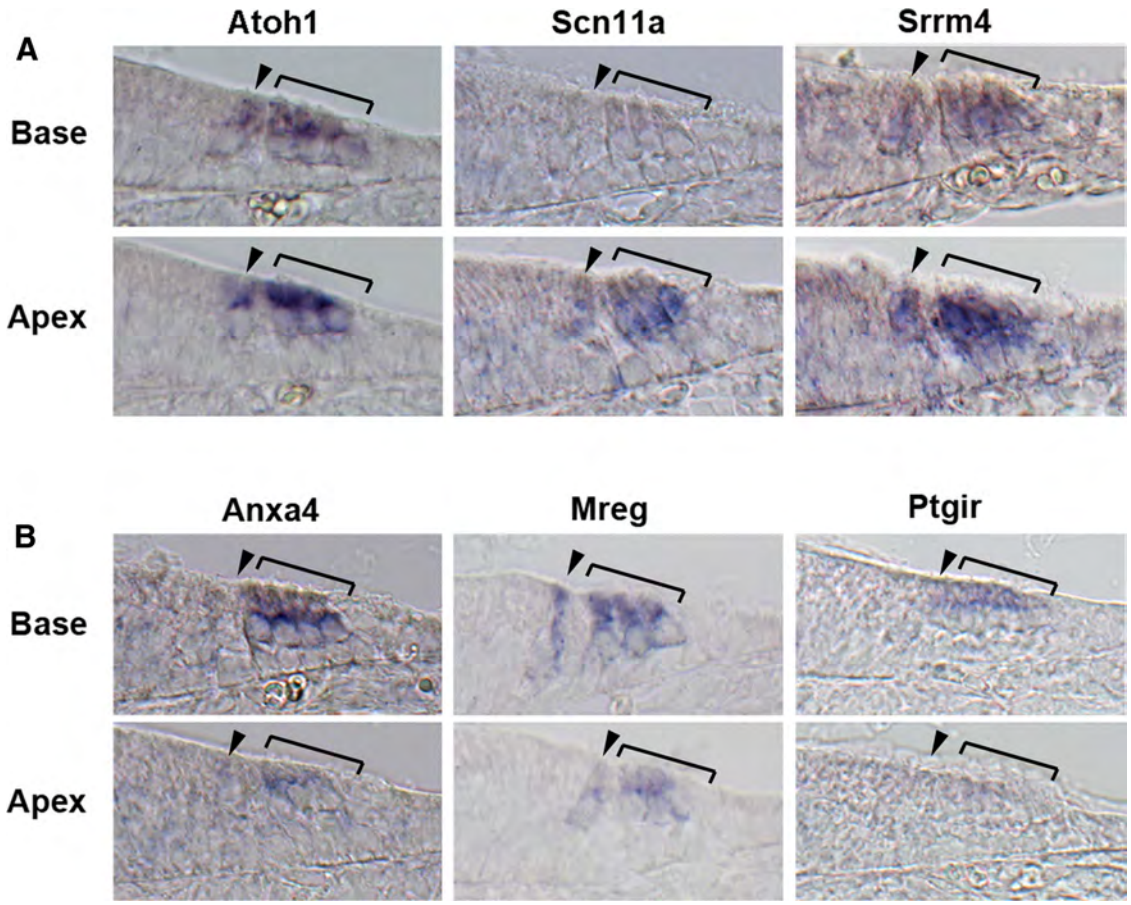

Figure 3. Examples of hair cell transcripts expressed in gradients along the neonatal cochlea. ***A***, *Atoh1*, *Scn11a*, and *Srrm4* are expressed more strongly in the apex than the base of the cochlea, consistent with their being downregulated as hair cells mature. ***B***, *Anxa4*, *Mreg*, and *Ptgir* are expressed more strongly in the base than the apex, consistent with their upregulation and maintenance as hair cells mature. Brackets mark the outer hair cell region; arrowhead marks the inner hair cell region.

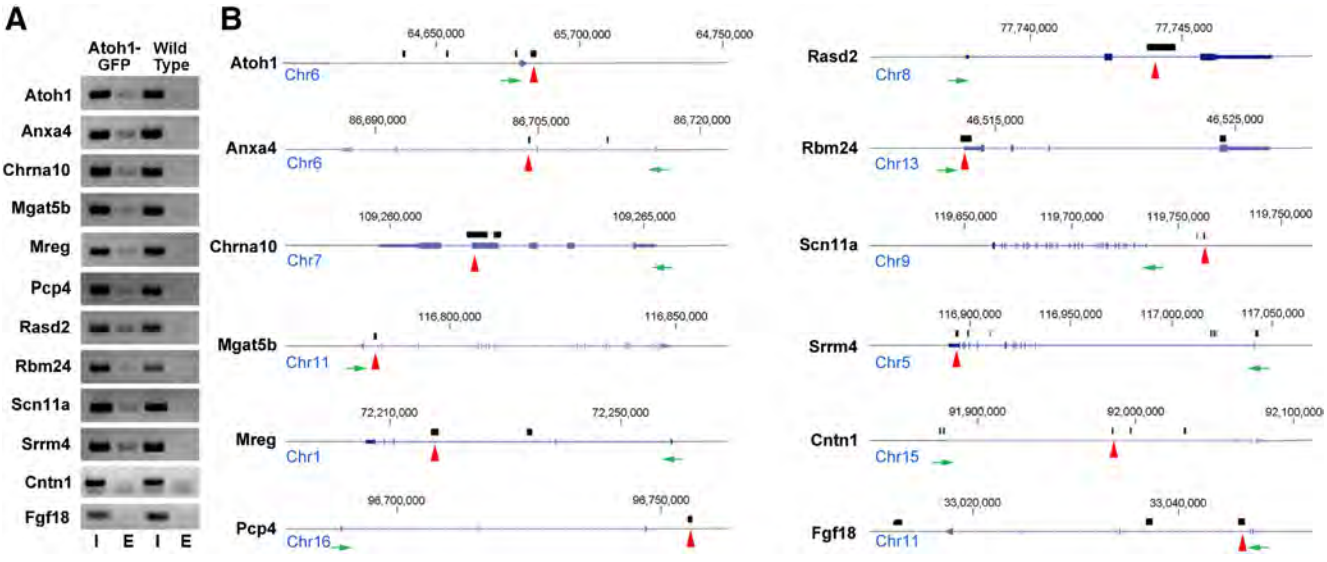

Figure 4. ***A***, Verification of direct targets of Atoh1 by ChIP-PCR. Ten genes that were identified as candidate Atoh1 targets (including *Atoh1* itself as a positive control) were analyzed by chromatin immunoprecipitation from sensory epithelium dissected from neonatal *Atoh1*$^{A1GFP/A1GFP}$ mice. Wild-type mice were used as a negative control. In addition, ChIP-PCR for two genes (*Fgf18* and *Cntn1*) that are directly regulated by Atoh1 in the cerebellum but are not expressed in hair cells were also used as a negative control. PCR amplification of candidate Atoh1 binding regions was performed as described in Materials and Methods. Input DNA and experimental lanes are indicated by I and E, respectively. ***B***, Schematic diagram showing the chromosomal location and structure of each gene, the direction of transcription (green arrows), and the location of Atoh1 binding sites (black bars) identified by ChIP-Seq from cerebellum (*Atoh1*, *Mgat5b*, *Mreg*, *Pcp4*, *Rasd2*, *Scn11a*, *Srrm4*, *Cntn1*, *Fgf18*; Klisch et al., 2011) or intestine (*Anxa4, Chrna10, Rbm24*; Kim et al., 2014). Regions used for ChIP-PCR in ***A*** are shown with red arrows.

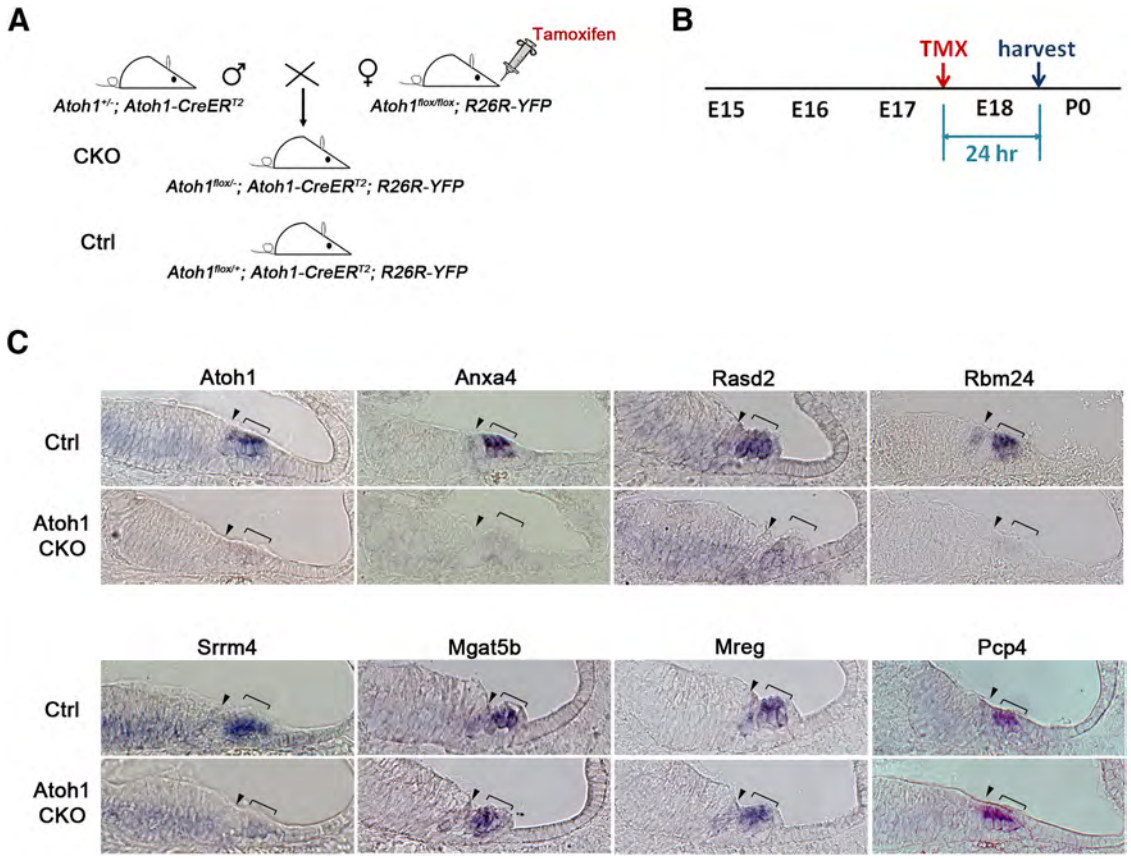

Figure 5. Some, but not all Atoh1 target genes are rapidly downregulated after deletion of *Atoh1*. ***A***, Breeding scheme to generate *Atoh1*-CKO mice. Female *Atoh1*$^{flox/flox}$; *R26R-YFP* mice were mated with *Atoh1*$^{\pm}$; *Atoh1-CreER*^{T2} males to generate mice that carried the *CreER*^{T2} allele, one copy of the *R26R-YFP* Cre reporter and either an *Atoh1*$^{flox/+}$ (50%) or *Atoh1*$^{flox/-}$ (50%) allele. Use of the *R26R-YFP* Cre reporter provides a readout of the leakiness, speed, and efficiency of the system. ***B***, Pregnant dams received one pulse of tamoxifen/progesterone (TMX) at E17.5, followed by kill 24 h later. ***C***, Four of seven genes tested (*Anxa4*, *Rasd2*, *Rbm24*, and *Srrm4*) showed rapid downregulation of transcripts 24 h after tamoxifen administration. However, three other genes (*Mgat5b*, *Mreg*, and *Pcp4*) were still expressed 24 h after tamoxifen administration. Brackets mark the outer hair cell region; arrowhead marks the inner hair cell region.

extent our verified Atoh1 target genes were sensitive to the loss of *Atoh1* by conditionally deleting *Atoh1* from hair cells at E17.5 as previously described (Cai et al., 2013). We crossed *Atoh1*$^{\pm}$; *Atoh1-CreER*^{T2} males with *Atoh1*$^{flox/flox}$; *R26R-YFP* female mice and administered tamoxifen and progesterone to female mice on the 17th day of pregnancy by oral gavage to generate *Atoh1* CKO (*Atoh1*$^{flox/-}$; *Atoh1-CreER*^{T2}; *R26R-YFP*) and control (*Atoh1*$^{flox/+}$; *Atoh1-CreER*^{T2}; *R26R-YFP*) animals. We collected embryos 24 h later, and examined the expression of seven verified Atoh1 target genes, as well as *Atoh1* itself as a positive control. Four genes (*Anxa4*, *Rasd2*, *Rbm24*, and *Srrm4*) were rapidly and completely downregulated in hair cells 24 h after deletion of *Atoh1* (Fig. 5). However, three other genes (*Mgat5b*, *Mreg*, and *Pcp4*) continued to be expressed in *Atoh1* CKO hair cells after 24 h at levels that were indistinguishable from their control counterparts. This persistence may simply reflect the stability of mRNA transcripts for these genes, or may indicate that these genes require Atoh1 for their initiation but not maintenance, due to the action of other transcription factors that can maintain transcription even after Atoh1 is downregulated.

Although Atoh1 is necessary and to some degree sufficient for hair cell development in the inner ear, its function is transient as it is downregulated shortly after birth (Groves et al., 2013). However, some of the genes we have verified to be direct targets of Atoh1, such as *Chrna10*, continue to be expressed in mature outer hair cells after Atoh1 ceases to be expressed (Elgoyhen et al., 2001), and were expressed strongly in basal regions of the cochlea even as *Atoh1* itself was being downregulated (Fig. 3). It is likely that Atoh1 participates in the assembly of transcriptional complexes at these loci, which remain active after Atoh1 expression ceases. For example, the *Pou4f3* gene, which is expressed in hair cells throughout life (Erkman et al., 1996; Xiang et al., 1998), has 5′ regulatory regions that are directly bound and regulated by Atoh1 (Masuda et al., 2011) but these regions also contain sites for other transcription factors such as Etv4, N-Myc, and Ets2 (Ikeda et al., 2015). It is possible that at least three of our verified Atoh1 targets, *Mgat5b*, *Mreg*, and *Pcp4* may be regulated in this way, as they continued to be expressed in the hair cells of *Atoh1* CKO mice (Fig. 3). Alternatively, it is also possible that the transcripts for these genes are quite stable and remain detectable in hair cells at least 24 h after loss of Atoh1 protein.

Discussion

We present one of the first RNA-seq studies to characterize purified cell populations from the mammalian cochlea. We were able to obtain high quality RNA-seq libraries from 100,000 purified Atoh1-GFP^{+} hair cells that gave excellent paired-end mapping of sequenced reads. A number of previous studies have produced valuable gene expression information from microarray profiling of different populations from the inner ear (Sato et al., 2009; Hertzano et al., 2011; Sinkkonen et al., 2011; Son et al., 2012). Our study, together with

other studies such as the recently described SHIELD database (shield.hms.harvard.edu) suggest that RNA-seq analysis of purified cell populations can be successfully accomplished with small numbers of inner ear hair cells; for example, we have recently been able to obtain RNA-seq data of similar quality from as few as 10,000 cells purified from the cochlea using standard RNA-seq library preparation reagents (M. L. Basch and A. K. Groves, unpublished observations).

We found 614 transcripts to be significantly enriched in hair cells, and of these at least 10% have been reported previously to be specifically expressed in hair cells. From our initial list of 614 genes, we selected 313 genes that were enriched >10-fold in Atoh1$^+$ cells, and which gave expression values of >3000 RPKM. Strikingly, when we analyzed 60 genes from this list by *in situ* hybridization, only ~50% (34 genes) showed exclusive and specific expression in hair cells. We note that one of our criteria for selecting genes for validation was the fold-change between Atoh1-GFP$^+$ hair cells and all other cell types in the ear. As such, it follows that a high degree of transcript enrichment in hair cells does not preclude that the transcript in question is present in other cell types in the ear; simply, that it is expressed at lower levels. This emphasizes that validation of RNA-seq data by analysis of mRNA *in situ* expression is a crucial step in the identification and confirmation of truly cell-type specific transcripts, even in cell populations enriched to >90% purity.

Our transcriptomic analysis was performed on hair cells purified from the newborn mouse cochlea. At this age, almost all hair cells have differentiated in the organ of Corti, although they continue to mature over the next 14 d until the onset of hearing at ~2 weeks of age. This maturation is reflected in many ways, for example, the elaboration of the stereociliary hair bundle (Frolenkov et al., 2004), the acquisition of functional mechanotransduction apparatus (Lelli et al., 2009), mature ion currents, and the divergence in morphology and function of inner and outer hair cells (Belyantseva et al., 2000). Some genes are specifically expressed in either inner or outer hair cells from an early age, for example, *Fgf8* is restricted to inner hair cells shortly after the onset of *Atoh1* expression (Jacques et al., 2007), and we observed *Kif21b* expression exclusively in inner hair cells at P1 (Fig. 2*B*). However, other genes, such as *Chrna9*, begin to be expressed in all cochlear hair cells before becoming restricted to outer hair cells (Elgoyhen et al., 1994; Liu et al., 2014; Fig. 2*A*), which may reflect radial (neural–abneural) gradients of differentiation signals. It will be of great interest to determine the transcriptional regulators that establish hair-cell-specific patterns of gene expression, either in development or during hair cell maturation.

At present, very little is known about changes in gene expression that accompany and regulate the maturation of hair cells. Our data suggest that at least some components of mature hair cells are already expressed in neonatal hair cells. First, gene ontology analysis of significantly enriched hair cell genes in our study identified cohorts of genes involved in motor activity, channel activity and calcium binding, synapse formation and function, in addition to genes associated with neural or sensory organ development (Table 2). Second, we were able to detect transcripts for some previously characterized components of the hair bundle (Shin et al., 2013), such as *Apba1*, *Calb2*, *Eps8l2*, *Fscn2*, *Hspa4l*, *Myo3b*, and *Stard10* in addition to the unconventional myosins *Myo6* and *Myo7a* that are expressed early in differentiating hair cells. Third, we compared our data to a recent study that used Affymetrix microarrays to identify the transcriptomes of 2000 individually isolated inner and outer hair cells from 25- to 30-d-old mice (Liu et al., 2014). Comparison of these transcriptomes to our neonatal hair cell data suggest that >80 genes expressed in neonatal hair cells continue to be expressed in mature inner or outer hair cells. Finally, we were also able to identify transcripts for 22 genes identified in syndromic or nonsyndromic forms of deafness.

The challenge and utility of identifying Atoh1 targets in hair cells

Atoh1 plays a central role in the differentiation and survival of hair cells (Jarman and Groves, 2013), and has been proposed as a candidate for gene therapy to restore hair cells lost through injury or aging (Baker et al., 2009; Husseman and Raphael, 2009). Discovering the direct transcriptional targets of Atoh1 is key to understanding its function and possible reasons for its reduced efficacy in promoting hair-cell formation in the aging ear (Kelly et al., 2012; Liu et al., 2012). However, genome-wide analysis of Atoh1 binding sites in hair cells by techniques, such as ChIP-seq, is confounded by the relatively small numbers of hair cells per cochlea and the fact that hair cells represent a small fraction of the total cell types in the cochlear duct. In contrast, it has been possible to obtain ChIP-seq data from Atoh1-expressing cerebellar granule cells (Klisch et al., 2011) and intestinal secretory cells (Kim et al., 2014). In an attempt to identify new Atoh1 targets in hair cells, we interrogated the transcriptome of cochlear hair cells obtained by RNA-sequencing to identify loci that are strongly and specifically expressed in Atoh1$^+$ hair cells and which have enhancers containing Atoh1 consensus binding sites (AtEAMs; Klisch et al., 2011), or which have been shown to be occupied by Atoh1 in the cerebellum or gut by ChIP-seq. This approach allowed us to identify 233 candidate Atoh1 target genes, of which 68 were common to our hair cell transcriptome and to ChIP-seq analyses from the cerebellum and gut. We verified 10 genes, including Atoh1 itself, as strong candidates to be direct targets of Atoh1. Previous studies have also identified several other direct targets of Atoh1 in hair cells, such as *Pou4f3* (Masuda et al., 2011; Ikeda et al., 2015), *Selm*, *Rassf4*, and *Rab15* (Lai et al., 2011).

Atoh1 can regulate a large and diverse array of genes in different cell types with functions including transcriptional control, cell-cycle regulation, cell migration, metabolic control, and even housekeeping functions (Klisch et al., 2011; Lai et al., 2011). These processes are not common to all *Atoh1*-expressing cells, for example, cerebellar granule neuron precursors are both migratory and proliferative, whereas hair cells are not. Clearly then, the cellular context in which Atoh1 functions will determine its selection of targets. Although Atoh1 is expressed in all inner ear hair cells, it is not known whether Atoh1 has distinct targets or overlapping targets in different types of hair cell, for example, auditory versus vestibular hair cells, inner hair cells versus outer hair cells, or type I versus type II vestibular hair cells, or instead simply regulates common, generic aspects of hair-cell development. All 10 of our validated Atoh1 targets showed comparable expression in inner and outer hair cells, and were also expressed in vestibular hair cells (Table 3); although the expression of many more validated Atoh1 targets will need to be tested to determine whether this trend is maintained. It is also possible that Atoh1 establishes a generic pattern of hair-cell gene expression, with later transcription factors modulating these targets in a hair-cell-specific manner after Atoh1 expression is downregulated.

Progress in identifying direct targets of Atoh1 may shed light on the function of this gene in regeneration as well as normal hair-cell differentiation. Ectopic expression of *Atoh1* in the inner

ear, either *in vivo* or *in vitro*, can lead to the formation of ectopic hair cells (Zheng and Gao, 2000; Kawamoto et al., 2003; Izumikawa et al., 2005; Gubbels et al., 2008; Kelly et al., 2012; Liu et al., 2012). Moreover, *Atoh1* is rapidly upregulated in supporting cells of nonmammalian vertebrates as a consequence of hair cell loss (Cafaro et al., 2007; Ma et al., 2008; Ma and Raible, 2009; Lewis et al., 2012). However, recent studies in mice suggest that the ability of inner ear cells to transdifferentiate into hair cells in the presence of ectopic Atoh1 declines with age (Kelly et al., 2012; Liu et al., 2012). There are a number of possible explanations for this decline, for example, the presence or absence of post-translational modifications of Atoh1 itself (Mulvaney and Dabdoub, 2012), an age-dependent upregulation of inhibitors of Atoh1, such as Id HLH factors, or an age-dependent decline in transcription factors or cofactors that cooperate with Atoh1 to activate hair cell genes (Ikeda et al., 2015). Finally, it is possible that direct epigenetic modification of Atoh1 target genes renders them unavailable for transcription, even in the presence of exogenously expressed Atoh1 (Groves et al., 2013). Our identification of direct Atoh1 targets in hair cells in the present study may allow the testing of these hypotheses.

Notes

Supplemental material for this article is available at **https://www.bcm.edu/research/labs/andrew-groves/publications**. Seven data tables and a legend document describe qPCR and PCR primers, a list of all 614 hair cell-enriched genes, 233 candidate *Atoh1* target genes, and comparisons of our hair cell-enriched genes with known deafness genes, genes identified in adult hair cells and genes identified in chick utricle hair cells, and expression levels of 19218 transcripts in Atoh1-GFP$^+$ hair cells at P1. This material has not been peer reviewed.

References

Ahmed ZM, Masmoudi S, Kalay E, Belyantseva IA, Mosrati MA, Collin RW, Riazuddin S, Hmani-Aifa M, Venselaar H, Kawar MN, Tlili A, van der Zwaag B, Khan SY, Ayadi L, Riazuddin SA, Morell RJ, Griffith AJ, Charfedine I, Caylan R, Oostrik J, et al. (2008) Mutations of LRTOMT, a fusion gene with alternative reading frames, cause nonsyndromic deafness in humans. Nat Genet 40:1335–1340. CrossRef Medline

Anders S, Huber W (2010) Differential expression analysis for sequence count data. Genome Biol 11:R106. CrossRef Medline

Avraham KB, Hasson T, Sobe T, Balsara B, Testa JR, Skvorak AB, Morton CC, Copeland NG, Jenkins NA (1997) Characterization of unconventional MYO6, the human homologue of the gene responsible for deafness in Snell's waltzer mice. Hum Mol Genet 6:1225–1231. CrossRef Medline

Baker K, Brough DE, Staecker H (2009) Repair of the vestibular system via adenovector delivery of Atoh1: a potential treatment for balance disorders. Adv Otorhinolaryngol 66:52–63. Medline

Belyantseva IA, Adler HJ, Curi R, Frolenkov GI, Kachar B (2000) Expression and localization of prestin and the sugar transporter GLUT-5 during development of electromotility in cochlear outer hair cells. J Neurosci 20:RC116. Medline

Ben-Arie N, Bellen HJ, Armstrong DL, McCall AE, Gordadze PR, Guo Q, Matzuk MM, Zoghbi HY (1997) Math1 is essential for genesis of cerebellar granule neurons. Nature 390:169–172. CrossRef Medline

Benjamini Y, Hochberg Y (1995) Controlling the false discovery rate: a practical and powerful approach to multiple testing. J R Stat Soc Ser B 57:289–300.

Ben-Yosef T, Belyantseva IA, Saunders TL, Hughes ED, Kawamoto K, Van Itallie CM, Beyer LA, Halsey K, Gardner DJ, Wilcox ER, Rasmussen J, Anderson JM, Dolan DF, Forge A, Raphael Y, Camper SA, Friedman TB (2003) Claudin 14 knockout mice, a model for autosomal recessive deafness DFNB29, are deaf due to cochlear hair cell degeneration. Hum Mol Genet 12:2049–2061. CrossRef Medline

Bermingham NA, Hassan BA, Price SD, Vollrath MA, Ben-Arie N, Eatock RA, Bellen HJ, Lysakowski A, Zoghbi HY (1999) Math1: an essential gene for the generation of inner ear hair cells. Science 284:1837–1841. CrossRef Medline

Birren SJ, Lo L, Anderson DJ (1993) Sympathetic neuroblasts undergo a developmental switch in trophic dependence. Development 119:597–610. Medline

Bodmer D, Brand Y, Radojevic V (2012) Somatostatin receptor types 1 and 2 in the developing mammalian cochlea. Dev Neurosci 34:342–353. CrossRef Medline

Cafaro J, Lee GS, Stone JS (2007) Atoh1 expression defines activated progenitors and differentiating hair cells during avian hair cell regeneration. Dev Dyn 236:156–170. CrossRef Medline

Cai T, Seymour ML, Zhang H, Pereira FA, Groves AK (2013) Conditional deletion of Atoh1 reveals distinct critical periods for survival and function of hair cells in the organ of Corti. J Neurosci 33:10110–10122. CrossRef Medline

Charpentier MS, Taylor JM, Conlon FL (2013) The CASZ1/Egfl7 transcriptional pathway is required for RhoA expression in vascular endothelial cells. Small GTPases 4:231–235. CrossRef Medline

Chen P, Johnson JE, Zoghbi HY, Segil N (2002) The role of Math1 in inner ear development: uncoupling the establishment of the sensory primordium from hair cell fate determination. Development 129:2495–2505. Medline

Dahl JA, Collas P (2009) MicroChIP: chromatin immunoprecipitation for small cell numbers. Methods Mol Biol 567:59–74. CrossRef Medline

Dechesne CJ, Winsky L, Moniot B, Raymond J (1993) Localization of calretinin mRNA in rat and guinea pig inner ear by *in situ* hybridization using radioactive and non-radioactive probes. Hear Res 69:91–97. CrossRef Medline

Dechesne CJ, Winsky L, Kim HN, Goping G, Vu TD, Wenthold RJ, Jacobowitz DM (1991) Identification and ultrastructural localization of a calretinin-like calcium-binding protein (protein 10) in the guinea pig and rat inner ear. Brain Res 560:139–148. CrossRef Medline

Deng M, Pan L, Xie X, Gan L (2006) Differential expression of LIM domain-only (LMO) genes in the developing mouse inner ear. Gene Expr Patterns 6:857–863. CrossRef Medline

Di Palma F, Belyantseva IA, Kim HJ, Vogt TF, Kachar B, Noben-Trauth K (2002) Mutations in Mcoln3 associated with deafness and pigmentation defects in varitint-waddler (Va) mice. Proc Natl Acad Sci U S A 99:14994–14999. CrossRef Medline

Ding D, He J, Allman BL, Yu D, Jiang H, Seigel GM, Salvi RJ (2011) Cisplatin ototoxicity in rat cochlear organotypic cultures. Hear Res 282:196–203. CrossRef Medline

Elgoyhen AB, Johnson DS, Boulter J, Vetter DE, Heinemann S (1994) Alpha 9: an acetylcholine receptor with novel pharmacological properties expressed in rat cochlear hair cells. Cell 79:705–715. CrossRef Medline

Elgoyhen AB, Vetter DE, Katz E, Rothlin CV, Heinemann SF, Boulter J (2001) alpha10: a determinant of nicotinic cholinergic receptor function in mammalian vestibular and cochlear mechanosensory hair cells. Proc Natl Acad Sci U S A 98:3501–3506. CrossRef Medline

Erkman L, McEvilly RJ, Luo L, Ryan AK, Hooshmand F, O'Connell SM, Keithley EM, Rapaport DH, Ryan AF, Rosenfeld MG (1996) Role of transcription factors Brn-3.1 and Brn-3.2 in auditory and visual system development. Nature 381:603–606. CrossRef Medline

Frolenkov GI, Belyantseva IA, Friedman TB, Griffith AJ (2004) Genetic insights into the morphogenesis of inner ear hair cells. Nat Rev Genet 5:489–498. CrossRef Medline

Goodyear RJ, Legan PK, Wright MB, Marcotti W, Oganesian A, Coats SA, Booth CJ, Kros CJ, Seifert RA, Bowen-Pope DF, Richardson GP (2003) A receptor-like inositol lipid phosphatase is required for the maturation of developing cochlear hair bundles. J Neurosci 23:9208–9219. Medline

Grillet N, Schwander M, Hildebrand MS, Sczaniecka A, Kolatkar A, Velasco J, Webster JA, Kahrizi K, Najmabadi H, Kimberling WJ, Stephan D, Bahlo M, Wiltshire T, Tarantino LM, Kuhn P, Smith RJ, Müller U (2009) Mutations in LOXHD1, an evolutionarily conserved stereociliary protein, disrupt hair cell function in mice and cause progressive hearing loss in humans. Am J Hum Genet 85:328–337. CrossRef Medline

Groves AK, George KM, Tissier-Seta JP, Engel JD, Brunet JF, Anderson DJ (1995) Differential regulation of transcription factor gene expression and phenotypic markers in developing sympathetic neurons. Development 121:887–901. Medline

Groves AK, Zhang KD, Fekete DM (2013) The genetics of hair cell development and regeneration. Annu Rev Neurosci 36:361–381. CrossRef Medline

Gubbels SP, Woessner DW, Mitchell JC, Ricci AJ, Brigande JV (2008) Functional auditory hair cells produced in the mammalian cochlea by in utero gene transfer. Nature 455:537–541. CrossRef Medline

Harland RM (1991) *In situ* hybridization: an improved whole-mount

method for *Xenopus* embryos. Methods Cell Biol 36:685–695. CrossRef Medline

Hartman BH, Hayashi T, Nelson BR, Bermingham-McDonogh O, Reh TA (2007) Dll3 is expressed in developing hair cells in the mammalian cochlea. Dev Dyn 236:2875–2883. CrossRef Medline

Hasson T, Heintzelman MB, Santos-Sacchi J, Corey DP, Mooseker MS (1995) Expression in cochlea and retina of myosin VIIa, the gene product defective in Usher syndrome type 1B. Proc Natl Acad Sci U S A 92:9815–9819. CrossRef Medline

Helms AW, Abney AL, Ben-Arie N, Zoghbi HY, Johnson JE (2000) Autoregulation and multiple enhancers control Math1 expression in the developing nervous system. Development 127:1185–1196. Medline

Hertzano R, Dror AA, Montcouquiol M, Ahmed ZM, Ellsworth B, Camper S, Friedman TB, Kelley MW, Avraham KB (2007) Lhx3, a LIM domain transcription factor, is regulated by Pou4f3 in the auditory but not in the vestibular system. Eur J Neurosci 25:999–1005. CrossRef Medline

Hertzano R, Elkon R, Kurima K, Morrisson A, Chan SL, Sallin M, Biedlingmaier A, Darling DS, Griffith AJ, Eisenman DJ, Strome SE (2011) Cell type-specific transcriptome analysis reveals a major role for Zeb1 and miR-200b in mouse inner ear morphogenesis. PLoS Genet 7:e1002309. CrossRef Medline

Huang DW, Sherman BT, Lempicki RA (2009a) Bioinformatics enrichment tools: paths toward the comprehensive functional analysis of large gene lists. Nucleic Acids Res 37:1–13. CrossRef Medline

Huang DW, Sherman BT, Lempicki RA (2009b) Systematic and integrative analysis of large gene lists using DAVID bioinformatics resources. Nat Protoc 4:44–57. CrossRef Medline

Husseman J, Raphael Y (2009) Gene therapy in the inner ear using adenovirus vectors. Adv Otorhinolaryngol 66:37–51. CrossRef Medline

Ikeda R, Pak K, Chavez E, Ryan AF (2015) Transcription factors with conserved binding sites near ATOH1 on the POU4F3 gene enhance the induction of cochlear hair cells. Mol Neurobiol 51:672–684. CrossRef Medline

Imtiaz A, Kohrman DC, Naz S (2014) A frameshift mutation in GRXCR2 causes recessively inherited hearing loss. Hum Mutat 35:618–624. CrossRef Medline

Izumikawa M, Minoda R, Kawamoto K, Abrashkin KA, Swiderski DL, Dolan DF, Brough DE, Raphael Y (2005) Auditory hair cell replacement and hearing improvement by Atoh1 gene therapy in deaf mammals. Nat Med 11:271–276. CrossRef Medline

Jacques BE, Montcouquiol ME, Layman EM, Lewandoski M, Kelley MW (2007) Fgf8 induces pillar cell fate and regulates cellular patterning in the mammalian cochlea. Development 134:3021–3029. CrossRef Medline

Jarman AP, Groves AK (2013) The role of atonal transcription factors in the development of mechanosensitive cells. Semin Cell Dev Biol 24:438–447. CrossRef Medline

Kalay E, Li Y, Uzumcu A, Uyguner O, Collin RW, Caylan R, Ulubil-Emiroglu M, Kersten FF, Hafiz G, van Wijk E, Kayserili H, Rohmann E, Wagenstaller J, Hoefsloot LH, Strom TM, Nürnberg G, Baserer N, den Hollander AI, Cremers FP, Cremers CW, et al. (2006) Mutations in the lipoma HMGIC fusion partner-like 5 (LHFPL5) gene cause autosomal recessive nonsyndromic hearing loss. Hum Mutat 27:633–639. CrossRef Medline

Kawamoto K, Ishimoto S, Minoda R, Brough DE, Raphael Y (2003) Math1 gene transfer generates new cochlear hair cells in mature guinea pigs in vivo. J Neurosci 23:4395–4400. Medline

Kawashima Y, Géléoc GS, Kurima K, Labay V, Lelli A, Asai Y, Makishima T, Wu DK, Della Santina CC, Holt JR, Griffith AJ (2011) Mechanotransduction in mouse inner ear hair cells requires transmembrane channel-like genes. J Clin Invest 121:4796–4809. CrossRef Medline

Kelly MC, Chang Q, Pan A, Lin X, Chen P (2012) Atoh1 directs the formation of sensory mosaics and induces cell proliferation in the postnatal mammalian cochlea in vivo. J Neurosci 32:6699–6710. CrossRef Medline

Kikkawa Y, Shitara H, Wakana S, Kohara Y, Takada T, Okamoto M, Taya C, Kamiya K, Yoshikawa Y, Tokano H, Kitamura K, Shimizu K, Wakabayashi Y, Shiroishi T, Kominami R, Yonekawa H (2003) Mutations in a new scaffold protein Sans cause deafness in Jackson shaker mice. Hum Mol Genet 12:453–461. CrossRef Medline

Kim TH, Li F, Ferreiro-Neira I, Ho LL, Luyten A, Nalapareddy K, Long H, Verzi M, Shivdasani RA (2014) Broadly permissive intestinal chromatin underlies lateral inhibition and cell plasticity. Nature 506:511–515. CrossRef Medline

Klisch TJ, Xi Y, Flora A, Wang L, Li W, Zoghbi HY (2011) In vivo Atoh1 targetome reveals how a proneural transcription factor regulates cerebellar development. Proc Natl Acad Sci U S A 108:3288–3293. CrossRef Medline

Krizhanovsky V, Soreq L, Kliminski V, Ben-Arie N (2006) Math1 target genes are enriched with evolutionarily conserved clustered E-box binding sites. J Mol Neurosci 28:211–229. CrossRef Medline

Krüger M, Schmid T, Krüger S, Bober E, Braun T (2006) Functional redundancy of NSCL-1 and NeuroD during development of the petrosal and vestibulocochlear ganglia. Eur J Neurosci 24:1581–1590. CrossRef Medline

Ku YC, Renaud NA, Veile RA, Helms C, Voelker CC, Warchol ME, Lovett M (2014) The transcriptome of utricle hair cell regeneration in the avian inner ear. J Neurosci 34:3523–3535. CrossRef Medline

Lai HC, Klisch TJ, Roberts R, Zoghbi HY, Johnson JE (2011) *In vivo* neuronal subtype-specific targets of Atoh1 (Math1) in dorsal spinal cord. J Neurosci 31:10859–10871. CrossRef Medline

Lanford PJ, Lan Y, Jiang R, Lindsell C, Weinmaster G, Gridley T, Kelley MW (1999) Notch signalling pathway mediates hair cell development in mammalian cochlea. Nat Genet 21:289–292. CrossRef Medline

Lelli A, Asai Y, Forge A, Holt JR, Géléoc GS (2009) Tonotopic gradient in the developmental acquisition of sensory transduction in outer hair cells of the mouse cochlea. J Neurophysiol 101:2961–2973. CrossRef Medline

Lewis RM, Hume CR, Stone JS (2012) Atoh1 expression and function during auditory hair cell regeneration in post-hatch chickens. Hear Res 289:74–85. CrossRef Medline

Li S, Price SM, Cahill H, Ryugo DK, Shen MM, Xiang M (2002) Hearing loss caused by progressive degeneration of cochlear hair cells in mice deficient for the Barhl1 homeobox gene. Development 129:3523–3532. Medline

Liu H, Pecka JL, Zhang Q, Soukup GA, Beisel KW, He DZ (2014) Characterization of transcriptomes of cochlear inner and outer hair cells. J Neurosci 34:11085–11095. CrossRef Medline

Liu Z, Dearman JA, Cox BC, Walters BJ, Zhang L, Ayrault O, Zindy F, Gan L, Roussel MF, Zuo J (2012) Age-dependent in vivo conversion of mouse cochlear pillar and deiters' cells to immature hair cells by atoh1 ectopic expression. J Neurosci 32:6600–6610. CrossRef Medline

Livak KJ, Schmittgen TD (2001) Analysis of relative gene expression data using real-time quantitative PCR and the $2^{-\delta\delta C(T)}$ method. Methods 25:402–408. CrossRef Medline

Longo-Guess CM, Gagnon LH, Cook SA, Wu J, Zheng QY, Johnson KR (2005) A missense mutation in the previously undescribed gene Tmhs underlies deafness in hurry-scurry (hscy) mice. Proc Natl Acad Sci U S A 102:7894–7899. CrossRef Medline

Lott SE, Villalta JE, Schroth GP, Luo S, Tonkin LA, Eisen MB (2011) Noncanonical compensation of zygotic X transcription in early *Drosophila* melanogaster development revealed through single-embryo RNA-seq. PLoS Biol 9:e1000590. CrossRef Medline

Ma EY, Raible DW (2009) Signaling pathways regulating zebrafish lateral line development. Curr Biol 19:R381–R386. CrossRef Medline

Ma EY, Rubel EW, Raible DW (2008) Notch signaling regulates the extent of hair cell regeneration in the zebrafish lateral line. J Neurosci 28:2261–2273. CrossRef Medline

Machanick P, Bailey TL (2011) MEME-ChIP: motif analysis of large DNA datasets. Bioinformatics 27:1696–1697. CrossRef Medline

Machold R, Fishell G (2005) Math1 is expressed in temporally discrete pools of cerebellar rhombic-lip neural progenitors. Neuron 48:17–24. CrossRef Medline

Maison SF, Liu XP, Vetter DE, Eatock RA, Nathanson NM, Wess J, Liberman MC (2010) Muscarinic signaling in the cochlea: presynaptic and postsynaptic effects on efferent feedback and afferent excitability. J Neurosci 30:6751–6762. CrossRef Medline

Maragh S, Miller RA, Bessling SL, Wang G, Hook PW, McCallion AS (2014) Rbm24a and rbm24b are required for normal somitogenesis. PLoS One 9:e105460. CrossRef Medline

Masuda M, Dulon D, Pak K, Mullen LM, Li Y, Erkman L, Ryan AF (2011) Regulation of POU4F3 gene expression in hair cells by 5′ DNA in mice. Neuroscience 197:48–64. CrossRef Medline

McGee J, Goodyear RJ, McMillan DR, Stauffer EA, Holt JR, Locke KG, Birch DG, Legan PK, White PC, Walsh EJ, Richardson GP (2006) The very large G-protein-coupled receptor VLGR1: a component of the ankle link complex required for the normal development of auditory hair bundles. J Neurosci 26:6543–6553. CrossRef Medline

Merritt RC, Manor U, Salles FT, Grati M, Dose AC, Unrath WC, Quintero OA, Yengo CM, Kachar B (2012) Myosin IIIB uses an actin-binding

motif in its espin-1 cargo to reach the tips of actin protrusions. Curr Biol 22:320–325. CrossRef Medline

Mitchem KL, Hibbard E, Beyer LA, Bosom K, Dootz GA, Dolan DF, Johnson KR, Raphael Y, Kohrman DC (2002) Mutation of the novel gene Tmie results in sensory cell defects in the inner ear of spinner, a mouse model of human hearing loss DFNB6. Hum Mol Genet 11:1887–1898. CrossRef Medline

Morrison A, Hodgetts C, Gossler A, Hrabé de Angelis M, Lewis J (1999) Expression of Delta1 and Serrate1 (Jagged1) in the mouse inner ear. Mech Dev 84:169–172. CrossRef Medline

Müller U (2008) Cadherins and mechanotransduction by hair cells. Curr Opin Cell Biol 20:557–566. CrossRef Medline

Mulvaney J, Dabdoub A (2012) Atoh1, an essential transcription factor in neurogenesis and intestinal and inner ear development: function, regulation, and context dependency. J Assoc Res Otolaryngol 13:281–293. CrossRef Medline

Nakamura E, Nguyen MT, Mackem S (2006) Kinetics of tamoxifen-regulated Cre activity in mice using a cartilage-specific CreER^T to assay temporal activity windows along the proximodistal limb skeleton. Dev Dyn 235:2603–2612. CrossRef Medline

Nakano Y, Jahan I, Bonde G, Sun X, Hildebrand MS, Engelhardt JF, Smith RJ, Cornell RA, Fritzsch B, Bánfi B (2012) A mutation in the Srrm4 gene causes alternative splicing defects and deafness in the Bronx Waltzer mouse. PLoS Genet 8:e1002966. CrossRef Medline

Neef J, Gehrt A, Bulankina AV, Meyer AC, Riedel D, Gregg RG, Strenzke N, Moser T (2009) The Ca2+ channel subunit β2 regulates Ca2+ channel abundance and function in inner hair cells and is required for hearing. J Neurosci 29:10730–10740. CrossRef Medline

Nunes FD, Lopez LN, Lin HW, Davies C, Azevedo RB, Gow A, Kachar B (2006) Distinct subdomain organization and molecular composition of a tight junction with adherens junction features. J Cell Sci 119:4819–4827. CrossRef Medline

Odeh H, Hunker KL, Belyantseva IA, Azaiez H, Avenarius MR, Zheng L, Peters LM, Gagnon LH, Hagiwara N, Skynner MJ, Brilliant MH, Allen ND, Riazuddin S, Johnson KR, Raphael Y, Najmabadi H, Friedman TB, Bartles JR, Smith RJ, Kohrman DC (2010) Mutations in Grxcr1 are the basis for inner ear dysfunction in the pirouette mouse. Am J Hum Genet 86:148–160. CrossRef Medline

Pack AK, Slepecky NB (1995) Cytoskeletal and calcium-binding proteins in the mammalian organ of Corti: cell type-specific proteins displaying longitudinal and radial gradients. Hear Res 91:119–135. CrossRef Medline

Pan N, Jahan I, Kersigo J, Duncan JS, Kopecky B, Fritzsch B (2012) A novel Atoh1 "self-terminating" mouse model reveals the necessity of proper Atoh1 level and duration for hair cell differentiation and viability. PLoS One 7:e30358. CrossRef Medline

Pearsall N, Bhattacharya G, Wisecarver J, Adams J, Cosgrove D, Kimberling W (2002) Usherin expression is highly conserved in mouse and human tissues. Hear Res 174:55–63. CrossRef Medline

Qian D, Radde-Gallwitz K, Kelly M, Tyrberg B, Kim J, Gao WQ, Chen P (2006) Basic helix-loop-helix gene Hes6 delineates the sensory hair cell lineage in the inner ear. Dev Dyn 235:1689–1700. CrossRef Medline

Rajab A, Kelberman D, de Castro SC, Biebermann H, Shaikh H, Pearce K, Hall CM, Shaikh G, Gerrelli D, Grueters A, Krude H, Dattani MT (2008) Novel mutations in LHX3 are associated with hypopituitarism and sensorineural hearing loss. Hum Mol Genet 17:2150–2159. CrossRef Medline

Rose MF, Ren J, Ahmad KA, Chao HT, Klisch TJ, Flora A, Greer JJ, Zoghbi HY (2009) Math1 is essential for the development of hindbrain neurons critical for perinatal breathing. Neuron 64:341–354. CrossRef Medline

Sato T, Doi K, Hibino H, Kubo T (2009) Analysis of gene expression profiles along the tonotopic map of mouse cochlea by cDNA microarrays. Acta Otolaryngol Suppl 562:12–17. Medline

Scheffer D, Sage C, Corey DP, Pingault V (2007a) Gene expression profiling identifies Hes6 as a transcriptional target of ATOH1 in cochlear hair cells. FEBS Lett 581:4651–4656. CrossRef Medline

Scheffer D, Sage C, Plazas PV, Huang M, Wedemeyer C, Zhang DS, Chen ZY, Elgoyhen AB, Corey DP, Pingault V (2007b) The α1 subunit of nicotinic acetylcholine receptors in the inner ear: transcriptional regulation by ATOH1 and co-expression with the gamma subunit in hair cells. J Neurochem 103:2651–2664. CrossRef Medline

Schmitz F, Königstorfer A, Südhof TC (2000) RIBEYE, a component of synaptic ribbons: a protein's journey through evolution provides insight into synaptic ribbon function. Neuron 28:857–872. CrossRef Medline

Shima Y, Copeland NG, Gilbert DJ, Jenkins NA, Chisaka O, Takeichi M, Uemura T (2002) Differential expression of the seven-pass transmembrane cadherin genes Celsr1–3 and distribution of the Celsr2 protein during mouse development. Dev Dyn 223:321–332. CrossRef Medline

Shin JB, Longo-Guess CM, Gagnon LH, Saylor KW, Dumont RA, Spinelli KJ, Pagana JM, Wilmarth PA, David LL, Gillespie PG, Johnson KR (2010) The R109H variant of fascin-2, a developmentally regulated actin cross-linker in hair-cell stereocilia, underlies early-onset hearing loss of DBA/2J mice. J Neurosci 30:9683–9694. CrossRef Medline

Shin JB, Krey JF, Hassan A, Metlagel Z, Tauscher AN, Pagana JM, Sherman NE, Jeffery ED, Spinelli KJ, Zhao H, Wilmarth PA, Choi D, David LL, Auer M, Barr-Gillespie PG (2013) Molecular architecture of the chick vestibular hair bundle. Nat Neurosci 16:365–374. CrossRef Medline

Shroyer NF, Helmrath MA, Wang VY, Antalffy B, Henning SJ, Zoghbi HY (2007) Intestine-specific ablation of mouse atonal homolog 1 (Math1) reveals a role in cellular homeostasis. Gastroenterology 132:2478–2488. CrossRef Medline

Simmons DD, Morley BJ (2011) Spatial and temporal expression patterns of nicotinic acetylcholine alpha9 and alpha10 subunits in the embryonic and early postnatal inner ear. Neuroscience 194:326–336. CrossRef Medline

Sinkkonen ST, Chai R, Jan TA, Hartman BH, Laske RD, Gahlen F, Sinkkonen W, Cheng AG, Oshima K, Heller S (2011) Intrinsic regenerative potential of murine cochlear supporting cells. Sci Rep 1:26. CrossRef Medline

Son EJ, Wu L, Yoon H, Kim S, Choi JY, Bok J (2012) Developmental gene expression profiling along the tonotopic axis of the mouse cochlea. PLoS One 7:e40735. CrossRef Medline

Srinivas S, Watanabe T, Lin CS, William CM, Tanabe Y, Jessell TM, Costantini F (2001) Cre reporter strains produced by targeted insertion of EYFP and ECFP into the ROSA26 locus. BMC Dev Biol 1:4. CrossRef Medline

Stern CD (1998) Detection of multiple gene products simultaneously by in situ hybridization and immunohistochemistry in whole mounts of avian embryos. Curr Top Dev Biol 36:223–243. Medline

Thomas S, Thiery E, Aflalo R, Vayssettes C, Verney C, Berthuy I, Créau N (2003) PCP4 is highly expressed in ectoderm and particularly in neuroectoderm derivatives during mouse embryogenesis. Gene Expr Patterns 3:93–97. CrossRef Medline

Togashi H, Kominami K, Waseda M, Komura H, Miyoshi J, Takeichi M, Takai Y (2011) Nectins establish a checkerboard-like cellular pattern in the auditory epithelium. Science 333:1144–1147. CrossRef Medline

Trapnell C, Pachter L, Salzberg SL (2009) TopHat: discovering splice junctions with RNA-Seq. Bioinformatics 25:1105–1111. CrossRef Medline

Verpy E, Masmoudi S, Zwaenepoel I, Leibovici M, Hutchin TP, Del Castillo I, Nouaille S, Blanchard S, Lainé S, Popot JL, Moreno F, Mueller RF, Petit C (2001) Mutations in a new gene encoding a protein of the hair bundle cause non-syndromic deafness at the DFNB16 locus. Nat Genet 29:345–349. CrossRef Medline

Walker RG, Hudspeth AJ, Gillespie PG (1993) Calmodulin and calmodulin-binding proteins in hair bundles. Proc Natl Acad Sci U S A 90:2807–2811. CrossRef Medline

Wallis D, Hamblen M, Zhou Y, Venken KJ, Schumacher A, Grimes HL, Zoghbi HY, Orkin SH, Bellen HJ (2003) The zinc finger transcription factor Gfi1, implicated in lymphomagenesis, is required for inner ear hair cell differentiation and survival. Development 130:221–232. CrossRef Medline

Walsh T, Walsh V, Vreugde S, Hertzano R, Shahin H, Haika S, Lee MK, Kanaan M, King MC, Avraham KB (2002) From flies' eyes to our ears: mutations in a human class III myosin cause progressive nonsyndromic hearing loss DFNB30. Proc Natl Acad Sci U S A 99:7518–7523. CrossRef Medline

Wheeler EF, Bothwell M, Schecterson LC, von Bartheld CS (1994) Expression of BDNF and NT-3 mRNA in hair cells of the organ of Corti: quantitative analysis in developing rats. Hear Res 73:46–56. CrossRef Medline

Woods C, Montcouquiol M, Kelley MW (2004) Math1 regulates development of the sensory epithelium in the mammalian cochlea. Nat Neurosci 7:1310–1318. CrossRef Medline

Xiang M, Gao WQ, Hasson T, Shin JJ (1998) Requirement for Brn-3c in maturation and survival, but not in fate determination of inner ear hair cells. Development 125:3935–3946. Medline

Yang J, Bouvron S, Lv P, Chi F, Yamoah EN (2012a) Functional features of trans-differentiated hair cells mediated by Atoh1 reveals a primordial mechanism. J Neurosci 32:3712–3725. CrossRef Medline

Yang SM, Chen W, Guo WW, Jia S, Sun JH, Liu HZ, Young WY, He DZ (2012b) Regeneration of stereocilia of hair cells by forced Atoh1 expression in the adult mammalian cochlea. PLoS One 7:e46355. CrossRef Medline

Ylikoski J, Pirvola U, Moshnyakov M, Palgi J, Arumäe U, Saarma M (1993) Expression patterns of neurotrophin and their receptor mRNAs in the rat inner ear. Hear Res 65:69–78. CrossRef Medline

Yoon H, Lee DJ, Kim MH, Bok J (2011) Identification of genes concordantly expressed with Atoh1 during inner ear development. Anat Cell Biol 44: 69–78. CrossRef Medline

Yu X, Lau D, Ng CP, Roy S (2011) Cilia-driven fluid flow as an epigenetic cue for otolith biomineralization on sensory hair cells of the inner ear. Development 138:487–494. CrossRef Medline

Zhang Y, Liu T, Meyer CA, Eeckhoute J, Johnson DS, Bernstein BE, Nusbaum C, Myers RM, Brown M, Li W, Liu XS (2008) Model-based analysis of ChIP-Seq (MACS). Genome Biol 9:R137. CrossRef Medline

Zheng JL, Gao WQ (2000) Overexpression of Math1 induces robust production of extra hair cells in postnatal rat inner ears. Nat Neurosci 3:580–586. CrossRef Medline

frontiers in Cellular Neuroscience

ORIGINAL RESEARCH
published: 31 March 2015
doi: 10.3389/fncel.2015.00110

Changes in the regulation of the Notch signaling pathway are temporally correlated with regenerative failure in the mouse cochlea

*Juan C. Maass[1,2,3,4], Rende Gu[1], Martin L. Basch[1], Joerg Waldhaus[5], Eduardo Martin Lopez[1], Anping Xia[5], John S. Oghalai[5], Stefan Heller[5] and Andrew K. Groves[1,6,7]**

[1] Department of Neuroscience, Baylor College of Medicine, Houston, TX, USA, [2] Department of Otolaryngology, Hospital Clínico Universidad de Chile, Santiago, Chile, [3] Interdisciplinary Program of Physiology and Biophysics, ICBM Universidad de Chile, Santiago, Chile, [4] Department of Otolaryngology, Clínica Alemana de Santiago, Facultad de Medicina Clínica Alemana-Universidad del Desarrollo, Santiago, Chile, [5] Department of Otolaryngology —Head and Neck Surgery, Stanford University School of Medicine, Palo Alto, CA, USA, [6] Department of Molecular and Human Genetics, Baylor College of Medicine, Houston, TX, USA, [7] Program in Developmental Biology, Baylor College of Medicine, Houston, TX, USA

OPEN ACCESS

Edited by:
Qi Yuan,
Memorial University, Canada

Reviewed by:
Fernando Giraldez,
Universitat Pompeu Fabra, Spain
Nicolas Daudet,
University College London, UK
Jian Zuo,
St. Jude Children's Research Hospital, USA

***Correspondence:**
Andrew K. Groves, Department of Molecular and Human Genetics, Baylor College of Medicine, BCM295, 1 Baylor Plaza, Houston, TX 77030, USA
akgroves@bcm.edu

Received: *16 December 2014*
Accepted: *10 March 2015*
Published: *31 March 2015*

Citation:
Maass JC, Gu R, Basch ML, Waldhaus J, Lopez EM, Xia A, Oghalai JS, Heller S and Groves AK (2015) Changes in the regulation of the Notch signaling pathway are temporally correlated with regenerative failure in the mouse cochlea. Front. Cell. Neurosci. 9:110. doi: 10.3389/fncel.2015.00110

Sensorineural hearing loss is most commonly caused by the death of hair cells in the organ of Corti, and once lost, mammalian hair cells do not regenerate. In contrast, other vertebrates such as birds can regenerate hair cells by stimulating division and differentiation of neighboring supporting cells. We currently know little of the genetic networks which become active in supporting cells when hair cells die and that are activated in experimental models of hair cell regeneration. Several studies have shown that neonatal mammalian cochlear supporting cells are able to trans-differentiate into hair cells when cultured in conditions in which the Notch signaling pathway is blocked. We now show that the ability of cochlear supporting cells to trans-differentiate declines precipitously after birth, such that supporting cells from six-day-old mouse cochlea are entirely unresponsive to a blockade of the Notch pathway. We show that this trend is seen regardless of whether the Notch pathway is blocked with gamma secretase inhibitors, or by antibodies against the Notch1 receptor, suggesting that the action of gamma secretase inhibitors on neonatal supporting cells is likely to be by inhibiting Notch receptor cleavage. The loss of responsiveness to inhibition of the Notch pathway in the first postnatal week is due in part to a down-regulation of Notch receptors and ligands, and we show that this down-regulation persists in the adult animal, even under conditions of noise damage. Our data suggest that the Notch pathway is used to establish the repeating pattern of hair cells and supporting cells in the organ of Corti, but is not required to maintain this cellular mosaic once the production of hair cells and supporting cells is completed. Our results have implications for the proposed used of Notch pathway inhibitors in hearing restoration therapies.

Keywords: notch, hair cell, supporting cell, cochlea, regeneration

Introduction

The Notch signaling pathway is an evolutionarily ancient form of cell-cell communication. During Notch signaling, the binding of membrane-bound ligands of the Delta and Jagged/Serrate families to Notch receptors causes the cleavage of the receptor and release of an intracellular domain which travels to the nucleus and participates in transcriptional activation (Artavanis-Tsakonas et al., 1999; Ilagan and Kopan, 2007; Artavanis-Tsakonas and Muskavitch, 2010; Hori et al., 2013). Notch signaling is deployed in the development of many tissues, and can influence cell fate through lateral inhibition with feedback (Chitnis, 1995; Formosa-Jordan et al., 2013), inductive signaling (frequently to establish boundaries of different cell types) or by the asymmetrical inheritance of fate determinants that affect Notch signaling (Bray, 2006).

Notch signaling regulates many aspects of inner ear development (Kelley, 2003, 2006, 2007; Murata et al., 2012). During the induction of the otic placode, the anlagen of the inner ear, Jagged1 activation of Notch signaling acts to strengthen otic placode fate in response to FGF and Wnt signals (Jayasena et al., 2008; Groves and Fekete, 2012). As the first neuroblasts begin to differentiate and delaminate from the otocyst, Notch-Delta signaling regulates the proportion of progenitor cells that differentiate as neurons by lateral inhibition (Adam et al., 1998; Abelló et al., 2007; Daudet et al., 2007; Kiernan, 2013; Neves et al., 2013a). As the first sensory regions of the inner ear begin to develop, Notch-Jagged1 signaling helps maintain and promote the fate of vestibular sensory regions of the ear through lateral induction (Eddison et al., 2000; Daudet and Lewis, 2005; Kiernan et al., 2005a; Brooker et al., 2006; Daudet et al., 2007; Hartman et al., 2010; Pan et al., 2010, 2013; Neves et al., 2011, 2013a,b), although it is less clear if this mode of sensory induction also occurs in the cochlea (Basch et al., 2011; Yamamoto et al., 2011). Finally, as hair cell and supporting cells begin to differentiate from sensory progenitor cells in prosensory patches, hair cells begin to express the Notch ligands Delta1 and Jagged2 (Dll1, Jag2) on their cell surface, and signaling by these ligands through the Notch1 receptor on nascent supporting cells induces and maintains supporting cell fate though lateral inhibition. Accordingly, pharmacological or genetic disruption of Notch1, Dll1 or Jag2, singly or in combination, leads to a failure of Notch signaling and an increase in the number of hair cells at the expense of supporting cells, likely through loss of lateral inhibition (Kiernan et al., 2005a; Brooker et al., 2006). Mutation or knock-down of downstream transcriptional effectors of Notch signaling, such as members of the Hes and Hey gene families, also leads to an increase in hair cell numbers at the expense of supporting cells (Zheng et al., 2000; Zine et al., 2001; Hayashi et al., 2008; Li et al., 2008; Doetzlhofer et al., 2009; Tateya et al., 2011; Benito-Gonzalez and Doetzlhofer, 2014).

A number of studies suggest that Notch signaling between hair cells and supporting cells continues in the sensory end organs of the mammalian inner ear after birth (Zine et al., 2000; Murata et al., 2006; Yamamoto et al., 2006; Hartman et al., 2007, 2009; Hori et al., 2007; Batts et al., 2009; Doetzlhofer et al., 2009; Lin et al., 2011; Liu et al., 2012a,b). Downstream effectors of Notch signaling can be detected in the cristae and maculae of the vestibular system (Hartman et al., 2009; Wang et al., 2010; Lin et al., 2011; Slowik and Bermingham-McDonogh, 2013), and blockade of Notch signaling in the adult vestibular system can induce the formation of ectopic hair cells at the expense of supporting cells (Lin et al., 2011; Slowik and Bermingham-McDonogh, 2013). Similarly, inhibition of Notch signaling in the neonatal organ of Corti also down-regulates some downstream effectors of Notch signaling in supporting cells and leads to the rapid formation of extra hair cells (Doetzlhofer et al., 2009; Korrapati et al., 2013; Mizutari et al., 2013; Bramhall et al., 2014). In both the neonatal cochlea and adult vestibular system, the generation of hair cells has been proposed to occur through a direct trans-differentiation of supporting cells without cell division (Doetzlhofer et al., 2009; Lin et al., 2011; Bramhall et al., 2014), a mode of differentiation that has also been observed during hair cell regeneration in birds (Stone and Cotanche, 2007).

Recently, application of gamma secretase inhibitors that attenuate the Notch pathway to the noise-damaged cochlea has been shown to generate small numbers of new hair cells and a partial restoration of hearing (Mizutari et al., 2013), suggesting that the Notch pathway may still be active in the mature cochlea. However, two issues remain unaddressed by this study. First, it is not clear to what extent components of the Notch signaling pathway—Notch receptors, Notch ligands and their downstream effectors—are expressed in the maturing cochlea (Batts et al., 2009). Indeed, two studies examining the presence of the active cleaved intracellular portion of the Notch1 receptor found very little evidence for Notch activation in the cochlea 1 week after birth (Murata et al., 2006; Liu et al., 2013). Moreover, although gamma secretase inhibitors are known to inhibit cleavage and activation of Notch receptors, they also cleave many other membrane proteins, and so it is possible that their effects in the cochlea may not be specific to the Notch pathway (Kopan and Ilagan, 2004).

In the present study, we compared the effects of gamma secretase inhibitors or blocking antibodies to the Notch1 receptor on the patterning of hair cells and supporting cells in organ cultures of the neonatal cochlea. In each case, we found that inhibitor treatment causes an increase in hair cell numbers at the expense of supporting cells, suggesting that both inhibitors are likely causing supporting cell trans-differentiation through inhibition of the Notch pathway. However, we find a precipitous age-dependent decline in the ability of these inhibitors to cause supporting cell trans-differentiation into hair cells. This decline in response to Notch inhibition progresses in a basal-apical gradient along the organ of Corti, consistent with the gradient of cellular maturation in the cochlea, and by 6 days after birth, the organ of Corti is essentially unresponsive to Notch inhibition in culture. We combined *in situ* hybridization, Q-PCR quantitation and single cell Fluidigm analysis of Notch pathway components and showed that Notch receptors,

ligands and effectors are down-regulated from the organ of Corti in basal-apical gradient during the first postnatal week, and are at least an order of magnitude lower in mature animals, even after noise damage. Our results suggest that the Notch signaling pathway is deployed to establish the pattern of hair cells and supporting cells in the cochlea, but is not required to maintain this pattern in the mature organ of Corti.

Materials and Methods

Mice

Atoh1$^{A1GFP/A1GFP}$ (MGI: *Atoh1*$^{tm4.1Hzo}$) knock-in mice and *Atoh1*^{GFP} transgenic reporter mice were generated as previously described (Lumpkin et al., 2003; Rose et al., 2009). ICR mice were used for Notch Intracellular Domain (NICD) immunostaining. Noise damage experiments were performed on wild type CBA/CaJ mice. Pillar cells and Deiters' cells were purified from *Fgfr3-iCreER*^{T2} (Young et al., 2010) mice mated with *Ai14:Rosa*^{tdTom} reporter mice (Jackson, #007908). All animal experiments were approved by the Baylor College of Medicine or Stanford University Institutional Animal Care and Use committees.

Cochlear Organ Culture

Cochleas were dissected in ice cold HBSS immediately after euthanasia. Briefly, the heads were bisected, the temporal bone was removed from the skull base and the otic capsule was removed with forceps until the intact membranous cochlea was separated from the bony structures. For P0 and P3 animals, the cochlear duct was peeled out from the modiolus and the medial structures (Kölliker and Corti's organs) were separated from the lateral wall, Reissner's membrane and the stria vascularis. For P6 mice, in order to preserve the structures in the organ of Corti, the cochlear duct was gently separated from the modiolus by cutting between them with forceps and the lateral wall, stria vascularis and Reissner's membrane were partially removed after cutting with 27 gauge needle. Immediately after dissection, the explants were placed on top of filter membranes with 1 μm pores (SPI-pore or Whatman) floating in DMEM/F12 (Hepes) supplemented with B27 supplements (Life Technologies), 1mM N-acetylcysteine (Sigma), 5 ng/ml EGF and 2.5 ng/ml FGF2 and 67 μg/ml penicillin. In some cultures DMEM/F12 medium was supplemented with N2 supplements (Life Technologies), N-acetylcysteine and penicillin. For Notch inhibition experiments, cultures were supplemented with 0.75–10 μM DAPT (Gamma secretase inhibitor IX, Calbiochem EMD) or DMSO 0.04% v/v (Life Technologies). Anti Notch1-specific antibodies and control IgD antibodies (Wu et al., 2010) were provided by Genentech and used at 2 μg/ml. The cultures were maintained for 1 h, 1, 2 or 3 days *in vitro* (DIV) at 37°C in 5% CO_2.

Immunostaining, Microscopy and Quantification

Whole cochlear explants were fixed in 4% paraformaldehyde, then permeabilized and blocked in 0.2% Triton X-100 and 10% donkey serum in PBS. The explants were incubated with primary antibodies overnight at 4°C, washed in PBST (0.1% Triton X-100 in PBS) and incubated with secondary antibodies for 2 h at room temperature, followed by 3 further washes in PBST and then incubated in 10 μg/ml DAPI for 10 min. Primary antibodies used were rabbit polyclonal anti-Myosin VIIa (1:500; Proteus Biosciences) and mouse monoclonal anti-GFP (1:200; Invitrogen). Secondary antibodies were Alexa Fluor 594 and 488 (Invitrogen). Images were obtained on an Axio Observer Zeiss microscope with an Apotome2 structured illumination attachment and analyzed in Axiovision 4.8 (Zeiss) and Image J (NIH) using Bioformat and the Cell Counter plugins. The cochlea was divided in five pieces: the tip, the apex, the middle, the base and the hook, and the center of each portion was analyzed, discarding the tip and the hook. Cell counts across different areas of the cochlea were normalized to cells per 100 μm and were expressed as a percentage increase with respect to control conditions. Significant differences were analyzed using a Mann-Whitney test for pairwise comparisons.

For NICD immunostaining in sections the protocol was modified from Morimoto et al. (2010). Briefly the heads of P0, P3 and P6 ICR mice were mounted in paraffin blocks and sectioned at 10 μm. The sections were rehydrated, bleached in H_2O_2 and boiled in a pressure cooker in antigen unmasking solution (Vectorlabs) for 20 min. The sections were then permeabilized, blocked and incubated with a cleaved Notch1 antibody (val1744; 1:100; Cell signaling) and anti- Myosin VIIa (1:500; Proteus Biosciences). The signal was amplified with Vectastain ABC Kit (rabbit IgG) (Vectorlabs) as indicated by manufacturer. The color was developed for 5–10 min with TSA Tyramide Cy3 Reagent (diluted 1:100 after reconstitution; Perkin Elmer) and then stained with DAPI. Images were obtained on a Zeiss Axio Observer microscope with an Apotome2 structured illumination attachment.

In Situ Hybridization

Digoxygenin-labeled *in situ* probe synthesis was performed on linearized plasmid DNA using standard protocols (Stern, 1998).The following mouse cDNA probes were used in the study and kindly provided by the investigators listed: *Notch1*, *Jag1*, *Dll1* (Gerry Weinmaster), *Notch3* (Urban Lendahl), *Hes5* (Ryoichiro Kageyama), *Hey1*, *Hey2*, *HeyL* (Manfred Gessler), and *Atoh1* (Huda Zoghbi). A cDNA clone for *Jag2* (BC010982) was purchased from open Biosystems. The *in situ* hybridization procedure for frozen sections was modified from previous protocols (Harland, 1991; Birren et al., 1993; Groves et al., 1995). Heads of perinatal mouse pups were fixed in 4% paraformaldehyde in PBS overnight at 4°C, cryoprotected in 30% sucrose in PBS at 4°C, embedded in OCT compound (Sakura Finetek), and cryosectioned at 14 μm. Sections were fixed in 4% paraformaldehyde in PBS, pH 7.2 for 10 min at room temperature, followed by three 5-min washes in DEPC-treated PBS. The sections were treated with 1 μg/ml Proteinase K in DEPC-PBS for 5 min at room temperature, followed by three 5-min washes in DEPC-PBS and re-fixation in 4% paraformaldehyde in PBS, pH 7.2 for 10 min at room

temperature. Sections were acetylated in 0.25% acetic anhydride in 0.1 M triethanolamine, pH 8.0 for 10 min at room temperature, followed by three 5-min washes in DEPC-PBS. Slides were incubated in hybridization buffer (50% formamide, 5 × SSC, 50 μg/ml Yeast tRNA, 100 μg/ml Heparin, 1 × Denhardt's Solution, 0.1% Tween 20, 0.1% CHAPS, 5 mM EDTA) for 1–2 h at 65°C. 100 μl of digoxygenin-labeled probe (1 mg/ml) was added to each slide and the slides covered with glass coverslips. The slides were incubated in a chamber humidified with 5 × SSC, 50% formamide at 65°C overnight. Coverslips were removed by rinsing in 0.2 × SSC and the slides washed in 0.2 × SSC at 65°C for 1 h. The slides were then washed in 0.2 × SSC for 5 min at room temperature, followed by another 5-min wash in 0.1% Tween-20 in PBS (PTw). The slides were blocked in 10% lamb serum in PTw at room temperature for 1 h and then stained with anti-digoxygenin-alkaline phosphatase antibody (1:2000) for 1–3 h at room temperature in a humidified chamber. The slides were then washed three times for 5 min each in PTw and equilibrated with freshly-made alkaline phosphatase buffer (100 mM Tris pH 9.5, 50 mM $MgCl_2$, 100 mM NaCl, 0.1% Tween 20) for 10 min. The slides were developed in alkaline phosphatase buffer containing 0.33 mg/ml NBT and 0.18 mg/ml BCIP in the dark at room temperature until the purple reaction product had developed to a satisfactory degree. The reaction was stopped by washing the slides in PBS three times for 15 min each, followed by fixation in 4% paraformaldehyde in PBS, pH 7.2 for 30 min. The slides were then rinsed and mounted in 80% glycerol in PBS. Whole mount *in situ* hybridization was carried out as recently described in detail (Khatri and Groves, 2013).

RNA Isolation and Q-PCR

For each experimental condition, total RNA was extracted from 4 uncultured whole cochlear explants or 3 cultured cochlear explants using the RNeasy mini kit (Qiagen). RNA yield ranged from 480 to 1200 ng and was used for cDNA preparation using random primers and SuperScript III First-Strand Synthesis System (Invitrogen). qPCR reaction was performed with SYBRGreen PCR Master Mix in StepOnePlus RealTime PCR System (Applied Biosystems), using in the reaction cDNA at 0.3–0.6 ng/μl and primers at 50 nM (excepting 100 nM for the Hes5 reaction). Primers sequences are provided in **Table 1**. *GAPDH* and *L19* primers were used as reference genes. Significant differences were analyzed using a Mann-Whitney test for pairwise comparisons. Multiple comparisons or pairwise correction for multiple comparisons were not performed.

TABLE 1 | Q-PCR primers for Figures 1, 3, 5, 7.

Gene	Forward primer	Reverse primer
Atoh1	5′-ATGCACGGGCTGAACCA-3′	5′-TCGTTGTTGAAGGAC GGGATA-3′
Notch1	5′-GCCGCAAGAGGCTTGAGAT-3′	5′-GGAGTCCTGGCATC GTTGG-3′
Notch3	5′-GCACTTGCCGTGGTTACATG-3′	5′-CCTCACAACTGTCACCAGC ATAG-3′
Hey1	5′-CACTGCAGGAGGGAAAGGTTAT-3′	5′-CCCCAAACTCCGATAG TCCAT-3′
Hey2	5′-AAGCGCCCTTGTGAGGAAA-3′	5′-TCGCTCCCCACGT CGAT-3′
HeyL	5′-GCGCAGAGGGATCATAGAGAA-3′	5′-TCGCAATTCAGAAAGGC TACTG-3′
Hes5	5′-GCACCAGCCCAACTCCAA-3′	5′-GGCGAAGGCTTTGC TGTGT-3′
Jag1	5′-AAAGACCACTGCCGTACCAC-3′	5′-GGGGACCACAGACG TTAGAA-3′
Jag2	5′-TGCGAACTAGAGTACGACAA-3′	5′-TTGGTTCACAGAGAT CCATG-3′
Dll1	5′-TCCGATTCCCCTTCGGCTTCA-3′	5′-TCTGTTGCGAGGTCA TCGGGA-3′
Dll3	5′-CCGCTTTCCCAGACGCTGAT-3′	5′-GGCCTGGCCCGAAA GAATGA-3′
Gapdh	5′-AGGTCGGTGTGAACGGATTTG-3′	5′-TGTAGACCATGTAGTTGA GGTCA-3′
Ll9	5′-GGTCTGGTTGGATCCCAATG-3′	5′-CCCGGGAATGGA CAGTCA-3′

Single Cell Purification and Q-PCR Analysis

Triple transgenic mice heterozygote for Fgfr3-iCreER^{T2} (Young et al., 2010), Ai14:Rosa^{tdTom} (Jackson, #007908) and Sox2-EGFP (Jackson, #017592) were analyzed at P2, and double transgenic animals (Fgfr3-iCreER^{T2} and Ai14:Rosa^{tdTom}) were analyzed at P21. Animals were injected with 0.2 mg/g body weight tamoxifen at P0 and P19 respectively. Animals were euthanized 2 days after the tamoxifen injection and organs of Corti were dissected. Single cell dissociation, flow cytometry, RNA isolation and single cell qRT-PCR were performed as described in Durruthy-Durruthy et al. (2014) using the primers listed in **Table 2**. Briefly, expression of Actb or Gapdh at levels lower or higher than 3 standard deviations from the mean was used to exclude compromised cells/empty wells or possible doublets, respectively. Ai14-Control primers detect recombination within the Ai14-tdTomato reporter locus and cells with no detectable recombination were excluded from the analysis. Single cell expression data is presented as Log2Ex values, calculated by subtracting experimentally determined Ct-values from the median limit of detection calculated for all primers used in the study. Single cell data were normalized using the median Log2Ex values as recommended by Fluidigm.

Noise Damage

Noise damage of six-week-old CBA/CaJ mice was performed as previously described (Liu et al., 2011). Briefly, a custom-built box contained six piezo horns (TW-125, Pyramid Car Audio, Brooklyn, NY, USA) inserted through the cover. Band-passed white noise (4–22 kHz) was generated digitally with RPvds software (Version 6.6, Tucker-Davis Technologies, Alachua, FL, USA), converted to analog by a digital-to-analog converter, and then transferred to the power amplifier (Servo 550, Sampson, Hauppauge, NY, USA) to drive the speakers. A cage containing the mice was placed inside the box and the mice were exposed to noise at 98 dB ± 2 dB for 4 h.

TABLE 2 | Q-PCR primers for Figure 6.

Gene	Forward primer	Reverse primer
Actb:	5′- CCCTAAGGCCAACCGTGAAA -3′	5′- CAGCCTGGATG GCTACGTAC -3′
Gapdh	5′- AGACGGCCGCATCTTCTT -3′	5′- TTCACACCGACC TTCACCAT -3′
Ai9-Control	5′- AGGAACTTCGTCGACATTTAAATCA -3′	5′- CTGCAGGTCGA GGGACCTAA -3′
Fgfr3	5′- AGGATTTAGACCGCATCCTCAC -3′	5′- CCTGGCGAGTAC TGCTCAAA -3′
Cdkn1b	5′- CAGTGTCCAGGGATGAGGAA -3′	5′- TTCGGGGAACCGTC TGAAA -3′
Sox2	5′- TGAAGGAGCACCCGGATTATA -3′	5′- CGGGAAGCGTGT ACTTATCC -3′
Jag1	5′- AACGACCGTAATCGCATCGTA -3′	5′- TCCACCAGCAAAGT GTAGGAC -3′
Jag2	5′- CTCGTCGTCATTCCCTTTCA -3′	5′- GGTGTCATTGTC CCAGTCC -3′
Hes1	5′- TGAAGCACCTCCGGAACC -3′	5′- CGCGGTATTTCC CCAACAC -3′
Hes5	5′- AAGAGCCTGCACCAGGACTA -3′	5′- GTGCAGGGTCAGG AACTGTAC -3′
Hey1	5′- ACGAGACCATCGAGGTGGAA -3′	5′- CGTTGGGGACAT GGAACACA -3′
Hey2	5′- ACTAGTGCCAACAGCTTTTGAA -3′	5′- TGTAGCCTGGAGC ATCTTCA -3′
LFng	5′- TCGATCTGCTGTTCGAGACC -3′	5′- CCTCCCCATCAG TGAAGATGAA -3′

Results

The Neonatal Cochlea Exhibits a Position-Dependent Variation of Supporting Cell Trans-Differentiation in Response to Gamma Secretase Inhibitors

A number of studies have demonstrated conversion or trans-differentiation of cochlear supporting cells into hair cells after treatment with gamma secretase inhibitors (Takebayashi et al., 2007; Hayashi et al., 2008; Doetzlhofer et al., 2009; Korrapati et al., 2013; Mizutari et al., 2013; Bramhall et al., 2014), although results in different studies have often been obtained with different gamma secretase inhibitors or at different concentrations of a given inhibitor. We confirmed these results in cochlear explant cultures from postnatal day 0 (P0) *Atoh1*$^{A1GFP/A1GFP}$ and *Atoh1-GFP* mice, using the gamma secretase inhibitor DAPT over a range of 0.75–10 μM. After 2 days in culture, we stained the cultures for Myosin VIIa and GFP to reveal the Atoh1-GFP fusion protein (*Atoh1*$^{A1GFP/A1GFP}$ mice) or GFP reporter (*Atoh1-GFP* mice). We observed a significant increase in the numbers of Myosin VIIa $^{+}$ hair cells at 2.5, 5 and 10 μM DAPT compared to DMSO vehicle (**Figures 1A,B**), but not at lower concentrations. We measured the levels of hair cell and supporting cell mRNAs in the *Atoh1-GFP* cultures and observed an increase of the hair cell markers *Atoh1* and *Jag2* and a decrease in the supporting cell markers *Jag1*, *Hey1* and *Hes5* (**Figure 1C**). As previously described (Doetzlhofer et al., 2009), *Hes5* was particularly sensitive to DAPT, with a strong reduction in mRNA levels being observed above 1 μM.

The organ of Corti differentiates in a broadly basal-apical direction, with the first differentiating Atoh1^{+} hair cells appearing near the base of the cochlea, and a wave of hair cell and supporting cell differentiation spreading basally to the hook region and in an apical direction to the tip of the cochlea (Chen et al., 2002; Cai et al., 2013). Consequently at birth, hair cells and supporting cells in the basal region of the cochlea can be considered to be slightly more mature than their counterparts at the apex and tip. To determine whether these differences in maturity affected the response to gamma secretase inhibitors, we cultured whole P0 cochleas from Atoh1-GFP mice in 10 μM DAPT or DMSO vehicle for 1–3 days and counted the numbers of Atoh1-GFP or Myosin VIIa-expressing hair cells in the apical, middle and basal regions of the cochlea (**Figures 2A,B**; the approximate positions of the three regions are indicated in **Figure 2C**). We excluded from our counts the most basal hook region as it was more susceptible to variable damage during dissection and the most apical tip region because of its more variable behavior. We observed a clear effect of position on the number of supernumerary hair cells generated in the cultures over the 3 day culture period, with the apex producing 202% more hair cells after 3 days, whereas the base generated only 32% more hair cells in the same time period (**Figures 2A,B**). These results suggested that more mature supporting cells at the base of the cochlea were far less likely to trans-differentiate into hair cells in response to DAPT than their younger counterparts at the apex.

The Response of Supporting Cells to Gamma Secretase Inhibition or Notch Inhibition Declines Rapidly with Age

To test whether the response of cochlear supporting cells to DAPT was indeed age-dependent, we established cochlear cultures from newborn (P0), 3 and 6 day old mice and cultured them for 2 days in 5 μM DAPT. We quantified the number of supernumerary hair cells in the apical region. We saw significant numbers of supernumerary hair cells in DAPT-treated P0 cochlear cultures compared to DMSO vehicle, but observed no significant increase in hair cell numbers when either P3 or P6 cultures were treated with DAPT (**Figures 3A,B**).

Most experiments in which gamma secretase inhibitors have been used to promote supporting cell trans-differentiation into hair cells are interpreted on the assumption that the inhibitors are targeting the cleavage of Notch receptors in cochlear supporting cells. However, since gamma secretases cleave many other membrane proteins (Kopan and Ilagan, 2004), it is possible that some of the effects of gamma secretase inhibitors may be due to the inhibition of cleavage of other membrane proteins. To test this, we used specific blocking antibodies to the Notch1 receptor (Wu et al., 2010) at a concentration of 2 μg/ml, previously shown to effectively inhibit Notch1 signaling *in vitro* (Wu et al., 2010). Cochlear cultures from P0 animals showed similar age-dependent responses to Notch1 blocking antibodies (48%

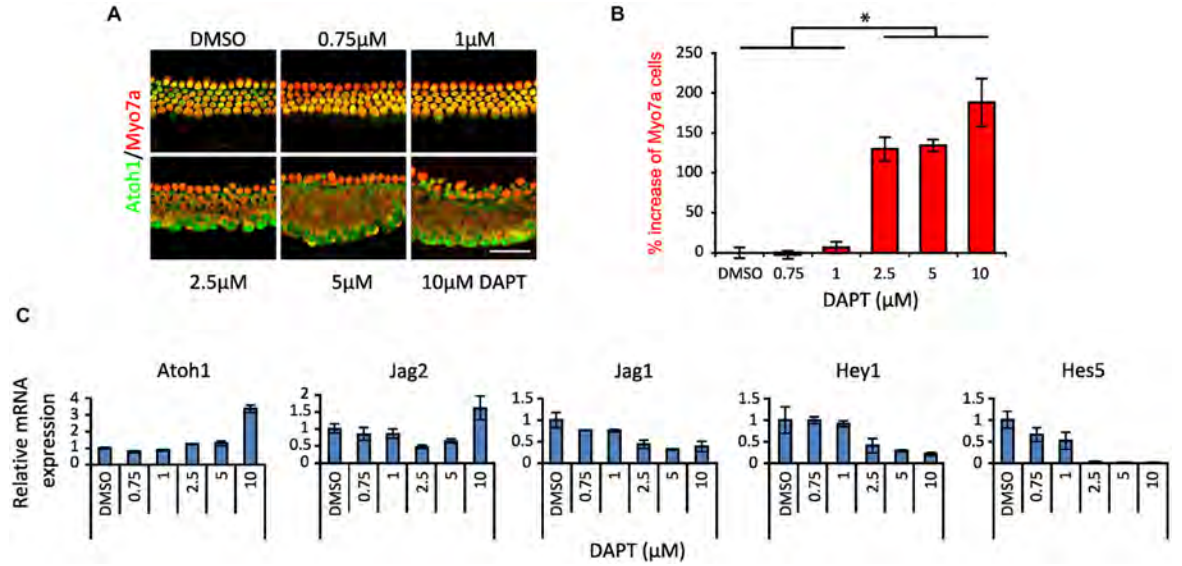

FIGURE 1 | Dose response of Notch inhibition in P0 cultures. **(A)** Immunostaining of apical portions of cochlear explants of newborn (P0) *Atoh1*$^{A1GFP/A1GFP}$ knock-in mice cultured 2 days *in vitro* (DIV) in DAPT from 0.75 to 10 μM or vehicle (DMSO). Atoh1: green. Myo7a: red. Scale 50 μm. **(B)** Quantitation of the increase in number of Myosin VIIa-labeled cells after different doses of DAPT compared to DMSO vehicle (same as shown in **A**). $N = 4$. $^*p = 0.030$ (Mann-Whitney pairwise comparisons). Error bars: SEM. **(C)** mRNA amount of hair cell, supporting cell and Notch pathway genes obtained by QPCR in whole cochlear explants from P0 *Atoh1*^{GFP} transgenic reporter mice treated with DAPT compared to DMSO vehicle. $N = 3$. Error bars: SEM. Note that error bars are present for each condition but are very small in some cases.

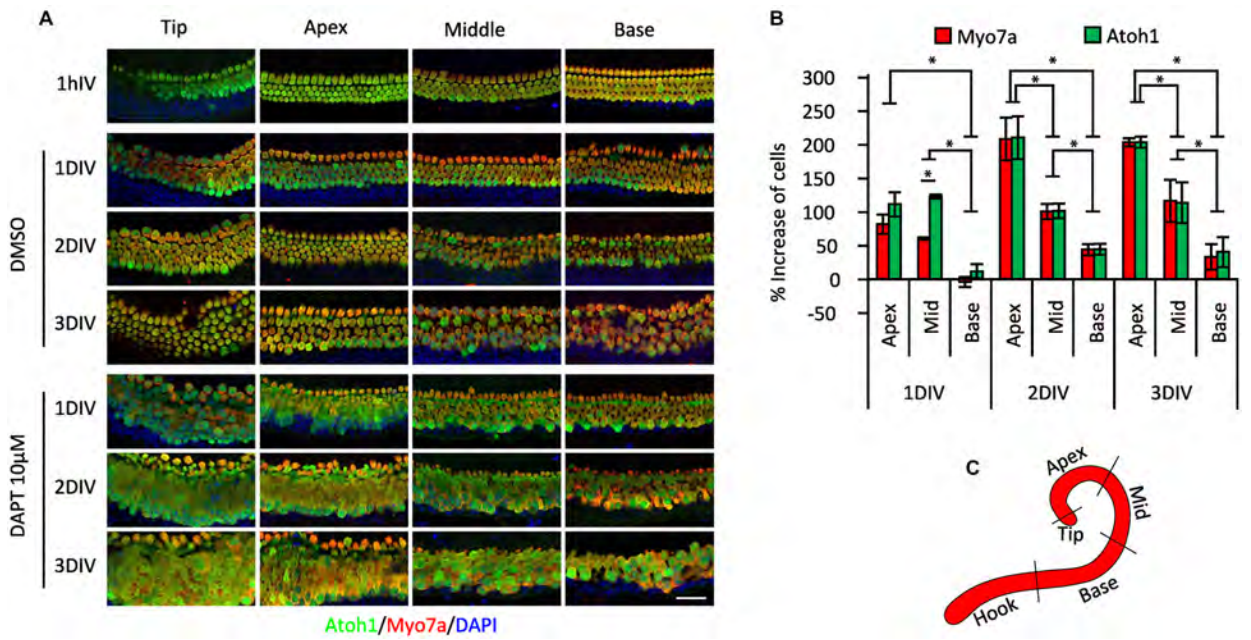

FIGURE 2 | Position-dependent effect of Notch inhibition in P0 cultures. **(A)** Immunostaining of different cochlear portions from newborn (P0) *Atoh1*$^{A1GFP/A1GFP}$ knock-in mice (shown in **C**) treated with 10 μM DAPT or vehicle (DMSO) for 1 h to 3 days *in vitro* (DIV). Atoh1: green. Myo7a: red. DAPI: Blue. **(B)** Percentage of increase in numbers of Myosin VIIa-labeled cells and GFP-labeled cells in the different regions of the cochlea after DAPT 10 μM treatment compared to vehicle (same as shown in **A**). $N = 4$. $^*p = 0.030$ (Mann-Whitney pairwise comparisons). Error bars: SEM. **(C)** Schematic view of the cochlear portions evaluated in **(A,B)**.

increase in Myosin VIIa $^+$ hair cells) as cultures incubated for 2 days in 5 μM DAPT (41% increase) compared to control cultures containing DMSO or a control IgD (**Figures 3A,B**). However, we saw no significant response when P3 or P6

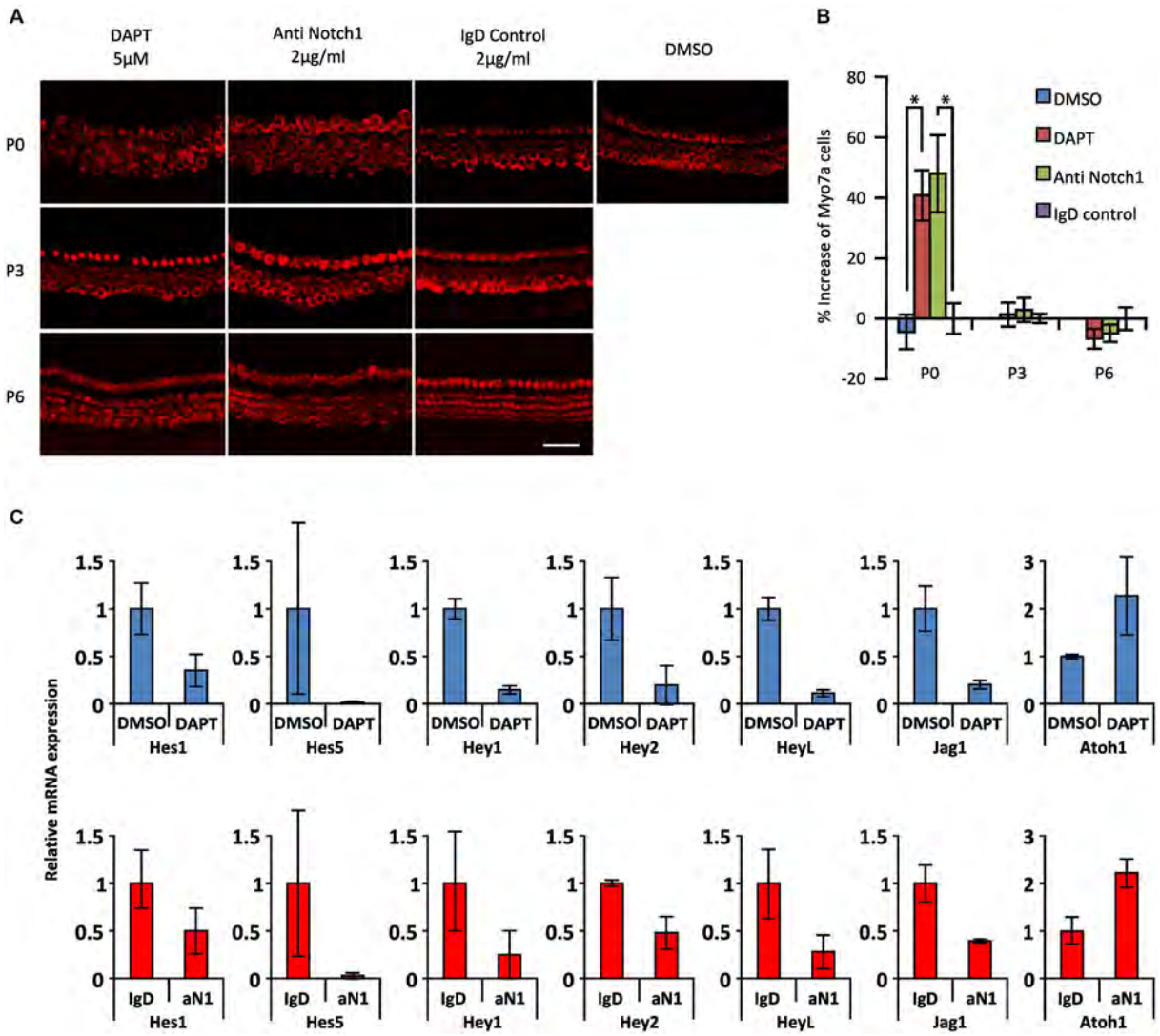

FIGURE 3 | Age-dependent decline in the effect of Notch inhibition on supporting cells in the presence of gamma secretase inhibitors or Notch1 blocking antibodies. (A) Immunostaining of apical portions of cochlear explants obtained at 0, 3 and 6 postnatal days (P0, P3 and P6) from *Atoh1*^{GFP} transgenic reporter mice treated with 5 μM DAPT, 2 μg/ml Notch1 antibodies (Anti Notch1), 2 μg/ml control IgD and DMSO cultured 2 days *in vitro* (DIV). Myo7a: red. Scale 50 μm. **(B)** The increase in numbers of Myosin VIIa-labeled cells in the apical portion of the cochleas shown in **(A)**. *N* = 6, 6 and 3 for P0, P3 and P6 respectively. **p* = 0.0044 and 0.0045 for DMSO/DAPT and Anti Notch1/Control IgD comparisons respectively (Mann Whitney). Error bars: SEM. **(C)** mRNA amount of Notch pathway genes obtained by QPCR in whole cochlear explants of *Atoh1*^{GFP} transgenic reporter P0 newborn mice cultured in the presence of DAPT or DMSO and in Notch1 antibodies or control IgD antibodies. Blue columns (top): level of expression after DAPT treatment relative to DMSO. Red columns (bottom): level of expression after anti Notch1 antibodies (aN1) relative to control IgD antibodies. *N* = 3. Error bars: SEM. Note that error bars are present for each condition but are very small in some cases.

cultures were treated with blocking antibodies as we previously saw with 5 μM DAPT (**Figures 3A,B**). We also observed a comparable down-regulation of supporting cell-specific *Hes* and *Hey* genes and the supporting cell marker *Jag1* in P0 cultures treated with DAPT or Notch1 blocking antibodies, together with a comparable up-regulation of *Atoh1* (**Figure 3C**). These results suggest that the majority of the effects of the gamma secretase inhibitor DAPT on supporting cell trans-differentiation in neonatal cultures are likely specific to the Notch pathway.

Notch Pathway Genes are Down-Regulated in the Cochlea During the First Postnatal Week

The preceding results suggest that the Notch pathway is deployed to stabilize supporting cell fate of neonatal cochlear supporting cells, but that inhibition of the Notch pathway has no effect on supporting cell fate even a few days later. To determine out if this change in the response of supporting cells to Notch inhibition was related to changes in the endogenous activity of the Notch pathway, we examined the expression of mRNA for Notch receptors (*Notch1* and *Notch3*), ligands (*Dll1*, *Jag1*

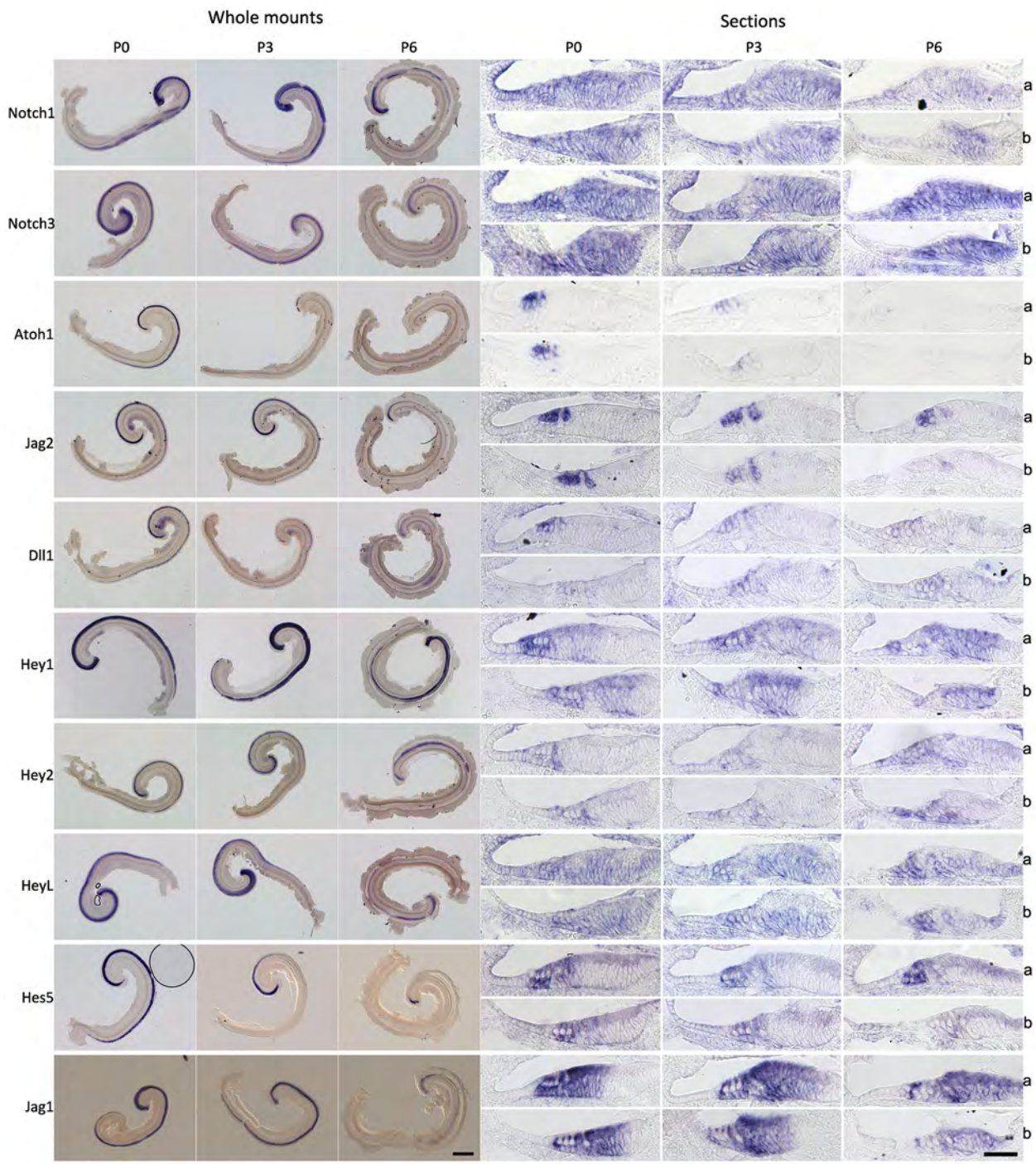

FIGURE 4 | Notch pathway components are down-regulated during the first postnatal week. *In situ* hybridization of Notch pathway genes in the cochlea at 0, 3 and 6 postnatal days (P0, P3 and P6). Left panels: Whole mount *in situs* of cochlear explants, with the samples curved clockwise from apex to base. Scale = 200 μm. Right panels: *In situ* hybridization of frozen sections; a: apex region, b: basal region. Scale 50 μm.

and *Jag2*) and downstream effectors of Notch signaling (*Hey1*, *Hey2*, *HeyL* and *Hes5*) in the cochlea from P0 to P6 by *in situ* hybridization on whole mount cochleas, sectioned cochleas and by Q-PCR of cochlear tissue (**Figures 4**, **5A**). In general, all components of the Notch pathway evinced a down-regulation between P0 and P6 starting at the base and proceeding down to the apex. Specifically, *Notch1* and *Notch3* were expressed throughout the supporting cell layer and into Kölliker's organ

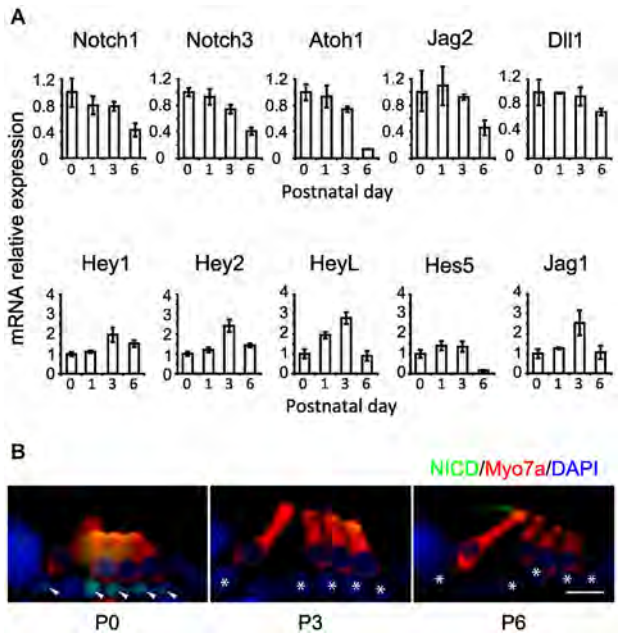

FIGURE 5 | Notch pathway components and Notch1 signaling activity decline during the first postnatal week. (A) Relative expression of some Notch pathway genes obtained by QPCR from whole cochlear explants at 1, 3 and 6 postnatal days relative to newborn (0 postnatal days). *N* = 3. Error bars: SEM. Note that error bars are present for each condition but are very small in some cases. **(B)** Notch1 intracellular domain (NICD) immunostaining in cochlear sections of ICR newborn mice, obtained at 0, 3 and 6 postnatal days (P0, P3 and P6 respectively). NICD: green. Myo7a: red. DAPI: blue. Arrow heads: supporting cells positive for NICD staining. Stars: same supporting cells pointed by arrow heads but negative for NICD staining. Scale = 20 μm.

and the outer sulcus, and both receptors showed a basal-apical down-regulation between P0 and P6. *Jag2* and *Dll1* were both down-regulated in hair cells between P0 and P6, along with the hair cell marker *Atoh1*. *Hey2* and *Hes5* were down-regulated from pillar cells and Deiters' cells respectively in a basal-apical gradient, whereas *Hey1*, *HeyL* and *Jag1* were expressed in all supporting cells and cells of Kölliker's organ, and down-regulated again in a basal-apical direction. The speed of down-regulation varied considerably from gene to gene—for example, *Dll1* was down-regulated in hair cells more quickly than *Jag2*, and *Hes5* was down-regulated much more quickly in supporting cells than *Hey1*. We also saw a general trend towards down-regulation of each gene by Q-PCR (**Figure 5A**), although the degree of down-regulation measured by this method was somewhat blunted as a result of including the entire basal-apical extent of the cochlear duct in each sample. To confirm that activation of the Notch1 receptor was also decreasing between P0 and P6, we immunostained cochlear sections with antibodies to the Notch1 intracellular domain (Notch1-ICD) which is released and localized to the nucleus after Notch activation (**Figure 5B**). We observed Notch1-ICD staining in Deiters' cells at P0, but could not detect staining in the supporting cells at later stages.

Although we did not see a significant increase in hair cells numbers at P3 or P6 after Notch inhibition in culture we did observe occasional isolated ectopic hair cells in our P3 (but not P6) cultures that may have been generated by trans-differentiation of supporting cells (**Figures 3A,B**) raising the possibility that a sub-population of supporting cells maintain Notch pathway expression at significant levels. To test whether small numbers of mature supporting cells maintain expression of some Notch pathway genes, we used the Fluidigm single cell handling system to compare gene expression in individual supporting cells purified from P2 and P21 mice. To label and purify pillar cells and Deiters' cells at P2, we injected triple transgenic mice (*FGFR3-iCreERT2/Ai14:Rosa*^{tdTom}*/Sox2-EGFP*) with tamoxifen at P0 and isolated TdTomato/EGFP double positive cells by flow cytometry. At this age, *FGFR3-iCreERT2* fate-labels pillar, Deiters', and outer hair cells, whereas EGFP is confined to all supporting cells. At P21, we used double transgenic (*FGFR3-iCreERT2/Ai14:Rosa*^{tdTom}) mice, injected with tamoxifen at P19, and sorted TdTomato-positive pillar and Deiters' cells, which were the only organ of Corti cell types labeled at this age. cDNA was prepared from individual P2 (N = 162) and P21 (n = 123) TdTomato cells using the Fluidigm single cell analysis system, and 96 genes analyzed from each sample by Q-PCR, including the Notch pathway genes *Jag1* and *2*, *Hes1* and *5*, *Hey1* and *2*, and the Notch target and ligand modulator *LFng* (**Figure 6**). In all cases, the numbers of cells with detectable amounts of Notch pathway genes declined from P2 to P21, (**Figure 6A**). The distribution in expression levels of Notch pathway genes in individual cells was visualized in violin plots and revealed a clear downward shift in expression across the population from P2 to P21 (**Figure 6B**), even when cells with undetectable levels of expression were removed from the analysis (**Figure 6C**). In some cases, we saw evidence for a small population of cells expressing high levels of a single Notch pathway gene at P21 (e.g., *Jag2*; **Figure 6C**), but we were unable to observe any single cells at P21 that co-expressed high levels of multiple Notch genes. These data suggest that the majority of P21 *FGFR3-iCreERT2* fate labeled supporting cells are unlikely to be transducing significant Notch signaling.

Notch Pathway Components are not Expressed at Significant Levels in the Normal and or Noise-Damaged Adult Organ of Corti

Several previous studies have suggested that some components of the Notch pathway may be re-activated in supporting cells following damage (Oesterle et al., 2008; Batts et al., 2009; Mizutari et al., 2013). However, these studies did not perform a direct quantitative comparison of message levels of Notch pathway components between neonatal animals (in which the Notch pathway is expressed and active) and mature animals before and after damage. We examined the expression of *Atoh1* and *Hes5* in cochleas isolated from cohorts of mice which received noise damage at P42 and were analyzed at one, three, or seven days later. Our controls were non-noise exposed cohorts of P0 and P49 mice. The level of noise we applied has been shown to be adequate to damage the cochlear epithelium and elicit changes in gene expression. In particular, it produces large temporary threshold

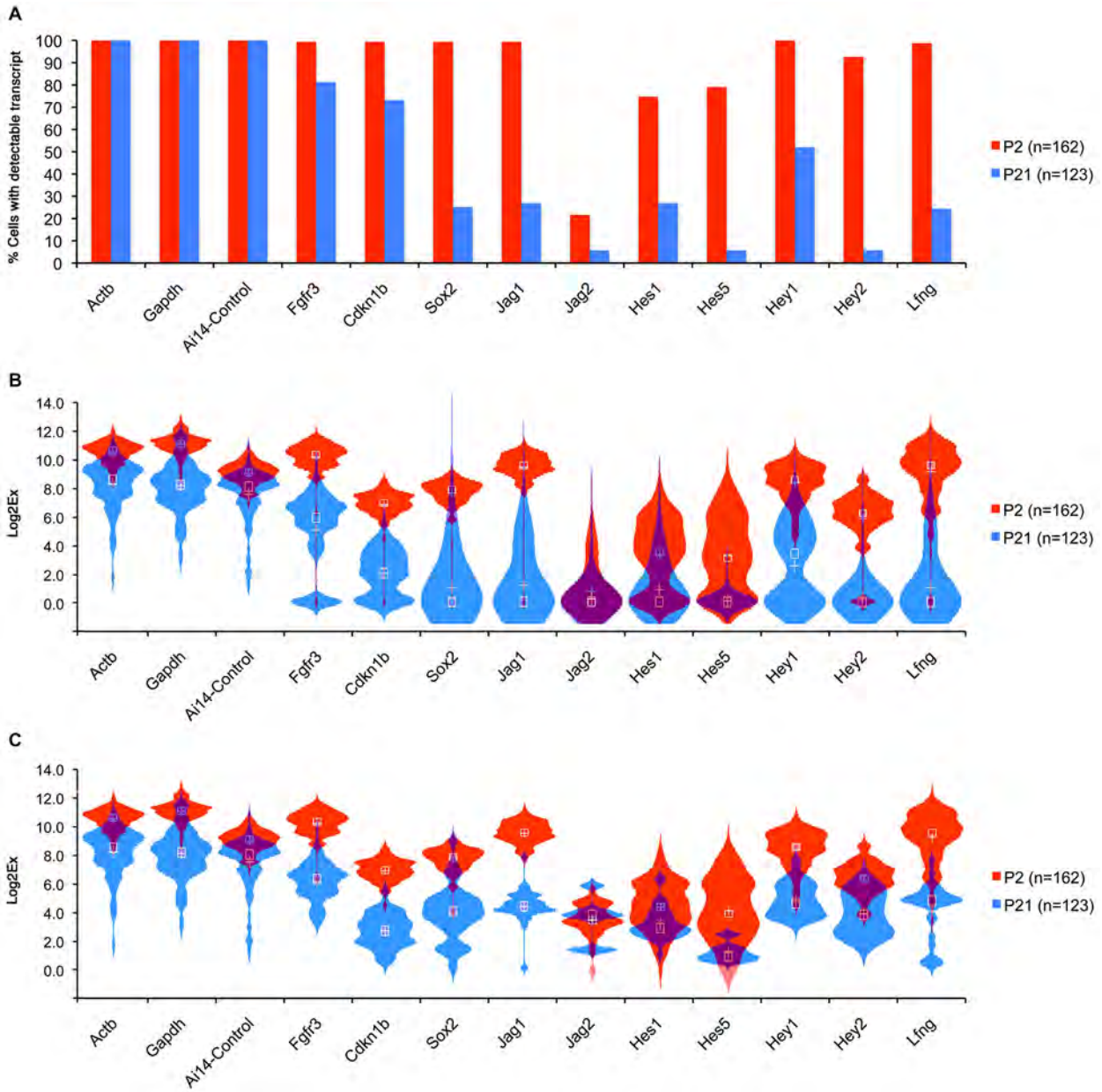

FIGURE 6 | Comparison of Notch pathway genes in P1 and P21 cochlea at the single cell level. Pillar and Deiters' cells were purified from P2 and P21 *FGFR3-CreER;ROSA-TdTomato* mice and RNA extracted from 162 (P2) and 123 (P21) single cells and subjected to QPCR analysis using the Fluidigm system (Durruthy-Durruthy et al., 2014) with primers for housekeeping genes and Notch pathway genes. **(A)** Graph showing the percentage of cells at each age that expressed detectable levels of each gene under analysis. **(B)** Violin plot showing the distribution of expression levels for each gene in all cells including the cells with no expression (Log2x = 0) presented in a combination of box plots and kernel density plots. White Crosses indicate the mean, white boxes the median expression levels. **(C)** Violin plot similar to **(B)**, excluding cells with undetectable levels of expression for each gene.

elevations, and mild permanent threshold shifts, 17% OHC loss and 3% IHC loss, and increases in prestin gene expression in residual OHCs (Wang et al., 2010; Xia et al., 2013). We found that levels of the hair cell-specific transcription factor *Atoh1* in 7 week old animals were less than 10% of their neonatal counterparts (**Figure 7**) and that these levels did not change significantly over a 7 day period after noise damage. Similar results were observed for *Hes5* (**Figure 7**). These data suggest that the Notch pathway remains down-regulated in the mature cochlea and that it is not significantly perturbed by noise damage.

Discussion

The Notch signaling pathway is deployed during the differentiation of hair cells and supporting cells and has been proposed to regulate the proportion of each cell type

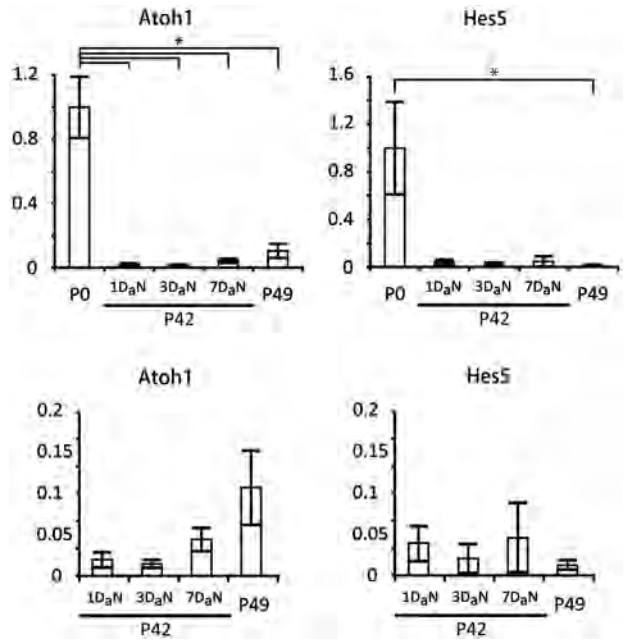

FIGURE 7 | Hes5 and Atoh1 remain expressed at very low levels in the mature organ of Corti, even after noise damage. Relative expression of *Atoh1* and *Hes5* obtained by QPCR in cochlear explants from neonatal (P0) and 6 to 7 week old mice exposed to noise. The mice exposed to noise on the 42nd postnatal day (P42) were evaluated after 1 ($1D_aN$), 3 ($3D_aN$), or 7 ($7D_aN$), days. As controls for the 7 day cohort we used 7 week old mice (P49) that had never been exposed to noise. The expression levels of *Atoh1* and *Hes5* were normalized to the level of expression at P0. $N = 3$ in all cases except P0, where $N = 6$. The values for adult animals are re-plotted on separate graphs; note that no significant changes occur in the adult samples. Error bars: SEM. $^*p = 0.03689$ (Mann-Whitney pairwise comparisons).

through lateral inhibition (Lewis, 1991; Eddison et al., 2000). The observation that inhibiting Notch signaling can generate ectopic hair cells at the expense of supporting cells (Takebayashi et al., 2007; Hayashi et al., 2008; Doetzlhofer et al., 2009; Korrapati et al., 2013; Mizutari et al., 2013; Bramhall et al., 2014), together with the observation that Notch signaling is re-deployed during avian hair cell regeneration (Stone and Rubel, 1999; Stone and Cotanche, 2007) has raised the possibility of targeting the Notch pathway in the damaged cochlea to effect hair cell replacement. However, results with Notch inhibitors in the adult cochlea have given variable results (Hori et al., 2007; Mizutari et al., 2013; Tona et al., 2014), prompting us to examine how this pathway is regulated as the cochlea matures. We show that the response of supporting cells to Notch inhibition drops dramatically in the first postnatal week, concomitant with a down-regulation of many components of the Notch signaling pathway.

Many studies have used gamma secretase inhibitors as a reagent to inhibit Notch signaling, despite the fact that gamma secretases are known to cleave scores of other transmembrane proteins in addition to Notch receptors (Kopan and Ilagan, 2004). Although it has generally been assumed that the conversion of supporting cells to hair cells in the presence of gamma secretase inhibitors is due to Notch inhibition, very few studies have tested this formally (Hayashi et al., 2008). We now show that the effects of the gamma secretase inhibitor DAPT on perinatal cochlear cultures—both in terms of the numbers of ectopic hair cells generated, in the down-regulation of Notch target genes and in the age-dependent response to these inhibitors—can be mimicked by blocking antibodies to the Notch1 receptor. While it remains formally possible that other gamma secretase-dependent signaling pathways are operating in perinatal supporting cells, our data suggest that the effect of inhibiting such pathways is negligible compared to their effect on Notch cleavage. We saw no evidence for supporting cell proliferation in our neonatal cultures treated with DAPT or Notch blocking antibodies (Doetzlhofer et al., 2009; data not shown). Conditional deletion of the Notch1 receptor, either at the otic placode stage (Kiernan et al., 2005a) or in neonatal mice (Li et al., 2015) has been reported to cause a small amount of supporting cell proliferation. Since these studies were both performed in intact animals, it is possible that the conditions used to establish organ cultures in our study militate against supporting cell proliferation when Notch signaling is blocked. Alternatively, it is possible that loss of a single allele in the *Sox2-CreER* and *Foxg1-Cre* knock-in lines used in these studies may interact genetically with *Notch1* mutants to cause abnormal proliferation. Indeed, haploinsufficiency of *Sox2* can modify the phenotype of $p27^{Kip1}$ mutants (Li et al., 2012), and *Foxg1-Cre* knock-in mice have been shown to have brain defects associated with proliferative defects on certain genetic backgrounds (Shen et al., 2006; Eagleson et al., 2007; Siegenthaler et al., 2008; see Cox et al., 2012 for further discussion).

We have characterized an age-dependent decline in the response of cochlear supporting cells to Notch inhibition in two ways. Our results from the most direct test of such age-dependence—treating cochlear tissue of different ages with Notch inhibitors (**Figure 3**)—are also supported by a careful analysis of basal-apical differences in the response of neonatal cochlear cultures to Notch inhibitors (**Figure 2**). Since hair cells and supporting cells in the mid-base of the cochlea differentiate at least 3 days before cells at the apex (Chen et al., 2002; Cai et al., 2013), analysis of whole cochlear explants allows us to directly compare different states of supporting cell differentiation in the same tissue. In P0 mice, we saw a higher proportion of ectopic outer hair cells vs. inner hair cells in the apex of the cochlea, and an even smaller proportion of ectopic inner hair cells at the base. Since inner hair cells begin to differentiate before outer hair cells in any given region of the cochlea (Chen et al., 2002; Cai et al., 2013), it is possible that these differences reflect a neural-abneural gradient of response to Notch inhibition as well as an apical-basal response. Alternatively, since different supporting cell types express different combinations of *Hes* and *Hey* genes (Zheng et al., 2000; Zine et al., 2001; Hayashi et al., 2008; Li et al., 2008; Doetzlhofer et al., 2009; Murata et al., 2009; Tateya et al., 2011), it is possible that these differences reflect the different sensitivities of these Notch target genes to Notch inhibition (Ong et al., 2006).

We observe a down-regulation of mRNA levels of Notch receptors, ligands and downstream effectors in the first postnatal week. The degree and rate of down-regulation varies, but analysis of Notch1 signaling in cochlear supporting cells over this time

period (**Figure 5**; Murata et al., 2006; Basch et al., 2011) suggests that very little cleavage of the Notch1 receptor is occurring by the end of the first postnatal week. The mechanism of this down-regulation is currently not known, although given the absence of significant Notch pathway expression in the adult cochlea, it is possible that the loci of Notch pathway genes are becoming epigenetically modified and placed beyond use. It is also possible that this epigenetic silencing is accompanied by silencing of the direct targets of Notch effectors such as the Hes and Hey genes. However, it should be noted that the Notch pathway appears to be down-regulated in mature supporting cells in the chicken basilar papilla, as this sensory organ also fails to respond to gamma secretase inhibitors in the undamaged state (Daudet et al., 2009). Nevertheless, after damage, the Notch pathway is once again deployed in chicken supporting cells and the differentiating hair cells that they generate (Stone and Rubel, 1999; Daudet et al., 2009). It will therefore be of great interest to identify the epigenetic state of Notch pathway genes and their targets in mature mammalian supporting cells. It should also be noted that the co-expression of Jag1 and Sox2, which is seen in sensory patches from their first appearance (Kiernan et al., 2005b; Pan et al., 2010, 2013; Neves et al., 2011, 2012), is maintained in adult mouse supporting cells (Oesterle et al., 2008). It is thus formally possible that low levels of Notch signaling may persist in the adult cochlea and may maintain expression of these two genes by lateral induction. If this is the case, such signaling does not appear to confer competence for regeneration on supporting cells.

A recent study demonstrated that a small but significant number of new hair cells could be generated from supporting cells by treating noise-damaged animals with gamma secretase inhibitors (Mizutari et al., 2013), leading to a partial restoration of function. How can we reconcile these results with our data in the present study? First, it is possible that the Notch pathway can continue to regulate hair cell and supporting cell fate in the adult animal when expressed at significantly lower levels. We feel this is unlikely since binding of the Notch-ICD-MAML-RBPj complex to its target sites in the genome is likely to be severely compromised at low concentrations of Notch-ICD (Ong et al., 2006). Second, it is possible that a sub-population of supporting cells continue to express Notch pathway components at significant levels, but that these would not be detected when analyzing gene expression in the entire cochlea. In our single cell analysis of 123 P21 pillar cells and Deiters' cells, we were able to detect a very small number of cells in which Notch pathway components were expressed at comparable levels to their neonatal counterparts (**Figure 6**), and levels of *Hes5* and the hair cell marker *Atoh1* are more than 10-fold lower in the adult, even after noise damage (**Figure 7**). This suggests that if such cells persist in the adult cochlea, they are present in extremely small numbers. Finally, it is also possible that a second, Notch-independent pathway that can be targeted by gamma secretase inhibitors is operating in a small number of mature supporting cells. The effect of inhibiting this second pathway would be overshadowed by Notch inhibition in the neonatal cochlea, but might be uncovered in the adult cochlea when the Notch pathway is no longer active. It should also be noted that the noise damage protocol (Liu et al., 2011) used in our study—98 dB for 4 h—is significantly less severe than the protocol used by Mizutari et al. (116 dB for 2 h). However, the large and significant drop in *Atoh1* and *Hes5* levels we observe in undamaged adult tissue compared to neonatal animals still supports our observed down-regulation of Notch pathway genes in the first postnatal week.

In conclusion, our results suggest that the canonical Notch pathway is not active to any significant degree in the adult organ of Corti, and that the down-regulation of signaling occurs prior to the onset of hearing. The Notch pathway can therefore be viewed as a developmental scaffold for the organ of Corti—it is partly necessary for establishing the pattern and proportion of hair cells and supporting cells, but not necessary to maintain this pattern once it has been established. This suggests that inhibition of Notch signaling in the adult organ of Corti in the absence of other manipulations is unlikely to promote significant numbers of new hair cells, and that alternative or supplementary therapeutic interventions should be considered.

Acknowledgments

We thank Alyssa Crowder, Hongyuan Zhang and Huiling Li for excellent technical support. We thank Gerry Weinmaster, Urban Lendahl, Ryoichiro Kageyama and Manfred Gessler for gifts of cDNA probes. This work was supported by Department of Defense Grant DOD W81XWH-11-2-004 (AKG) and Hearing Restoration Project consortium grants from the Hearing Health Foundation (AKG and SH), NIH grant DC004563 (SH), NIH grant P30 DC010363 (SH, JSO), and NIH R01 DC014450 (JSO).

References

Abelló, G., Khatri, S., Giráldez, F., and Alsina, B. (2007). Early regionalization of the otic placode and its regulation by the Notch signaling pathway. *Mech. Dev.* 124, 631–645. doi: 10.1016/j.mod.2007.04.002

Adam, J., Myat, A., Le Roux, I., Eddison, M., Henrique, D., Ish-Horowicz, D., et al. (1998). Cell fate choices and the expression of Notch, Delta and Serrate homologues in the chick inner ear: parallels with Drosophila sense-organ development. *Development* 125, 4645–4654.

Artavanis-Tsakonas, S., and Muskavitch, M. A. (2010). Notch: the past, the present and the future. *Curr. Top. Dev. Biol.* 92, 1–29. doi: 10.1016/s0070-2153(10)92001-2

Artavanis-Tsakonas, S., Rand, M. D., and Lake, R. J. (1999). Notch signaling: cell fate control and signal integration in development. *Science* 284, 770–776. doi: 10.1126/science.284.5415.770

Basch, M. L., Ohyama, T., Segil, N., and Groves, A. K. (2011). Canonical Notch signaling is not necessary for prosensory induction in the mouse cochlea: insights from a conditional mutant of RBPjkappa. *J. Neurosci.* 31, 8046–8058. doi: 10.1523/jneurosci.6671-10.2011

Batts, S. A., Shoemaker, C. R., and Raphael, Y. (2009). Notch signaling and Hes labeling in the normal and drug-damaged organ of corti. *Hear. Res.* 249, 15–22. doi: 10.1016/j.heares.2008.12.008

Benito-Gonzalez, A., and Doetzlhofer, A. (2014). Hey1 and hey2 control the spatial and temporal pattern of mammalian auditory hair cell differentiation

downstream of hedgehog signaling. *J. Neurosci.* 34, 12865–12876. doi: 10.1523/jneurosci.1494-14.2014

Birren, S. J., Lo, L., and Anderson, D. J. (1993). Sympathetic neuroblasts undergo a developmental switch in trophic dependence. *Development* 119, 597–610.

Bramhall, N. F., Shi, F., Arnold, K., Hochedlinger, K., and Edge, A. S. (2014). Lgr5-positive supporting cells generate new hair cells in the postnatal cochlea. *Stem Cell Reports* 2, 311–322. doi: 10.1016/j.stemcr.2014.01.008

Bray, S. J. (2006). Notch signalling: a simple pathway becomes complex. *Nat. Rev. Mol. Cell Biol.* 7, 678–689. doi: 10.1038/nrm2009

Brooker, R., Hozumi, K., and Lewis, J. (2006). Notch ligands with contrasting functions: Jagged1 and Delta1 in the mouse inner ear. *Development* 133, 1277–1286. doi: 10.1242/dev.02284

Cai, T., Seymour, M. L., Zhang, H., Pereira, F. A., and Groves, A. K. (2013). Conditional deletion of Atoh1 reveals distinct critical periods for survival and function of hair cells in the organ of corti. *J. Neurosci.* 33, 10110–10122. doi: 10.1523/JNEUROSCI.5606-12.2013

Chen, P., Johnson, J. E., Zoghbi, H. Y., and Segil, N. (2002). The role of Math1 in inner ear development: uncoupling the establishment of the sensory primordium from hair cell fate determination. *Development* 129, 2495–2505.

Chitnis, A. B. (1995). The role of Notch in lateral inhibition and cell fate specification. *Mol. Cell. Neurosci.* 6, 311–321. doi: 10.1006/mcne.1995.1024

Cox, B. C., Liu, Z., Lagarde, M. M., and Zuo, J. (2012). Conditional gene expression in the mouse inner ear using Cre-loxP. *J. Assoc. Res. Otolaryngol.* 13, 295–322. doi: 10.1007/s10162-012-0324-5

Daudet, N., Ariza-Mcnaughton, L., and Lewis, J. (2007). Notch signalling is needed to maintain, but not to initiate, the formation of prosensory patches in the chick inner ear. *Development* 134, 2369–2378. doi: 10.1242/dev.001842

Daudet, N., Gibson, R., Shang, J., Bernard, A., Lewis, J., and Stone, J. (2009). Notch regulation of progenitor cell behavior in quiescent and regenerating auditory epithelium of mature birds. *Dev. Biol.* 326, 86–100. doi: 10.1016/j.ydbio.2008.10.033

Daudet, N., and Lewis, J. (2005). Two contrasting roles for Notch activity in chick inner ear development: specification of prosensory patches and lateral inhibition of hair-cell differentiation. *Development* 132, 541–551. doi: 10.1242/dev.01589

Doetzlhofer, A., Basch, M. L., Ohyama, T., Gessler, M., Groves, A. K., and Segil, N. (2009). Hey2 regulation by FGF provides a Notch-independent mechanism for maintaining pillar cell fate in the organ of corti. *Dev. Cell* 16, 58–69. doi: 10.1016/j.devcel.2008.11.008

Durruthy-Durruthy, R., Gottlieb, A., Hartman, B. H., Waldhaus, J., Laske, R. D., Altman, R., et al. (2014). Reconstruction of the mouse otocyst and early neuroblast lineage at single-cell resolution. *Cell* 157, 964–978. doi: 10.1016/j.cell.2014.03.036

Eagleson, K. L., Schlueter Mcfadyen-Ketchum, L. J., Ahrens, E. T., Mills, P. H., Does, M. D., Nickols, J., et al. (2007). Disruption of Foxg1 expression by knock-in of cre recombinase: effects on the development of the mouse telencephalon. *Neuroscience* 148, 385–399. doi: 10.1016/j.neuroscience.2007.06.012

Eddison, M., Le Roux, I., and Lewis, J. (2000). Notch signaling in the development of the inner ear: lessons from Drosophila. *Proc. Natl. Acad. Sci. U S A* 97, 11692–11699. doi: 10.1073/pnas.97.22.11692

Formosa-Jordan, P., Ibañes, M., Ares, S., and Frade, J. M. (2013). Lateral inhibition and neurogenesis: novel aspects in motion. *Int. J. Dev. Biol.* 57, 341–350. doi: 10.1387/ijdb.120259jf

Groves, A. K., and Fekete, D. M. (2012). Shaping sound in space: the regulation of inner ear patterning. *Development* 139, 245–257. doi: 10.1242/dev.067074

Groves, A. K., George, K. M., Tissier-Seta, J. P., Engel, J. D., Brunet, J. F., and Anderson, D. J. (1995). Differential regulation of transcription factor gene expression and phenotypic markers in developing sympathetic neurons. *Development* 121, 887–901.

Harland, R. M. (1991). *In situ* hybridization: an improved whole-mount method for Xenopus embryos. *Methods Cell Biol.* 36, 685–695. doi: 10.1016/s0091-679x(08)60307-6

Hartman, B. H., Basak, O., Nelson, B. R., Taylor, V., Bermingham-Mcdonogh, O., and Reh, T. A. (2009). Hes5 expression in the postnatal and adult mouse inner ear and the drug-damaged cochlea. *J. Assoc. Res. Otolaryngol.* 10, 321–340. doi: 10.1007/s10162-009-0162-2

Hartman, B. H., Hayashi, T., Nelson, B. R., Bermingham-Mcdonogh, O., and Reh, T. A. (2007). Dll3 is expressed in developing hair cells in the mammalian cochlea. *Dev. Dyn.* 236, 2875–2883. doi: 10.1002/dvdy.21307

Hartman, B. H., Reh, T. A., and Bermingham-Mcdonogh, O. (2010). Notch signaling specifies prosensory domains via lateral induction in the developing mammalian inner ear. *Proc. Natl. Acad. Sci. U S A* 107, 15792–15797. doi: 10.1073/pnas.1002827107

Hayashi, T., Kokubo, H., Hartman, B. H., Ray, C. A., Reh, T. A., and Bermingham-Mcdonogh, O. (2008). Hesr1 and Hesr2 may act as early effectors of Notch signaling in the developing cochlea. *Dev. Biol.* 316, 87–99. doi: 10.1016/j.ydbio.2008.01.006

Hori, R., Nakagawa, T., Sakamoto, T., Matsuoka, Y., Takebayashi, S., and Ito, J. (2007). Pharmacological inhibition of Notch signaling in the mature guinea pig cochlea. *Neuroreport* 18, 1911–1914. doi: 10.1097/wnr.0b013e3282f213e0

Hori, K., Sen, A., and Artavanis-Tsakonas, S. (2013). Notch signaling at a glance. *J. Cell Sci.* 126, 2135–2140. doi: 10.1242/jcs.127308

Ilagan, M. X., and Kopan, R. (2007). SnapShot: notch signaling pathway. *Cell* 128, 1246.e1–1246.e2. doi: 10.1016/j.cell.2007.03.011

Jayasena, C. S., Ohyama, T., Segil, N., and Groves, A. K. (2008). Notch signaling augments the canonical Wnt pathway to specify the size of the otic placode. *Development* 135, 2251–2261. doi: 10.1242/dev.017905

Kelley, M. W. (2003). Cell adhesion molecules during inner ear and hair cell development, including notch and its ligands. *Curr. Top. Dev. Biol.* 57, 321–356. doi: 10.1016/s0070-2153(03)57011-9

Kelley, M. W. (2006). Regulation of cell fate in the sensory epithelia of the inner ear. *Nat. Rev. Neurosci.* 7, 837–849. doi: 10.1038/nrn1987

Kelley, M. W. (2007). Cellular commitment and differentiation in the organ of corti. *Int. J. Dev. Biol.* 51, 571–583. doi: 10.1387/ijdb.072388mk

Khatri, S. B., and Groves, A. K. (2013). Expression of the Foxi2 and Foxi3 transcription factors during development of chicken sensory placodes and pharyngeal arches. *Gene Expr. Patterns* 13, 38–42. doi: 10.1016/j.gep.2012.10.001

Kiernan, A. E. (2013). Notch signaling during cell fate determination in the inner ear. *Semin. Cell Dev. Biol.* 24, 470–479. doi: 10.1016/j.semcdb.2013.04.002

Kiernan, A. E., Cordes, R., Kopan, R., Gossler, A., and Gridley, T. (2005a). The Notch ligands DLL1 and JAG2 act synergistically to regulate hair cell development in the mammalian inner ear. *Development* 132, 4353–4362. doi: 10.1242/dev.02002

Kiernan, A. E., Pelling, A. L., Leung, K. K., Tang, A. S., Bell, D. M., Tease, C., et al. (2005b). Sox2 is required for sensory organ development in the mammalian inner ear. *Nature* 434, 1031–1035. doi: 10.1038/nature03487

Kopan, R., and Ilagan, M. X. (2004). Gamma-secretase: proteasome of the membrane? *Nat. Rev. Mol. Cell Biol.* 5, 499–504. doi: 10.1038/nrm1406

Korrapati, S., Roux, I., Glowatzki, E., and Doetzlhofer, A. (2013). Notch signaling limits supporting cell plasticity in the hair cell-damaged early postnatal murine cochlea. *PLoS One* 8:e73276. doi: 10.1371/journal.pone.0073276

Lewis, J. (1991). Rules for the production of sensory cells. *Ciba Found. Symp.* 160, 25–39; discussion 40–53.

Li, H., Collado, M., Villasante, A., Matheu, A., Lynch, C. J., Cañamero, M., et al. (2012). p27(Kip1) directly represses Sox2 during embryonic stem cell differentiation. *Cell Stem Cell* 11, 845–852. doi: 10.1016/j.stem.2012.09.014

Li, S., Mark, S., Radde-Gallwitz, K., Schlisner, R., Chin, M. T., and Chen, P. (2008). Hey2 functions in parallel with Hes1 and Hes5 for mammalian auditory sensory organ development. *BMC Dev. Biol.* 8:20. doi: 10.1186/1471-213X-8-20

Li, W., Wu, J., Yang, J., Sun, S., Chai, R., Chen, Z. Y., et al. (2015). Notch inhibition induces mitotically generated hair cells in mammalian cochleae via activating the Wnt pathway. *Proc. Natl. Acad. Sci. U S A* 112, 166–171. doi: 10.1073/pnas.1415901112

Lin, V., Golub, J. S., Nguyen, T. B., Hume, C. R., Oesterle, E. C., and Stone, J. S. (2011). Inhibition of Notch activity promotes nonmitotic regeneration of hair cells in the adult mouse utricles. *J. Neurosci.* 31, 15329–15339. doi: 10.1523/JNEUROSCI.2057-11.2011

Liu, C. C., Gao, S. S., Yuan, T., Steele, C., Puria, S., and Oghalai, J. S. (2011). Biophysical mechanisms underlying outer hair cell loss associated with a shortened tectorial membrane. *J. Assoc. Res. Otolaryngol.* 12, 577–594. doi: 10.1007/s10162-011-0269-0

Liu, Z., Liu, Z., Walters, B. J., Owen, T., Kopan, R., and Zuo, J. (2013). *In vivo* visualization of Notch1 proteolysis reveals the heterogeneity of Notch1 signaling activity in the mouse cochlea. *PLoS One* 8:e64903. doi: 10.1371/journal.pone.0064903

Liu, Z., Owen, T., Fang, J., Srinivasan, R. S., and Zuo, J. (2012a). *In vivo* Notch reactivation in differentiating cochlear hair cells induces Sox2 and Prox1

expression but does not disrupt hair cell maturation. *Dev. Dyn.* 241, 684–696. doi: 10.1002/dvdy.23754

Liu, Z., Owen, T., Fang, J., and Zuo, J. (2012b). Overactivation of Notch1 signaling induces ectopic hair cells in the mouse inner ear in an age-dependent manner. *PLoS One* 7:e34123. doi: 10.1371/journal.pone.0034123

Lumpkin, E. A., Collisson, T., Parab, P., Omer-Abdalla, A., Haeberle, H., Chen, P., et al. (2003). Math1-driven GFP expression in the developing nervous system of transgenic mice. *Gene Expr. Patterns* 3, 389–395. doi: 10.1016/s1567-133x(03)00089-9

Mizutari, K., Fujioka, M., Hosoya, M., Bramhall, N., Okano, H. J., Okano, H., et al. (2013). Notch inhibition induces cochlear hair cell regeneration and recovery of hearing after acoustic trauma. *Neuron* 77, 58–69. doi: 10.1016/j.neuron.2012.10.032

Morimoto, M., Liu, Z., Cheng, H. T., Winters, N., Bader, D., and Kopan, R. (2010). Canonical Notch signaling in the developing lung is required for determination of arterial smooth muscle cells and selection of Clara versus ciliated cell fate. *J. Cell Sci.* 123, 213–224. doi: 10.1242/jcs.058669

Murata, J., Ikeda, K., and Okano, H. (2012). Notch signaling and the developing inner ear. *Adv. Exp. Med. Biol.* 727, 161–173. doi: 10.1007/978-1-4614-0899-4_12

Murata, J., Ohtsuka, T., Tokunaga, A., Nishiike, S., Inohara, H., Okano, H., et al. (2009). Notch-Hes1 pathway contributes to the cochlear prosensory formation potentially through the transcriptional down-regulation of p27Kip1. *J. Neurosci. Res.* 87, 3521–3534. doi: 10.1002/jnr.22169

Murata, J., Tokunaga, A., Okano, H., and Kubo, T. (2006). Mapping of notch activation during cochlear development in mice: implications for determination of prosensory domain and cell fate diversification. *J. Comp. Neurol.* 497, 502–518. doi: 10.1002/cne.20997

Neves, J., Abelló, G., Petrovic, J., and Giraldez, F. (2013a). Patterning and cell fate in the inner ear: a case for Notch in the chicken embryo. *Dev. Growth Differ.* 55, 96–112. doi: 10.1111/dgd.12016

Neves, J., Parada, C., Chamizo, M., and Giráldez, F. (2011). Jagged 1 regulates the restriction of Sox2 expression in the developing chicken inner ear: a mechanism for sensory organ specification. *Development* 138, 735–744. doi: 10.1242/dev.060657

Neves, J., Uchikawa, M., Bigas, A., and Giraldez, F. (2012). The prosensory function of Sox2 in the chicken inner ear relies on the direct regulation of Atoh1. *PLoS One* 7:e30871. doi: 10.1371/journal.pone.0030871

Neves, J., Vachkov, I., and Giraldez, F. (2013b). Sox2 regulation of hair cell development: incoherence makes sense. *Hear. Res.* 297, 20–29. doi: 10.1016/j.heares.2012.11.003

Oesterle, E. C., Campbell, S., Taylor, R. R., Forge, A., and Hume, C. R. (2008). Sox2 and JAGGED1 expression in normal and drug-damaged adult mouse inner ear. *J. Assoc. Res. Otolaryngol.* 9, 65–89. doi: 10.1007/s10162-007-0106-7

Ong, C. T., Cheng, H. T., Chang, L. W., Ohtsuka, T., Kageyama, R., Stormo, G. D., et al. (2006). Target selectivity of vertebrate notch proteins. Collaboration between discrete domains and CSL-binding site architecture determines activation probability. *J. Biol. Chem.* 281, 5106–5119. doi: 10.1074/jbc.m506108200

Pan, W., Jin, Y., Chen, J., Rottier, R. J., Steel, K. P., and Kiernan, A. E. (2013). Ectopic expression of activated notch or SOX2 reveals similar and unique roles in the development of the sensory cell progenitors in the mammalian inner ear. *J. Neurosci.* 33, 16146–16157. doi: 10.1523/JNEUROSCI.3150-12.2013

Pan, W., Jin, Y., Stanger, B., and Kiernan, A. E. (2010). Notch signaling is required for the generation of hair cells and supporting cells in the mammalian inner ear. *Proc. Natl. Acad. Sci. U S A* 107, 15798–15803. doi: 10.1073/pnas.1003089107

Rose, M. F., Ren, J., Ahmad, K. A., Chao, H. T., Klisch, T. J., Flora, A., et al. (2009). Math1 is essential for the development of hindbrain neurons critical for perinatal breathing. *Neuron* 64, 341–354. doi: 10.1016/j.neuron.2009.10.023

Shen, L., Nam, H. S., Song, P., Moore, H., and Anderson, S. A. (2006). FoxG1 haploinsufficiency results in impaired neurogenesis in the postnatal hippocampus and contextual memory deficits. *Hippocampus* 16, 875–890. doi: 10.1002/hipo.20218

Siegenthaler, J. A., Tremper-Wells, B. A., and Miller, M. W. (2008). Foxg1 haploinsufficiency reduces the population of cortical intermediate progenitor cells: effect of increased p21 expression. *Cereb. Cortex* 18, 1865–1875. doi: 10.1093/cercor/bhm209

Slowik, A. D., and Bermingham-McDonogh, O. (2013). Hair cell generation by notch inhibition in the adult mammalian cristae. *J. Assoc. Res. Otolaryngol.* 14, 813–828. doi: 10.1007/s10162-013-0414-z

Stern, C. D. (1998). Detection of multiple gene products simultaneously by *in situ* hybridization and immunohistochemistry in whole mounts of avian embryos. *Curr. Top. Dev. Biol.* 36, 223–243. doi: 10.1016/s0070-2153(08)60505-0

Stone, J. S., and Cotanche, D. A. (2007). Hair cell regeneration in the avian auditory epithelium. *Int. J. Dev. Biol.* 51, 633–647. doi: 10.1387/ijdb.072408js

Stone, J. S., and Rubel, E. W. (1999). Delta1 expression during avian hair cell regeneration. *Development* 126, 961–973.

Takebayashi, S., Yamamoto, N., Yabe, D., Fukuda, H., Kojima, K., Ito, J., et al. (2007). Multiple roles of Notch signaling in cochlear development. *Dev. Biol.* 307, 165–178. doi: 10.1016/j.ydbio.2007.04.035

Tateya, T., Imayoshi, I., Tateya, I., Ito, J., and Kageyama, R. (2011). Cooperative functions of Hes/Hey genes in auditory hair cell and supporting cell development. *Dev. Biol.* 352, 329–340. doi: 10.1016/j.ydbio.2011.01.038

Tona, Y., Hamaguchi, K., Ishikawa, M., Miyoshi, T., Yamamoto, N., Yamahara, K., et al. (2014). Therapeutic potential of a gamma-secretase inhibitor for hearing restoration in a guinea pig model with noise-induced hearing loss. *BMC Neurosci.* 15:66. doi: 10.1186/1471-2202-15-66

Wang, G. P., Chatterjee, I., Batts, S. A., Wong, H. T., Gong, T. W., Gong, S. S., et al. (2010). Notch signaling and Atoh1 expression during hair cell regeneration in the mouse utricle. *Hear. Res.* 267, 61–70. doi: 10.1016/j.heares.2010.03.085

Wu, Y., Cain-Hom, C., Choy, L., Hagenbeek, T. J., de Leon, G. P., Chen, Y., et al. (2010). Therapeutic antibody targeting of individual Notch receptors. *Nature* 464, 1052–1057. doi: 10.1038/nature08878

Xia, A., Song, Y., Wang, R., Gao, S. S., Clifton, W., Raphael, P., et al. (2013). Prestin regulation and function in residual outer hair cells after noise-induced hearing loss. *PLoS One* 8:e82602. doi: 10.1371/journal.pone.0082602

Yamamoto, N., Chang, W., and Kelley, M. W. (2011). Rbpj regulates development of prosensory cells in the mammalian inner ear. *Dev. Biol.* 353, 367–379. doi: 10.1016/j.ydbio.2011.03.016

Yamamoto, N., Tanigaki, K., Tsuji, M., Yabe, D., Ito, J., and Honjo, T. (2006). Inhibition of Notch/RBP-J signaling induces hair cell formation in neonate mouse cochleas. *J. Mol. Med. (Berl)* 84, 37–45. doi: 10.1007/s00109-005-0706-9

Young, K. M., Mitsumori, T., Pringle, N., Grist, M., Kessaris, N., and Richardson, W. D. (2010). An Fgfr3-iCreER(T2) transgenic mouse line for studies of neural stem cells and astrocytes. *Glia* 58, 943–953. doi: 10.1002/glia.20976

Zheng, J. L., Shou, J., Guillemot, F., Kageyama, R., and Gao, W. Q. (2000). Hes1 is a negative regulator of inner ear hair cell differentiation. *Development* 127, 4551–4560.

Zine, A., Aubert, A., Qiu, J., Therianos, S., Guillemot, F., Kageyama, R., et al. (2001). Hes1 and Hes5 activities are required for the normal development of the hair cells in the mammalian inner ear. *J. Neurosci.* 21, 4712–4720.

Zine, A., Van De Water, T. R., and de Ribaupierre, F. (2000). Notch signaling regulates the pattern of auditory hair cell differentiation in mammals. *Development* 127, 3373–3383.

Conflict of Interest Statement: The authors declare that the research was conducted in the absence of any commercial or financial relationships that could be construed as a potential conflict of interest.